Fast Solution Techniques for Energy Management in Smart Homes

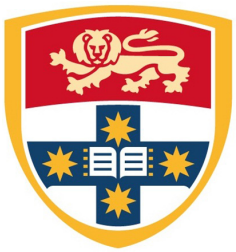

Chanaka Keerthisinghe

School of Electrical and Information Engineering
University of Sydney

A thesis submitted in fulfilment of the requirements for the degree of
Doctor of Philosophy

December 2016

I would like to dedicate this thesis to everyone who helped. …

Declaration

I hereby declare that except where specific reference is made to the work of others, the contents of this dissertation are original and have not been submitted in whole or in part for consideration for any other degree or qualification in this, or any other university. This dissertation is my own work and contains nothing which is the outcome of work done in collaboration with others, except as specified in the text and Acknowledgements. This dissertation contains fewer than 65,000 words including appendices, bibliography, footnotes, tables and equations and has fewer than 150 figures.

Chanaka Keerthisinghe
December 2016

Acknowledgements

First of all I would like to thank my supervisors, Dr. Gregor Verbič and Dr. Archie C. Chapman, for their valuable guidance, advice and help throughout my PhD.

Next, I would like to appreciate the scholarships from the following: Australian Postgraduate Award (APA) from the Australian Government; Norman I prize supplementary scholarship from the University of Sydney (1 year); and Postgraduate Scholarship in Smart Grids from Ausgrid (few months).

Last but not least, I would like to deeply thank my friends and family for their support.

Abstract

In the future, residential energy users will seize the full potential of demand response schemes by using an automated *smart home energy management system* (SHEMS) to schedule their distributed energy resources. The underlying optimisation problem facing a SHEMS is a sequential decision making problem under uncertainty because the states of the devices depend on the past state. There are two major challenges to optimisation in this domain; namely, handling uncertainty, and planning over suitably long decision horizons. In more detail, in order to generate high quality schedules, a SHEMS should consider the stochastic nature of the *photovoltaic* (PV) generation and energy consumption. In addition, the SHEMS should accommodate predictable inter-daily variations over several days. Ideally, the SHEMS should also be able to integrate into an existing smart meter or a similar device with low computational power. However, extending the decision horizon of existing solution techniques for sequential stochastic decision making problems is computationally difficult and moreover, these approaches are only computationally feasible with a limited number of storage devices and a daily decision horizon. Given this, the research investigates, proposes and develops fast solution techniques for implementing efficient SHEMSs.

Specifically, three novel methods for overcoming these challenges: a *two-stage lookahead stochastic optimisation* framework; an *approximate dynamic programming* (ADP) approach with *temporal difference learning*; and a *policy function approximation* (PFA) algorithm using *extreme learning machines* (ELM) are presented. Throughout the thesis, the performance of these solution techniques are benchmarked against dynamic programming (DP) and stochastic mixed-integer linear programming (MILP) using a range of residential PV-storage (thermal and battery) systems. We use empirical data collected during the Smart Grid Smart City project in New South Wales, Australia, to estimate the parameters of a Markov chain model of PV output and electrical demand using an hierarchical approach, which first cluster empirical data and then learns probability density functions using kernel regression (Chapter 2).

The two-stage lookahead method uses deterministic MILP to solve a longer decision horizon, while its end-of-day battery state of charge is used as a constraint for a daily DP approach (Chapter 4). Here DP is used for the daily horizon as it is shown to provide

close-to-optimal solutions when the state, decision and outcome spaces are finely discretised (Chapter 3). However, DP is computationally difficult because of the dimensionalities of state, decision and outcome spaces, so we resort to MILP to solve the longer decision horizon. The two-stage lookahead results in significant financial benefits compared to daily DP and stochastic MILP approaches (8.54% electricity cost savings for a very suitable house), however, the benefits decreases as the actual PV output and demand deviates from their forecast values.

Building on this, ADP is proposed in Chapter 5 to implement a computationally efficient SHEMS. Here we obtain policies from value function approximations (VFAs) by stepping forward in time, compared to the value functions obtained by backward induction in DP. Similar to DP, we can use VFAs generated during the offline planning phase to generate fast real-time solutions using the Bellman optimality condition, which is computationally efficient compared to having to solve the entire stochastic MILP problem. The decisions obtained from VFAs at a given time-step are optimal regardless of what happened in the previous time-steps. Our results show that ADP computes a solution much faster than both DP and stochastic MILP, and provides only a slight reduction in quality compared to the optimal DP solution. In addition, incorporating a thermal energy storage unit using the proposed ADP-based SHEMS reduces the daily electricity cost by up to 57.27% for a most suitable home, with low computational burden. Moreover, ADP with a two-day decision horizon reduces the average yearly electricity cost by a 4.6% over a daily DP method, yet requires less than half of the computational effort. However, ADP still takes a considerable amount of time to generate VFAs in the off-line planning phase and require us to estimate PV and demand models.

Given this, a PFA algorithm that uses ELM is proposed in Chapter 6 to overcome these difficulties. Here ELM is used to learn models that map input states and output decisions within seconds, without solving an optimisation problem. This off-line planning process requires a training data set, which has to be generated by solving the deterministic SHEMS problem over couple of years. Here we can use a powerful cloud or home computer as it is only needed once. PFA models can be used to make fast real-time decisions and can easily be embedded in an existing smart meter or a similar low power device. Moreover, we can use PFA models over a long period of time without updating the model and still obtain similar quality solutions. Collectively, ADP and PFA using ELM can overcome challenges of considering the stochastic variables, extending the decision horizon and integrating multiple controllable devices using existing smart meters or a device with low computational power, and represent a significant advancement to the state of the art in this domain.

Table of contents

List of figures

List of tables

Nomenclature

Roman Symbols

k	Time-step
K	Total number of time-steps
i	Index of controllable devices
I	Total number of controllable devices
j	Index of stochastic variables
J	Total number of stochastic variables
$s_k^{\{i,j\}}$	State of i or j at time-step k
x_k^i	Decision of controllable device i at time-step k
ω_k^j	Variation of stochastic variable j at time-step k
C_k	Cost or reward at time-step k
π	Policy
r	Realisation of random information
R	Total number of random realisations
α	Stepsize
V_k^π	Expected future cost/reward for following π from k
$s^{i,\max}$	Maximum state of a controllable device
$s^{i,\min}$	Minimum state of a controllable device

μ^i Efficiency of a controllable device [%]

l^i Losses of a controllable device per time-step

a Index of a segment in the VFA

A_k Total number of segments at time-step k

z_{ka} Capacity of a segment

$\bar{v}_{ka}$ Slope of a segment

n A particular scenario

N Total number of scenarios in stochastic MILP

Acronyms / Abbreviations

ACT Australian Capital Territory

ADP Approximate dynamic programming

AEMO Australian Energy Market Operator

ANN Artificial neural networks

DG Distributed generation

DLC Direct load control

DP Dynamic programming

DR Demand response

DSM Demand side management

ELM Extreme learning machines

EMS Energy management system

EV Electric vehicle

FDNNE Fast decorrelated neural networks ensembles

FiTs Feed-in-tariffs

HVAC Heating, ventilation and air conditioning

MAE Mean-absolute error

MILP Mixed-integer linear programming

NSW New South Wales

PFA Policy function approximation

PSO Particle swarm optimisation

PV Photovoltaic

RES Renewable energy sources

RMSE Root-mean-square error

SGSC Smart Grid Smart City

SHEMS Smart home energy management system

SOC State of charge

SVM Support vector machines

TES Thermal energy storage

ToUP Time-of-use pricing

VFA Value function approximation

Chapter 1

Introduction

Traditional electrical power systems are based on a "supply-following-demand" paradigm, where electrical power generation follows electrical power demand in real-time. This is possible because conventional thermal and hydro generation is dispatchable. However, in recent times, growing concerns about climate change because of CO_2 emissions have resulted in a movement away from fossil-fuel-based generation towards *renewable energy sources* (RES), such as wind farms, rooftop *photovoltaic* (PV) systems, and concentrated solar plants. In Australia, the aim is to increase the penetration of RES to 50% of the total generation by 2030, abreast with California, USA [1] and more examples are in Section 1.1. However, the intermittent nature of the RES means that the requirements to smooth electrical power fluctuations and balance the supply and demand in real-time will be more challenging. One technology for achieving this is by using batteries to store excess energy when the power generation from RES is high, however, batteries are very costly.

Given these insights, in order to accommodate increasing penetration of intermittent RES, several key reports [2–4] have identified the requirement for future electrical power systems to shift to a "demand-following-supply" paradigm. Also referred to as the smart grid, the aim is a more efficient, reliable and green electrical power system. A cornerstone of achieving this future electrical power grid is *demand side management* (DSM), which refers to methods of influencing the energy and peak power use of end-users of electrical power [3]. Specifically, DSM schemes provide additional capacity to the electrical power system without costly new infrastructure, which reduces both the price of electricity for end users and expenditure by network and generation utilities.

In more detail, DSM can be divided into *demand response* (DR) programs [5–8] and *direct load control* (DLC) [9]. In this research we focus on DR, which encourages customers to reduce loads during periods of critical network congestion (i.e. periods of high energy costs) or shift it to off-peak periods, as depicted in Fig 1.1, in return reducing their energy

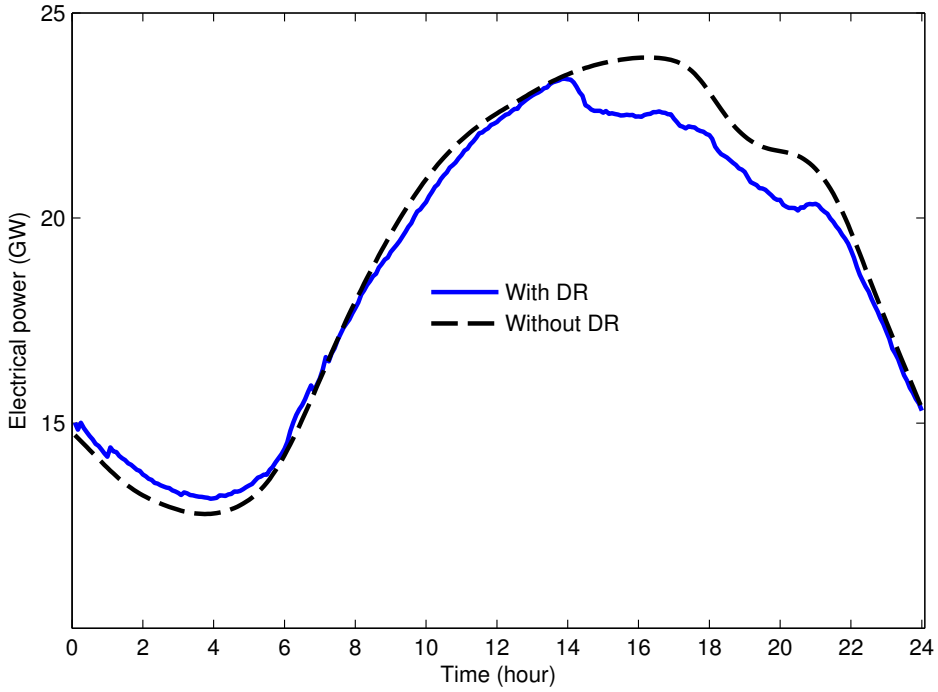

Fig. 1.1 An example of the effect on aggregated electrical demand with and without DR over a day.

costs. As shown in Fig. 1.1, DR can reduce the electrical demand during the peak periods (2 pm to 8 pm) and shift all or part of it to off peak periods (12 am to 6 am). The DR data was obtained from New England on 24th June, 2010 [10].

Currently, DR is implemented using small-scale voluntary programs and the same pricing strategy for all the customers. The main drawback of using the same pricing strategy for all the customers is the possibility of inducing unwanted peaks in the demand curve as customers respond to prices. Also, it is not possible for residential and small commercial users to directly participate in wholesale energy or ancillary services markets because of the regulatory regimes and computational requirements. As such, DR revolves around the interaction between an *aggregator* and customers, as shown in Fig. 1.2. In many cases, the retailer acts as the aggregator. The aggregator's task is to construct a scheme that coordinates, schedules or otherwise controls part of a participating user's load via interaction with its *energy management system* (EMS) [3]. In the context of DR, the aggregator sends control signals in the form of electricity price signals to the EMS. The EMS then schedules and coordinates customer's energy use to minimise energy costs while maintaining a suitable level of comfort. More details on the customer's expected benefits from an EMS are in Section 1.2.2. Given this context, EMSs in residential and commercial buildings will play a major role in DR programs, and this thesis focuses on energy management in residential

buildings because roughly 30% of the energy use in Australia is comprised of residential loads [11] and their diurnal patterns drive daily and seasonal peak loads.

In particular, this research study investigated, proposed and developed fast and efficient EMSs for smart homes that can be embedded into existing smart meters or a device with low computational power. Currently used smart meters in Australia allow customers to accurately access real-time information about their electricity consumption using an in-home display or a web portal; and can automatically send electricity data (i.e. every 30 minutes) back to the electricity distribution company for billing and load forecasting. These smart meters have limited computational power and memory. Given this, Reposit, a company that develops home EMSs in Australia, uses a Beagle board for installing their home EMSs [12]. In the future, they are planning to use a slightly higher powered Raspberry Pi board. This can be a $35 Raspberry Pi Zero with 1 GHz Broadcom BCM2835 ARM11 core processor and 512 MB of LPDDR2 SDRAM, or $69 Raspberry Pi 3 Model B that has a 1 GB RAM and 1.2 GHz Broadcom BCM2837 64-bit ARMv8 quad core processor [13].

This thesis assumes that the exact electricity price signals are available from a DR aggregator/retailer in the form of *time-of-use pricing* (ToUP). ToUP is chosen as it is prevalent in Australia [14, 15], however, the proposed EMSs (details in Section 1.4) will work under any pricing strategy. Note that this thesis does not focus on the aggregation of smart homes as it is a different research field. An interested reader can refer to [3].

1.1 Energy Management in Smart Homes

This section is divided into two parts. In the first section, the smart home considered in this thesis is presented along with the motivation for its choice. The second section discuses the benefits of a *smart home energy management system* (SHEMS) and the underlying optimisation problem.

1.1.1 Smart homes

A *smart home* is envisioned as an automated residential building that uses *distributed energy resources* (DER) for managing energy consumption and providing suitable levels of comfort to the end-user. The DER in a smart home can consist of:

- Distributed generation (DG) units, such as rooftop PV systems, fuel cells and micro-turbines;
- Energy storage units, such as a battery storage, electric vehicle (EV) battery storage and *thermal energy storage* (TES) units (i.e. hot water tank), and;

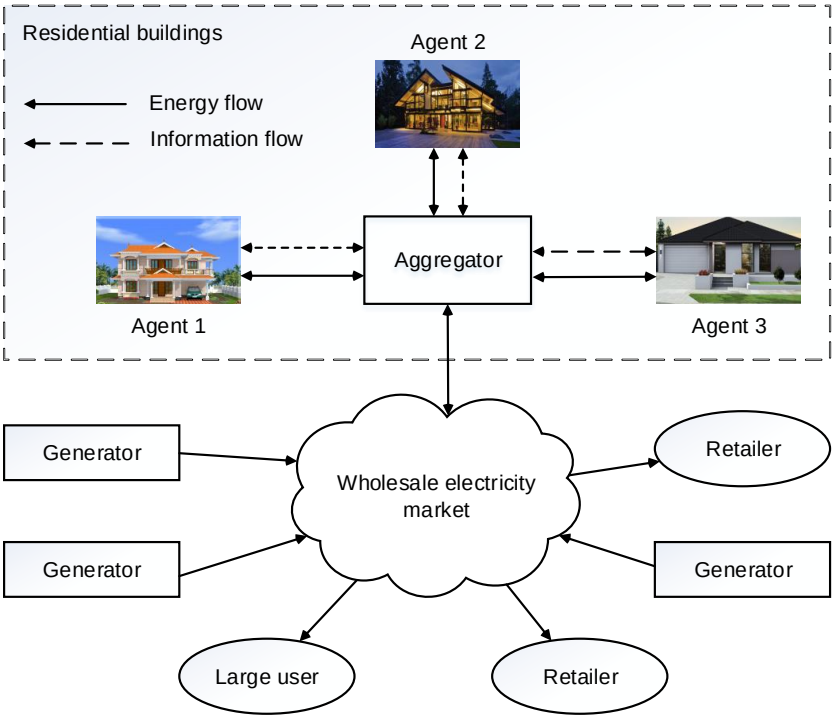

Fig. 1.2 Customers, aggregator and the wholesale electricity market.

- End-user loads, such as cyclical loads (i.e. heating, ventilation and air conditioning (HVAC) system, refrigerator and hot water heater) and shiftable loads (i.e. washing machine, dryer and dishwasher).

Specifically, the smart homes considered in this thesis comprise a PV, battery and TES units, as depicted in Fig. 1.3. In the existing literature, a range of DER have been used to achieve DR [7, 8, 5, 6, 16–22]. However, our choice stems from increasing penetration of rooftop PV and battery storage systems in Australia, New Zealand, some parts of USA and Europe, in response to rising electricity costs, government incentives, decreasing capital costs, growing concerns about climate change and existing fleet of hot water storage devices. In more detail:

- In January 2016, Australia reached 5 GW solar PV from residential and commercial users [23], while global solar PV had increased from 4 GW in 2003 to 128 GW in 2013 [24];

- Tesla Energy's Powerwall 2 batteries, which were announced in October 2016, provide a possible solution for storage in residential buildings [25]. A comparison with other price-competitive batteries is in [26];

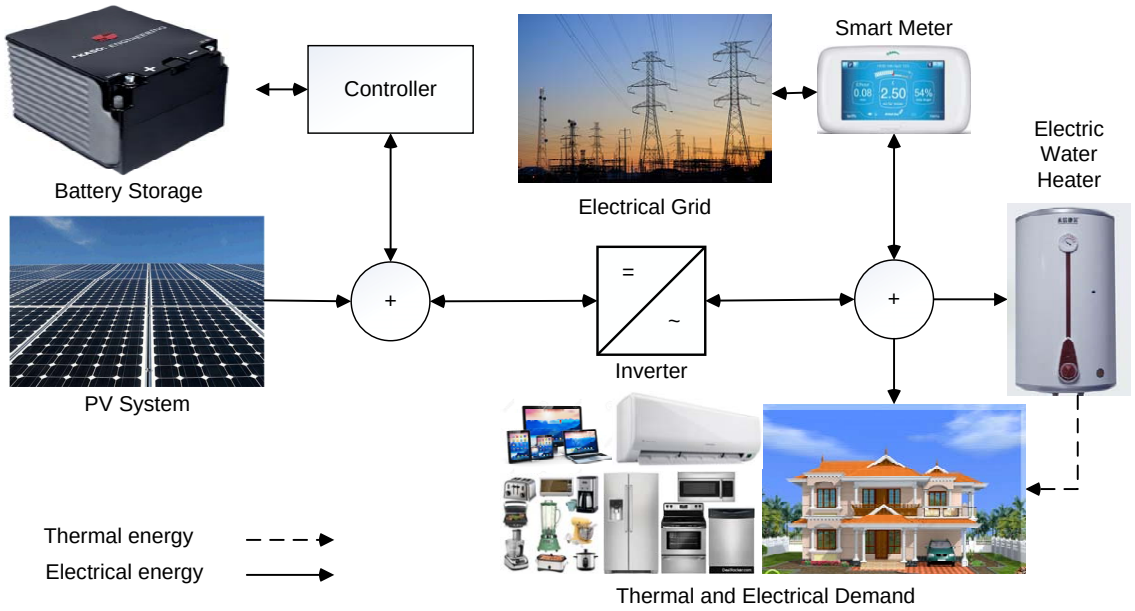

Fig. 1.3 Illustration of electrical and thermal energy flows in a smart home.

- Australian Capital Territory (ACT) government recently opened auctions to provide financial support for the installation of 36 MW of battery storage that will support solar PV installed in residential and commercial buildings in ACT [27].
- According to the Australian Energy Market Operator (AEMO), the payback period for residential PV-storage systems is already below 15 years in South Australia, with the other states to follow suit in less than a decade [28];
- Residential users with PV-storage systems in the USA have been forecast to reach grid parity within the next decade [4];
- Vector, a distribution company in New Zealand has a package to install solar panels with Tesla Energy's Powerwall batteries in residential buildings. They even offered it free to 100 residential buildings [29];
- Germany offers incentives to residential users who install PV-storage systems, which is now extended until 2018 [30].

In a similar vein, Ausgrid, a distribution company in New South Wales (NSW), Australia and their consortium partners recently completed *Smart Grid Smart City* (SGSC) project, which investigated the benefits and costs of implementing a range of smart grid technologies in Australian households [31]. This involved collecting PV and electrical and thermal demand data from a range of residential buildings in Sydney, Newcastle, and Central Coast regions of

NSW. The PV and demand data from data sets collected during this SGSC project [32] are use to estimate future PV and demand models using an hierarchical approach, in Chapter 2.

1.1.2 Smart home energy management systems (SHEMSs)

An illustration of electrical and thermal energy flows in the smart home considered in this thesis is depicted in Fig. 1.3. In order to maximise the benefits of PV-storage systems, it is assumed that residential energy users will use an automated SHEMS to schedule and coordinate their energy use. This is for the following reasons:

- When the PV generation is higher than the electrical demand, extra electrical power will be either stored, consumed by shiftable and controllable loads or/and fed back to the electrical grid. However, in Australia, selling power back to the electrical grid is uneconomical since retail feed-in tariffs (FiTs) are significantly less than the retail tariffs paid by the households. In some countries, the FiT for small generators (such as households) acts as a generation subsidy, rather than a grid export subsidy [33]. Coupled with ever dropping PV costs, there is a strong incentive for PV owners to self-consume as much locally generated power as possible. Our conjecture is that in the near future this may happen in other parts of the world too.

- Time varying pricing methods, such as ToUP means that the users will want to operate the battery and TES in such a way that their *state of charge* (SOC) is maximised at the beginning of time periods with peak price signals.

- An automated SHEMS can control the PV-storage system to achieve demand response [7, 8, 5, 6, 3] or direct load control[3, 9] on behalf of customers but without human interaction.

The underlying optimisation problem undertaken by the SHEMS can be thought of as a sequential decision making process under uncertainty. The specific formulation of the SHEMS problem is detailed in Chapter 2. The problem contains stochastic variables, such as PV output and electrical and thermal demand. Typical variations of the PV output and electrical demand from estimates of these variations are shown as error bars in Fig. 1.4. These variations in the electrical demand depends on the customers' behaviour, which varies for different days. Similarly, the variations in the PV output depends on the type of day (i.e sunny, normal or cloudy). For example on a sunny day there is a higher probability of PV output decreasing than increasing, and the converse is true for cloudy days. Given this, a first major focus of this thesis is to consider these stochastic variables, using appropriate

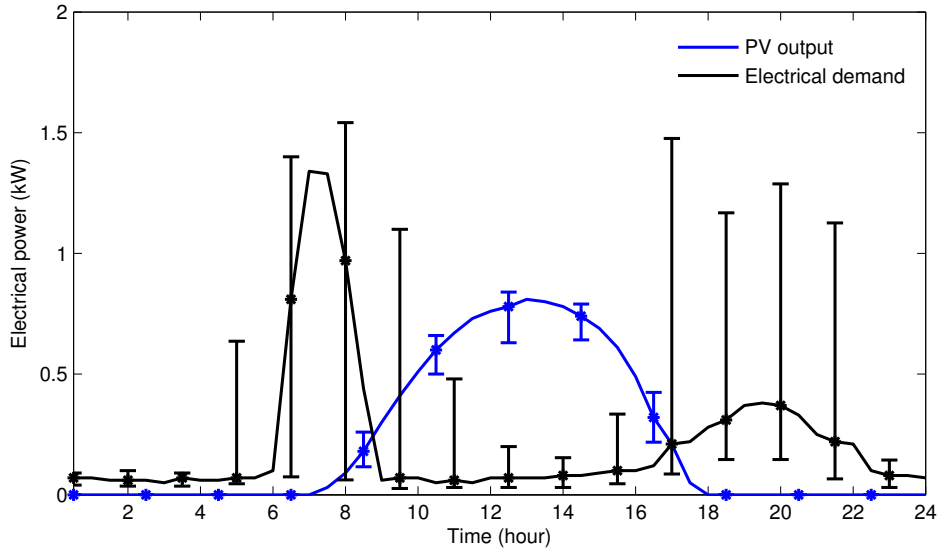

Fig. 1.4 The PV output and electrical demand over a day (error bars as 10^{th} and 90^{th} percentiles).

probability distributions, which is expected to yield better quality schedules compared to ones obtained from deterministic optimisations using off-the-shelf solvers [34].

In the literature, the start-of-day and end-of-day battery SOC are often assumed to be the same [35, 36] and its value is set to 50% of the battery capacity in [36] and 30% in [35]. On days with a medium to high evening demand, having the minimum battery SOC at the end of the day gives the best results because the battery can be used to supply the evening demand and there is no need to charge it back. This means the next day's electricity cost can significantly increase if anticipating a high morning demand and low PV output. Because of such situations, it is beneficial to capture inter-daily variations in consumption and solar-insolation patterns over several days [37], either by extending the decision horizon or controlling the end-of-day battery SOC of the SHEMS problem, which is a second major focus of attention in this thesis.

Against this background, next section explain in detail the requirements of a suitable solution technique that can be use to implement a SHEMS.

1.2 Requirements

Overall, we need a computationally efficient SHEMS that minimises a household's energy costs while maintaining a suitable level of user comfort. Moreover, the SHEMS should be able to integrate into an existing smart meter or a similar device with low computational power. This requires a solution technique that can achieve the following with low computational burden:

- Integrate additional DER to a PV-battery system, such as a EV battery, TES unit and controllable loads;
- Incorporate the stochastic nature of the input variables using appropriate probabilistic models;
- Consider uncertainties over several days by extending the decision horizon of the SHEMS problem. To illustrate this, consider a few sunny days with low demand (e.g. a weekend) followed by a few cloudy days with high demand; in anticipation of this, the SHEMS may adjust the end-of-day battery SOC to reap significant financial benefits. Note that adjusting the end-of-day battery SOC using an extended decision horizon and fixing the end-of-day battery SOC of a daily optimisation to capture future uncertainties are two different approaches investigated in Chapter 5 and Chapter 4, respectively.

Moreover, the SHEMS problem is highly stochastic in nature (i.e. the actual and estimated PV output and demand are different most of the time) so we can not always rely on fixed schedules for the DER obtained before the decision horizon. Instead, the SHEMS needs to make real-time decisions without having to solve an entire optimisation problem that is computationally expensive or requires user interaction. Finally, the SHEMS should be implemented using an anytime optimisation solution technique, so that it always gives a solution regardless of the constraints and the input parameters, which avoids the necessity for user interaction. Note that an anytime algorithm is an algorithm that returns a feasible solution even if it is interrupted prematurely. The quality of the solution, however, improves if the algorithm is allowed to run until the desired convergence.

Next, a review of the existing solution techniques that can solve this sequential stochastic decision making problem is presented.

1.3 Solution Techniques

First, a review of the existing solution techniques used to solve the SHEMS problem and their drawbacks are presented. Second, the four fundamental classes of policies that can be applied to any stochastic optimisation problem is presented [38].

1.3.1 Existing solution techniques

Currently, proposed methods for implementing a SHEMS include:

- Mixed-integer linear programming (MILP) [34, 39–46],
- Particle swarm optimisation (PSO) [47, 35, 48–52],
- Dynamic programming (DP) [53–55].

These methods are discussed below. First, MILP optimises a linear objective function subject to linear constraints with continuous and integer variables. In order to use MILP, the constraints have to be linearised and the sequential stochastic optimisation problem has to be formulated as a mathematical programming problem (more details in Chapter 2 and 3). As presented in [39, 40, 45], MILP is widely used in SHEMSs mainly because of the simplicity associated with off-the-shelf MILP solvers, such as CPLEX, MATLAB, AMPL and MOSEK. However, MILP does not consider the uncertainties in a household's energy use and the intermittent nature of its DG. MILP can incorporate the stochastic variables by using a scenario-based approach [56]. A comparison of a scenario based stochastic and deterministic optimisations using MILP is presented in [34]. The paper concluded that stochastic optimisation has the better quality solutions as it considers the uncertainties in the household. However, the energy management problem becomes computationally challenging as the number of scenarios increases. More drawbacks associated with MILP are as follows:

- The whole SHEMS problem is solved at once so the computational time increases exponentially as the number of decision variables increases. This means:
  - The number of controllable devices that we can include is limited;
  - The length of the decision horizon is limited to one day in a SHEMS with larger number of controllable devices, which means we can not consider uncertainties over several days.
- It is computationally difficult to solve the entire stochastic optimisation problem at every time-step using existing smart meters. Note that the PV output and electrical and thermal demand are hard to estimate accurately in real world, so there is a strong requirement to solve either the entire optimisation problem or a part of it at each time-step.
- Any non-linear constraints will have to be linearised when using MILP, as depicted in Fig. 1.5, which results in lower quality schedules (device constraints are listed in detail in Chapter 2 and comparisons are in Chapter 3). Note that a piecewise linear approximations of the non-linear constraints will result in further increase in the computational burden.

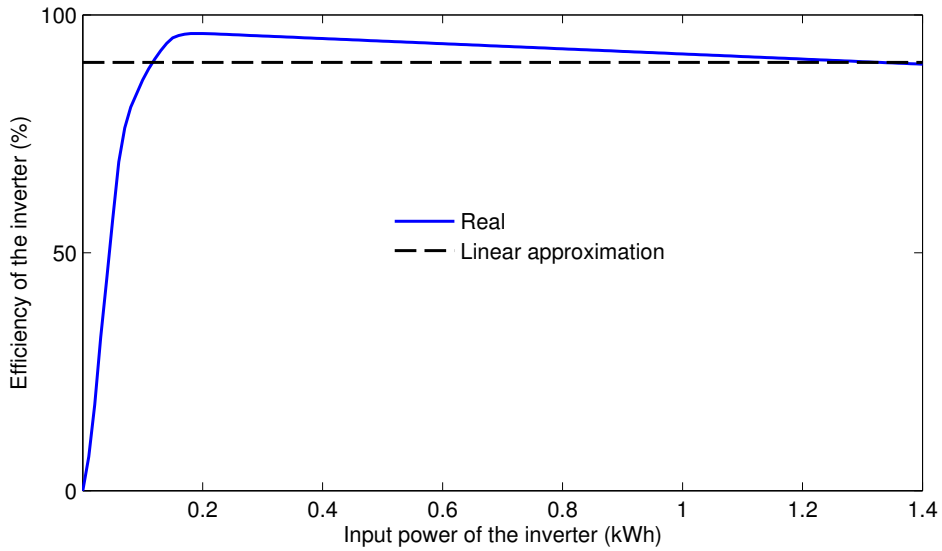

Fig. 1.5 The non-linear inverter efficiency is approximated by a linear function.

- MILP fails to find a solution when the constraints are not satisfied. From our experience, this often happens when the end-of-day TES SOC is fixed, because the energy out of the TES unit can not be controlled, which is the thermal demand of the household. We can overcome this by either removing the end-of-day TES constraint or by having a range of values. However, this means we end up with a sub-optimal level of TES SOC at the end-of-day or require user interaction to adjust the end-of-day TES SOC, which we should avoid in practical applications (more details in Chapter 3).

Second, PSO is a population-based stochastic optimisation technique, which is inspired by social behaviour of bird flocking or fish schooling [57]. In [47, 35, 48], PSO is used for robust scheduling of the DERs in a smart home. However, these papers do not consider the stochastic variables of the SHEMS problem. Robust scheduling of DERs with stochastic programming using scenario-based PSO is presented in [48], which is computationally difficult and the accuracy of the results depends on the selection method used for reducing the number of scenarios. More drawbacks associated with PSO are as follows:

- The PSO approach is a local search heuristic technique so we might end up in the local optimum instead of the global optimum. This means we can never ascertain the quality of the solutions.

- Similar to MILP, the number of decision variables increases as the length of the decision horizon and the number of controllable devices increases. This means the computational time increases because the number of iterations needed to reach reasonably quality solutions increases.

- Similar to MILP, it is computationally difficult to solve the entire stochastic optimisation problem at every time-step using existing smart meters.

Third, DP is used to implement a SHEMS in [53]. Here the sequential stochastic optimisation problem is modelled as a *Markov decision process* (MDP) and solved by computing a value function using the Bellman optimality condition. A value function consists of the expected future cost of following a policy from every state (more details are given in Chapter 3). This approach considers the non-linear constraints and the stochastic variables of the household. Note that the DP approach gives close-to-optimal solutions when the state, decision and outcome spaces are finely discretised. More benefits of using DP in SHEMSs are explained in Section 1.4 and Chapter 3, as a contribution of this thesis. However, the computational complexity of DP increases exponentially with dimensionalities of state, outcome and action spaces, making it impractical in large-scale or long-horizon problems. One way of overcoming this problem is to approximate the value function, while maintaining the benefits of DP. We can approximate the value functions using *approximate dynamic programming* (ADP), which is the special focus of attention in Chapter 5.

Given these insights, the aim is to find a solution technique that is computationally efficient compared to DP but that returns similar quality solutions.

1.3.2 Four classes of policies

In order to map the space of alternative approaches to SHEMSs, we now review four fundamental classes of policies for stochastic optimisations. Following [38], there are four fundamental classes of policies that can be applied to any stochastic optimisation problem are:

1. Myopic policies,
2. Lookahead policies,
3. *Policy function approximations* (PFAs),
4. Policies based on *value function approximations* (VFAs).

These policies are described below. First, myopic policies optimise costs/rewards of the current time-step without considering the impact on future decisions. One way to improve myopic policies is to include a tunable parameter to capture the future information. These are called cost function approximations (CFAs), which are widely used in high dimensional resource allocation problems where we can get desired behavior by manipulating the cost

function. This thesis does not consider CFAs as they provide lower quality solutions compared to the below methods in energy storage problems [38].

Second, lookahead policies make decisions in the current time-step using an approximation of the future information. The future information can be found by solving a deterministic optimisation over a longer decision horizon. According to [38], lookahead policies work best for a time-dependent problem with daily load, energy and price patterns, relatively low noise and very accurate forecasts [38]. The proposed approach in Chapter 4 is a two-stage lookahead, which uses a deterministic MILP approach to approximate the end-of-day battery SOC of a more detail daily DP optimisation. The future uncertainties are captured in the end-of-day battery SOC.

Third, PFAs are look-up tables, parametric models and non-parametric models that return a decision for a given state without having to solve an optimisation problem. PFAs are most suitable for stationary problems with unknown price signals that are variable throughout the day, relatively low noise and moderately accurate forecasts [38]. Chapter 6 of this thesis proposes a PFA algorithm, which uses a suitable non-parametric technique to make fast real-time decisions. The non-parametric learning technique can be *extreme learning machines* (ELM), which is developed in [58], *artificial neural networks* (ANN) [59], *support vector machines* (SVM) [60] and *fast decorrelated neural network ensembles* (FDNNE) [61].

Fourth, VFAs are the policies that are often associated with DP and ADP, and obtained using the Bellman optimality condition. The VFAs work best in time-dependent problems with regular load, energy and price patterns, relatively high noise and less accurate forecasts (errors grow with the horizon) [38]. This thesis implements a DP based SHEMS in Chapter 3 and proposes an ADP approach with *temporal difference learning* in Chapter 5 to overcome the computational burden of DP but with similar quality solutions. This ADP approach has successfully been applied for the control of grid level storage in [62]. Other ADP methods are better suited to applications with different characteristics [63–73].

The next section presents the details of the three proposed fast solution techniques that falls into lookahead policies, PFAs and policies based on VFAs. According to [38], VFAs are the most suited to solve the SHEMS problem, followed by PFAs.

1.4 Contributions and the Scope of the Thesis

As residential PV-storage systems are becoming more popular, this research study investigated, proposed and developed fast solution techniques for energy management in smart homes. Note that as mentioned before, we need a computationally feasible SHEMS that can efficiently minimise energy costs while maintaining a suitable level of user comfort, and the

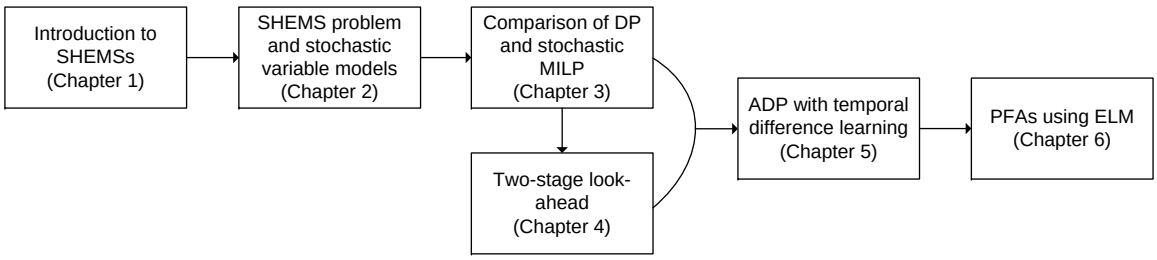

Fig. 1.6 The summary of contributions and how the chapters are structured.

smart home considered in this thesis comprise of PV, battery and TES units. Given this, the contributions of this thesis are summarised in Fig. 1.6, and explained in more detail below:

The first contribution is an hierarchical approach to estimate PV and demand models using empirical data (Chapter 2). In brief, we first cluster empirical data into different day types and then estimate PV and demand models using kernel regression. The draws from the kernel estimates within a day type are independent so the clustering is done to capture inter-daily variations in the PV and demand profiles. The benefits of these estimations are as follows:

- It conforms with the MDP construction, which is needed to solve the SHEMS problem using DP and ADP;
- In practical applications user will only need to choose the type of day for demand and PV output compared to having to estimate the entire days PV and demand profiles using PV [74] and demand prediction algorithms [75, 76].

The second contribution is a comparison of SHEMSs using a scenario based MILP approach, which is referred to as stochastic MILP in [56], and DP (Chapter 3) and guidelines for their practical implementations. In summary, DP approach generates value functions for every time-step during the offline planning phase. Note that a value function consists of the expected future cost of following a policy from every state. Once we have the value functions, we can make faster online solutions using the Bellman optimality condition (more details in Chapter 3). This idea of making fast on-line solutions using a value function has significant benefits in practical applications. They are as follows:

- Computationally easy to solve a simple linear problem compared to having to solve an entire optimisation problem.
- In case of a DR event or high electricity price signal at a certain time-step, the battery will discharge its maximum possible power to the household. From the next time-step, battery operation will continue to be optimal regardless of what happened in the previous time-step.

- The user will have more flexibility to use controllable loads. In detail, under ToUP, the controllable loads can be used at any time as long as the user does not exceed the battery discharge limit during peak periods.

Moreover, we can always obtain a solution with DP regardless of the constraints and the inputs while MILP fails to find a solution when constraints are violated. However, it is computationally difficult to extend the decision horizon, consider stochastic nature or incorporate additional controllable devices with DP as we have to loop around all the possible combinations of state and outcome spaces. Note that we do not have to loop over all the possible decisions in our problem, which is achieved using a matrix operation in MATLAB (evident in Chapter 3).

The third contribution is a multi-stage lookahead stochastic optimisation framework to explore the benefits of using an extended decision horizon. This is a two-stage lookahead optimisation, which uses deterministic MILP to solve a longer decision horizon and its end-of-day one battery SOC is used in a daily DP (Chapter 4) [37]. The two-stage lookahead is expected to work well only when the forecasts are accurate because we resort to deterministic MILP. Note that extending the decision horizon is computationally difficult using DP or stochastic MILP. This means a stochastic optimisation technique that enables us to extend the decision horizon with less computational burden is needed.

Given these insights, the fourth contribution is an ADP approach with temporal difference learning to overcome the computational burden of DP but with similar quality solutions (Chapter 5) [77, 78]. ADP enables us to:

- incorporate stochastic nature of the input variables without a noticeable increase in the computational burden;
- extend the decision horizon with less computational burden to consider uncertainties over several days, which results in significant financial benefits;
- enable integration of multiple controllable devices with less computational burden;
- integrate the SHEMS into an existing smart meter as it uses less computer memory compared to existing methods.

Although ADP is computationally fast compared to DP and stochastic MILP, it still takes a considerable amount of time to compute value functions.

Given this, the fifth contribution is a PFA algorithm that can use non-parametric learning techniques, such as ELM, ANN, SVM and FDNNE, to make fast online decisions (Chapter 6). In the off-line planning phase, the training data is clustered into different day types and then

a non-parametric learning technique is used to quickly learn a model that maps inputs and output decisions. These models can be used in real-time to make fast online solutions, which is approximately the same speed as with making decisions using VFAs. The computational simplicity of PFAs over VFAs using ADP is only for the off-line planning phase. The PFA models of different day-types can be used over a longer period of time (i.e. months) without updating and it will still results in similar quality solutions. The training data set can be generated by solving the deterministic SHEMS problem over couple of years. A powerful cloud or home computer can be used for this task as we only have to do it once.

Throughout the thesis, the benefits of PV-storage systems coupled with a SHEMS are highlighted using real data collected during SGSC project. Specifically, the benefits of a PV-battery system and PV-battery-TES system are shown separately. Note that the benefits of a TES unit coupled with a PV-battery system has not been done before using real data. Furthermore, the comparisons of DP, stochastic MILP and our proposed techniques such as ADP with temporal difference learning, two-stage lookahead and PFAs using ELM, ANN, SVM and FDNNE will be helpful in the future when finding a suitable technique to implement a fast and an efficient SHEMS. A summary of these techniques are in Fig. 1.7. MATLAB is used to implement all the SHEMS on a computer with a Intel(R) Core(TM) i5-3470 CPU @3.2 Ghz processor and 16 GB RAM.

The thesis is structured into 7 chapters (see Fig. 1.6) as follows:

- Chapter 2 is divided into two parts. The first part presents a general formulation of a sequential stochastic optimisation problem and then formulate the smart home energy management problem as a sequential stochastic optimisation problem. This includes the state, decision and stochastic variables, constraints and all the simulation parameters used through out the thesis. The second part estimates the stochastic variable models using an hierarchical approach that first clusters empirical data and then estimate probability distributions using kernel regression. These stochastic variables are used in the subsequent chapters.

- Chapter 3 first explains the implemented SHEMSs using stochastic MILP and DP. Second, presents comparisons of deterministic and stochastic DP and MILP. These implemented SHEMS are used in Chapter 4 and as a benchmark in the subsequent chapters.

- Chapter 4 presents the two-stage lookahead stochastic optimisation framework for considering uncertainties over a longer decision horizon. The two-stage lookahead uses deterministic MILP to solve the longer decision horizon and DP to solve the daily

	ADP (Chapter 5)	DP (Chapter 3)	Two-stage lookahead (Chapter 4)	PFA using ELM (Chapter 6)	Stochastic MILP (Chapter 3)
Non-linear constraints	Yes	Yes	Yes	Yes	No Linear constraints
Probability distributions	Yes	Yes	Yes	Not needed	Yes
Solution quality (accurate forecasts)	Good	Good	Good	Reasonably good	Reasonably good
Solution quality (less accurate forecasts)	Good	Good	Good, but can get worse with forecast error	Good, no impact from forecast errors	Not good, unless problem solved at every time-step
Computational burden offline planning	Medium	High	High	Low	Medium
Computational speed online phase	Fast	Fast	Fast	Fast	Need to solve the entire problem
User interaction	Not needed	Not needed	Not needed	Not needed	Yes, if the MILP solver can' not find a solution
PV and demand models	Needed	Needed	Needed	Not needed	Needed
Anytime algorithm	Yes	No	No	Not an issue	No

Fig. 1.7 A summary of ADP, DP, two-stage lookahead, stochastic MILP and PFAs using ELM employed for implementing a SHEMS.

horizon. Here the two-stage lookahead is benchmarked against a one-stage daily DP approach.

- Chapter 5 presents the proposed computationally efficient ADP approach with temporal difference learning and practical guidelines for its implementation. In order to show the performance of ADP, we use it with a two-day decision horizon over three years using a rolling horizon approach where the expected electricity cost of each day is minimised considering the uncertainties over the next day. The daily performance is benchmarked against DP and stochastic MILP by applying them to three different scenarios with different electrical and thermal demand patterns and PV outputs. The three year evaluation is benchmarked against daily DP and stochastic MILP approaches by applying it to ten smart homes.

- Chapter 6 first describes the strategies used in PFAs and then explains the ELM algorithm. The implementation section presents the proposed PFA algorithm, which can be used in conjunction with any learning method. The simulation results section compares PFAs using ELM, ANN, SVM and FDNNE with ADP, DP, stochastic MILP and the two-stage lookahead.
- Chapter 7 summarises the conclusions reached in the thesis.

Chapter 2

Smart Home Energy Management Problem and Stochastic Variable Models

This chapter presents the SHEMS problem and the inputs to the algorithms derived later. The chapter is divided into two parts. The first is to present the SHEMS problem for the DER considered in this thesis, which comprise a PV unit, battery, and TES unit. The second is to present the hierarchical approach use to estimate the stochastic variable models, such as the PV output and electrical demand.

In more detail, Chapter 2 is structured as follows: First section describes the general formulation of the sequential stochastic optimisation problem (Section 2.1). Second section formulates the stochastic SHEMS problem as a sequential stochastic optimisation problem (Section 2.2). Third section explains the effects of stochastic variables on the SHEMS problem and presents the hierarchical approach use to estimate the stochastic variable models (Section 2.3). Fourth section estimates PV and demand models of eight scenarios, which consists of four days each for two residential buildings (Section 2.4). These PV and demand models will be used in later chapters.

2.1 General Sequential Stochastic Optimisation Problem

A sequential stochastic optimisation problem comprises:

- *A sequence of time-steps*, $\mathcal{K} = \{1 \dots k \dots K\}$, where k and K denote a particular time-step and the total number of time-steps in the decision horizon, respectively.
- *A set of non-controllable inputs,* $\mathcal{J} = \{1 \dots j \dots J\}$, where each j is represented using:
    - A state variable, $s_k^j \in \mathcal{S}$.

- A random variable, $\omega_k^j \in \Omega$, capturing exogenous information or perturbations.

• *A set of controllable devices,* $\mathcal{I} = \{1 \dots i \dots I\}$, where each i is represented using:

- A state variable, $s_k^i \in \mathcal{S}$;
- A decision variable, $x_k^i \in \mathcal{X}$, which is a control action;
- Constraints for the state and control variables;
- A transition function $s_{k+1}^i = \mathbf{s}^M \left(s_k^i, x_k^i, \omega_k^j \right)$, describing the evolution of a state from k to $k+1$, where $s^M(.)$ is the system model that consists of controllable device i's operational constraints such as power flow limits, efficiencies and losses.

Given this, let: $\mathbf{s}_k = [\ s_k^i \dots s_k^I, s_k^j \dots s_k^J\ ]^\mathsf{T}$, $\mathbf{x}_k = [\ x_k^i \dots x_k^I\ ]^\mathsf{T}$, and $\omega_k = [\ \omega_k^j \dots \omega_k^J\ ]^\mathsf{T}$. The state variables contain the information that is necessary and sufficient to make the decisions and compute costs, rewards and transitions. The compact form of the transition functions is given as $\mathbf{s}_{k+1} = \mathbf{s}^M(\mathbf{s}_k, \mathbf{x}_k, \omega_k)$. Note that in our problem transition functions are only required for the controllable devices and ω_k (without a superscript) is the combined random variables vector of the non-controllable inputs.

• *An objective function:*

$$F = \mathbb{E}\left\{ \sum_{k=1}^{K} C_k(\mathbf{s}_k, \mathbf{x}_k, \omega_k) \right\}, \tag{2.1}$$

where $C_k(\mathbf{s}_k, \mathbf{x}_k, \omega_k)$ is the contribution (i.e cost or reward of energy, or a discomfort penalty) incurred at time-step k, which accumulates over time.

2.2 Instantiation

The objective of the SHEMS is to minimise energy costs over a decision horizon. The sequential stochastic optimisation problem is solved before the start of each day, using either a daily or a two day decision horizon. This thesis considers a system consisting of a PV unit, battery and a hot water system (TES unit), as depicted in Fig. 2.1. A single inverter is used for both the battery and the PV, which is becoming popular in Australia.

In order to optimise performance, a SHEMS needs to incorporate the variations in PV output, electrical and thermal demand of the household. Given this, the stochastic variables are modelled using their mean as state variables and variation as random variables.

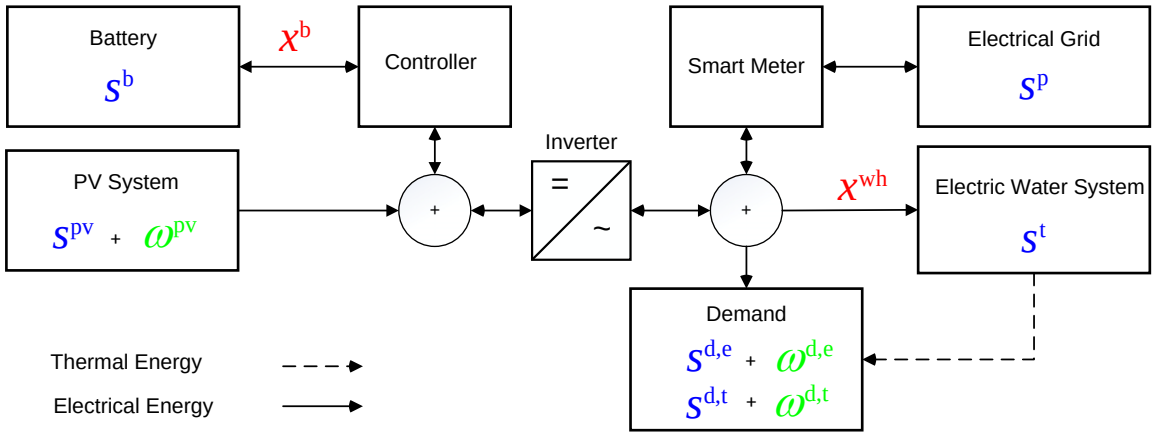

Fig. 2.1 Illustration of electrical and thermal energy flows in a smart home, and the state, decision and random variables use to formulate the problem.

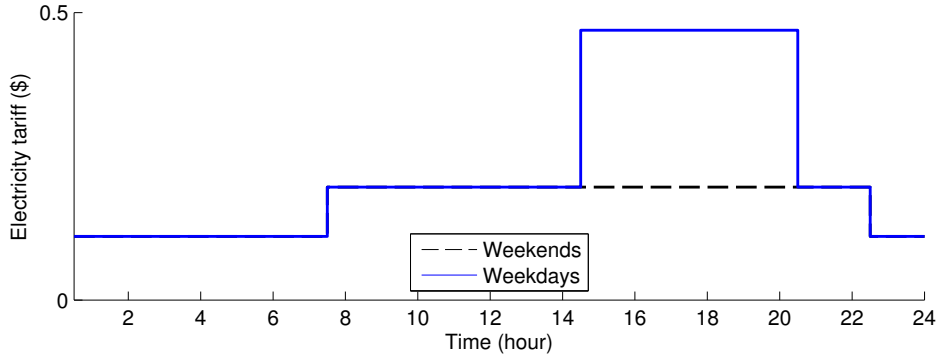

Fig. 2.2 The time-of-use electricity tariff over a day for all the scenarios.

This enabled the use of an algorithmic strategy that separates the transition function into a deterministic term, using the mean, and a random term, using variation (discussed in Chapter 5). In some cases, electricity prices may be considered as a stochastic variable. However, this thesis assumes that the exact electricity prices are available before the start of the decision horizon from an residential DR aggregator/retailer in the form of ToUP (time-of-use pricing), as shown in Fig. 2.2. Given this, there is no random variable associated with the electricity tariff.

In more detail, we cast our SHEMS problem as the sequential stochastic optimisation formulation in Section 2.1 as follows:

- The daily decision horizon is a 24 hour period, divided into $K = 48$ time-steps with a 30 minutes resolution. We do this similarly for the two day decision horizon. Here 30 minutes time resolution is chosen to match with typical dispatch time lines because the PV and demand data from the SGSC project [32] are only available at 30 minutes

intervals. If required, the proposed ADP approach can increase the time resolution with less computational burden compared to existing methods.

- The non-controllable inputs are the PV output, the electrical and thermal demand, and electricity tariff, which are represented using:
  - State variables for the mean PV output, s_k^{pv}, mean electrical demand, $s_k^{\mathrm{d,e}}$, mean thermal demand, $s_k^{\mathrm{d,t}}$, and electricity tariff, s_k^{p}.
  - Random variables for the variations in PV output, ω_k^{pv}, variations in thermal demand, $\omega_k^{\mathrm{d,t}}$, and variations in electrical demand, $\omega_k^{\mathrm{d,e}}$. We use empirical data to estimate the probability distributions associated with the uncertain variables using kernel regression, which are more realistic than assuming parametric approaches (discussed in detail in Section 3.3).
- The controllable devices are the battery and the TES, which are represented using:
  - State variables for the battery SOC, s_k^{b}, and TES SOC, s_k^{t}.
  - Control variables for charge and discharge rates of the battery, x_k^{b} and electric water heater input, x_k^{wh}.

    Given this, $\mathbf{x}_k = [x_k^{\mathrm{b}}, x_k^{\mathrm{wh}}]$, $\mathbf{s}_k = [s_k^{\mathrm{b}}, s_k^{\mathrm{t}}, s_k^{\mathrm{d,e}}, s_k^{\mathrm{pv}}, s_k^{\mathrm{d,t}}, s_k^{\mathrm{p}}]$, and $\omega_k = [\omega_k^{\mathrm{pv}}, \omega_k^{\mathrm{d,e}}, \omega_k^{\mathrm{d,t}}]$, are defined for each time-step, k, in the decision horizon, as depicted in Fig. 2.1.
  - The energy balance constraint is given by:

$$s_k^{\mathrm{d,e}} + \omega_k^{\mathrm{d,e}} + x_k^{\mathrm{wh}} = \mu^{\mathrm{i}} x_k^{\mathrm{i}} + x_k^{\mathrm{g}}, \tag{2.2}$$

    where x_k^{g} is the electrical grid power; μ^{i} is the efficiency of the inverter (note that the efficiency is $1/\mu^{\mathrm{i}}$ when the inverter power is negative); and x_k^{i} is the inverter power at the DC side (positive value means power into the inverter), given by:

$$x_k^{\mathrm{i}} = s_k^{\mathrm{pv}} + \omega_k^{\mathrm{pv}} - \mu^{\mathrm{b}} x_k^{\mathrm{b}}, \tag{2.3}$$

    where $\mu^{\mathrm{b}} \in \{\mu^{\mathrm{b+}}, \mu^{\mathrm{b-}}\}$ is the efficiency of the battery action corresponding to either charging ($1/\mu^{\mathrm{b+}}$ as power flows into the battery) or discharging. The charge rate of the battery is constrained by the maximum charge rate $x_k^{\mathrm{b+}} \leq \gamma^c$ and discharge rate of the battery is constrained by the maximum discharge rate $x_k^{\mathrm{b-}} \leq \gamma^d$. The electric water heater input should never exceed the maximum possible electric water heater input $x_k^{\mathrm{wh}} \leq \gamma^{\mathrm{wh}}$. In order to satisfy thermal demand at all time-steps, we make sure that the TES has enough energy at each time-step,

$s_k^{\mathrm{t,req}}$ to satisfy thermal demand for the next 2 hours. We do this because there are no instant hot water systems in practical application. Therefore, the energy stored in the TES is always within the limits:

$$s^{\mathrm{t,req}} \leq s_k^{\mathrm{t}} \leq s^{\mathrm{t,max}}. \tag{2.4}$$

The energy stored in the battery should be within the limits $s^{\mathrm{b,min}} \leq s_k^{\mathrm{b}} \leq s^{\mathrm{b,max}}$.

- Transition functions govern how the state variables evolve over time. The battery SOC, denoted $s_k^{\mathrm{b}} \in [s^{\mathrm{b,min}}, s_k^{\mathrm{b,max}}]$, progresses by:

$$s_{k+1}^{\mathrm{b}} = \left(1 - l^{\mathrm{b}}(s_k^{\mathrm{b}})\right)\left(s_k^{\mathrm{b}} - x_k^{\mathrm{b\text{-}}} + \mu^{\mathrm{b+}} x_k^{\mathrm{b+}}\right), \tag{2.5}$$

where $l^{\mathrm{b}}(s_k^{\mathrm{b}})$ models the self-discharging process of the battery. The TES SOC is denoted $s_k^{\mathrm{t}} \in [s^{\mathrm{t,req}}, s_k^{\mathrm{t,max}}]$, and evolves according to:

$$s_{k+1}^{\mathrm{t}} = \left(1 - l^{\mathrm{t}}(s_k^{\mathrm{t}})\right)\left(s_k^{\mathrm{t}} - s_k^{\mathrm{d,t}} - \omega_k^{\mathrm{d,t}} + \mu^{\mathrm{wh}} x_k^{\mathrm{wh}}\right), \tag{2.6}$$

where $l^{\mathrm{t}}(s_k^{\mathrm{t}})$ models the thermal loss of the TES and μ^{wh} is the efficiency of the electric water heater.

The discharge efficiency of the battery, efficiency of the inverter and the maximum possible charge rate with respect to the battery SOC are non-linear. The different ways that the stochastic MILP, DP and ADP approaches represent them are illustrated in Fig 2.3. These indicate that DP and ADP can directly incorporate non-linear characteristics, while linear approximations have to be made with stochastic MILP. The remaining device characteristics for the implemented SHEMSs in this thesis are as follows: the charging efficiency of the battery is $\mu^{\mathrm{b+}} = 1$; the maximum and minimum battery SOC are 2 kWh and 10 kWh, respectively; the maximum charge and discharge rates of the battery are 2 kWh; electric water heater efficiency is $\mu^{\mathrm{wh}} = 0.9$ while its maximum possible input is 3 kWh; and TES limit is set to 12 kWh. The losses of both the battery and the TES are 0.01 kWh. All of these parameters are given in Table 2.1.

- The optimal policy, π^*, is a choice of action for each state $\pi : \mathcal{S} \to \mathcal{X}$, that minimises the expected sum of future costs over the decision horizon; that is:

$$F^{\pi^*} = \min_{\pi^*} \quad \mathbb{E}\left\{\sum_{k=0}^{K} C_k(\mathbf{s}_k, \pi(\mathbf{s}_k), \omega_k)\right\}, \tag{2.7}$$

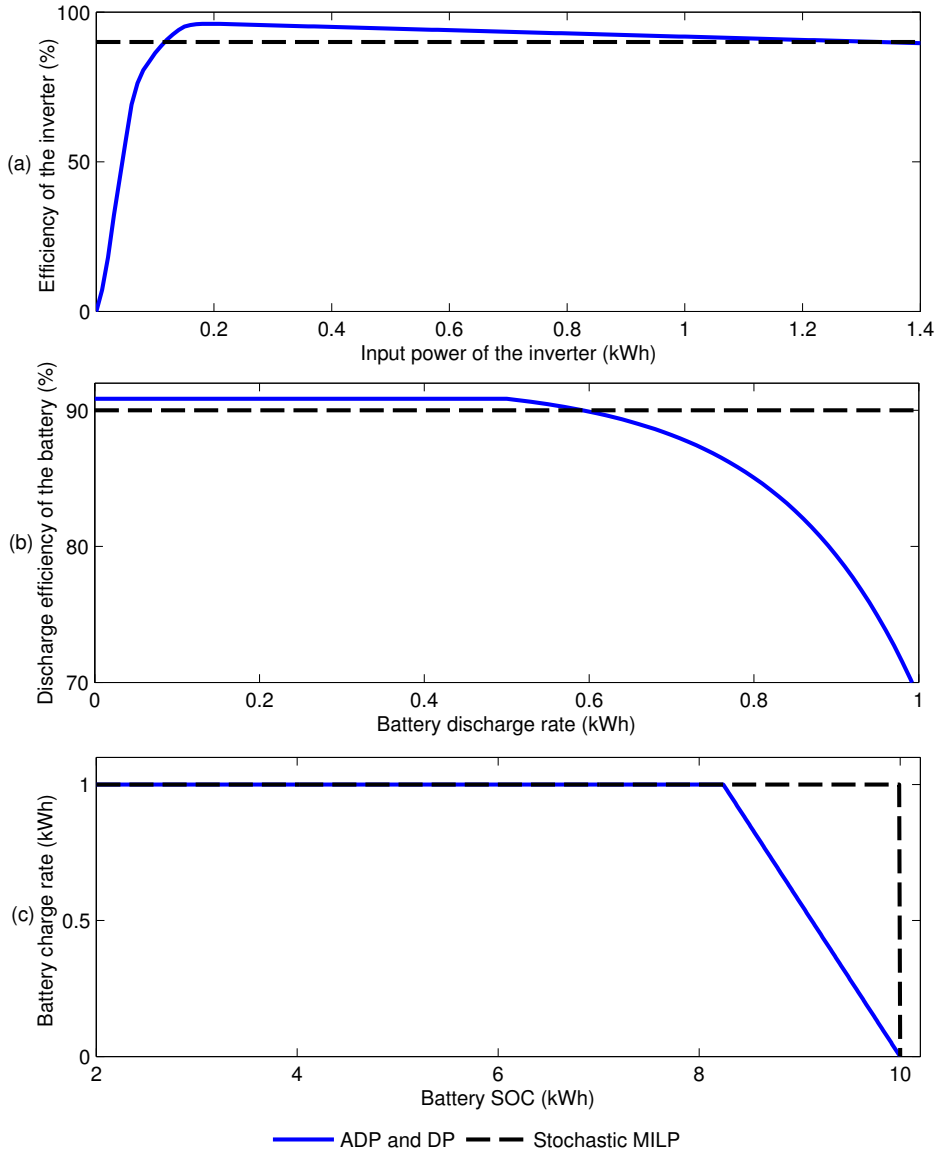

Fig. 2.3 Characteristics of the battery and the inverter.

where $C_k(\mathbf{s}_k, \mathbf{x}_k, \omega_k)$ is the cost incurred at a given time-step, which is given by:

$$C_k(\mathbf{s}_k, \mathbf{x}_k, \omega_k) = s_k^{\mathrm{p}} \left(s_k^{\mathrm{d,e}} + \omega_k^{\mathrm{d,e}} - \mu^{\mathrm{i}} x_k^{\mathrm{i}} + x_k^{\mathrm{wh}} \right). \tag{2.8}$$

Note that we don't use any specific user comfort criteria in the contribution function. However, we endeavour to supply the thermal demand at all time-steps without any user discomfort by penalising undesired states of the TES in DP and ADP, and directly using the constraint (2.4) in stochastic MILP . The problem is formulated as an optimisation of the expected contribution because the contribution is generally a random variable due

Table 2.1 The simulation parameters

Maximum battery charge rate	2 kWh
Maximum battery discharge rate	2 kWh
Maximum electric water heater input	3 kWh
Electric water heater efficiency	90 %
Battery charging efficiency	100 %
Battery losses	0.01 kWh
TES losses	0.01 kWh
Maximum battery capacity	10 kWh
Minimum battery discharge limit	2 kWh
TES capacity	12 kWh

to the effect of ω_k. In all the SHEMSs, we obtain the decisions $\mathbf{x}_k = \pi(\mathbf{s}_k) = [x_k^{\mathrm{b}}, x_k^{\mathrm{wh}}]$, depending on the state variables $\mathbf{s}_k = [s_k^{\mathrm{b}}, s_k^{\mathrm{t}}, s_k^{\mathrm{d,e}}, s_k^{\mathrm{pv}}, s_k^{\mathrm{d,t}}, s_k^{\mathrm{p}}]$, and realisations of random variables $\omega_k = [\omega_k^{\mathrm{pv}}, \omega_k^{\mathrm{d,e}}, \omega_k^{\mathrm{d,t}}]$ at each time-step. Note that the electrical demand here is the aggregated household demand.

Next section explains the effects of stochastic variables on the SHEMS problem and presents the algorithm use to estimate their probabilistic models.

2.3 Stochastic Variable Models

In order to optimise performance, it is important for a SHEMS to incorporate variations in the PV output and electrical and thermal demand, and to do so over a horizon of several days. This requires a stochastic optimisation technique and its benefits over a deterministic optimisation are discussed in Chapter 3 and 5, and in [34, 48, 35, 53, 56]. Given this, SHEMSs require the mean PV output and the demand with its appropriate probability distributions before the start of the decision horizon. This section first discusses the stochastic variables and their effects on the SHEMS problem and then presents a hierarchical approach based on clustering and kernel regression used to estimate the stochastic variables models. Note that the kernel estimator conforms to the MDP construction (i.e. Markov property of the transition functions), which is needed to solve the problem using DP (Chapter 3 and 4) and ADP (Chapter 5).

2.3.1 Stochastic variables

The stochastic variables in the SHEMS problem considered in this thesis are PV output and electrical and thermal demand. The effects of these random variations on the SHEMS problem are discussed below:

- PV output depends on solar insolation and cloud coverage, a forecast of which can be obtained before the horizon starts from weather forecasting services. The solar insolation can be obtained with a good accuracy as it only depends on the position of the sun, time of day in the year and geographic coordinates. However, cloud coverage is much harder to predict, especially for a particular location with a sufficient level of granularity (e.g. 1/2 hour). PV output is important to the SHEMS problem as it is a key source of energy and is expected to be closely coupled with the battery storage profile. Failing to accommodate for variation in PV generation would be expected to increase costs to the household as more power is imported from the grid.

- Electrical demand of the household depends on the number of occupants and their behavioural patterns, which is difficult to predict in the real world. In the context of SHEMSs, electrical demand should be supplied from the DG units, storage units and the electrical grid. Failure to accommodate variations in electrical demand may result in additional costs to the household.

- Thermal demand is also difficult to predict in the real world so failure to accommodate variations in thermal demand may result in user discomfort.

Note that a deterministic optimisation can only use the mean estimated PV output and demand while a stochastic optimisation can incorporate appropriate probability distributions. Currently proposed SHEMSs estimate mean PV output using the weather forecast [74] and the mean electrical demand using a suitable demand prediction algorithm [75, 76]. These existing approaches have several drawbacks, such as:

- The accuracy of their estimates depends on user inputs or the quality of the user behaviour prediction algorithm. In detail, in order to improve the accuracy of the estimated electrical demand profile, the demand prediction algorithms consider all the individual appliances separately. However, this means the details of each appliance's use has to be either predicted from the user behaviour prediction algorithm or input by the user.

- They are only suitable for certain scenarios, because predicting human behaviour is difficult in real life. For example, [75] is more appropriate for a family with a predictable lifestyle compared to students sharing a house.

- In most cases, the probability distributions associated with the PV output and demand will have to be obtained as follows:
  - Assume prior knowledge as in [48]. In detail, [48] used a occupancy transition matrix with 3 occupancy states (i.e. all home, some home, and all away) to incorporate the uncertainty associated with the electrical demand. This is only practically possible for users with a continuous life style. Note that we can't always assume that the users have a prior knowledge.
  - Model using parametric approaches, such as Gaussian or skew-Laplace distributions [53]. However, this does not always represent a real scenario.

Given this, we propose a hierarchical approach, where we first cluster daily empirical data according to a certain criteria, and then estimate probability distributions within each cluster using kernel regression. The means that the predictions from the users should only be accurate enough to identify the type of day and hence the corresponding cluster.

The mean PV output and electrical demand used throughout the thesis are from a data set collected during SGSC project. The data set [32] consists of PV output and electrical demand measurements at 30 minutes intervals over 3 years for 50 households. In more detail, we use this data in two ways: (1) Firstly, as inputs to the SHEMS along with a parametric or a non-parametric probability distribution; and (2) secondly, for estimating the PV and demand models using the hierarchical approach described below.

Finally, we construct the magnitudes of the thermal demand and the time they occur making use of Australian Standard AS4552 [79] and the hot water plug readings in [31]. We assume a Gaussian distribution for the thermal demand because there is not enough empirical data to obtain a reasonable distribution using the hierarchical approach described below.

2.3.2 An hierarchical approach

This thesis estimates the probability distributions of PV-output and electrical demand using an hierarchical approach, where we first cluster daily empirical data according to certain attributes, and then kernel estimate probability distributions at each time-step within each cluster. In more detail, we obtain the probability distributions of the PV output, which depend on the time and type of day (sunny, normal or cloudy days) in two steps.

1. First we separate daily empirical data into seasons and then we cluster them using a k-means algorithm according to certain attributes to obtain clusters with different daily PV generations. We compare two attributes: (1) total daily PV output so the clusters corresponds to sunny, partially sunny, normal, partially cloudy and cloudy

days; and (2) total morning and evening PV output so the clusters corresponds to sunny morning and cloudy evening etc. We use a *genetic algorithm* (GA) to optimise the time that separates morning and the evening. The objective of the GA is to minimise the *mean absolute error* (MAE) between the actual and estimated PV output profiles (more details are in the next section).

2. Second, for each time-step in the corresponding clusters, we estimate a probability distribution of the PV output using an *Epanechnikov* kernel estimating technique [80]. The bandwidth of the PV generation kernel estimates are slightly increased from the default MATLAB values to obtain a smoother distribution in some residential buildings (more details are in the next section).

Note that the draws from the kernel estimates at each time-step within a day-type are independent so the Markov property of the transition functions is satisfied. The inter-daily transition probabilities are captured in the clustering process. The probability distributions of the electrical demand are obtained in a similar way except the attributes of the k-means clustering algorithm are for different time periods throughout the day. Similar to the PV output, we optimise these time periods and the best number of clusters using GA. As a result, the clusters are according to days with high, normal or low demand levels on different times of the day. The bandwidth of the kernel estimates vary rapidly so we stick with the default MATLAB values. It is worthwhile to note that before the start of the decision horizon, the SHEMS uses the predicted mean PV-output and the electrical demand to determine the type of day and hence the corresponding probability distribution.

2.4 Results and Discussion

This section first optimises the number of clusters and the time periods of their attributes using GA for the PV output and electrical demand (Section 2.4.1), and then estimate the PV and electrical demand models using the optimised number of clusters and their attributes as well as a benchmark with no clustering (Section 2.4.2). The stochastic variable models are for four scenarios each for two residential buildings. The two residential buildings are as follows:

1. Central coast, NSW, Australia based residential building with a 2.22 kWp PV system.

2. Sydney, NSW, Australia based residential building with a 3.78 kWp PV system.

For each residential building we investigate four scenarios corresponding to four different days: July 15$^{\text{th}}$, 2012; October 10$^{\text{th}}$, 2012; January 5$^{\text{th}}$, 2013; and April 15$^{\text{th}}$, 2013. These

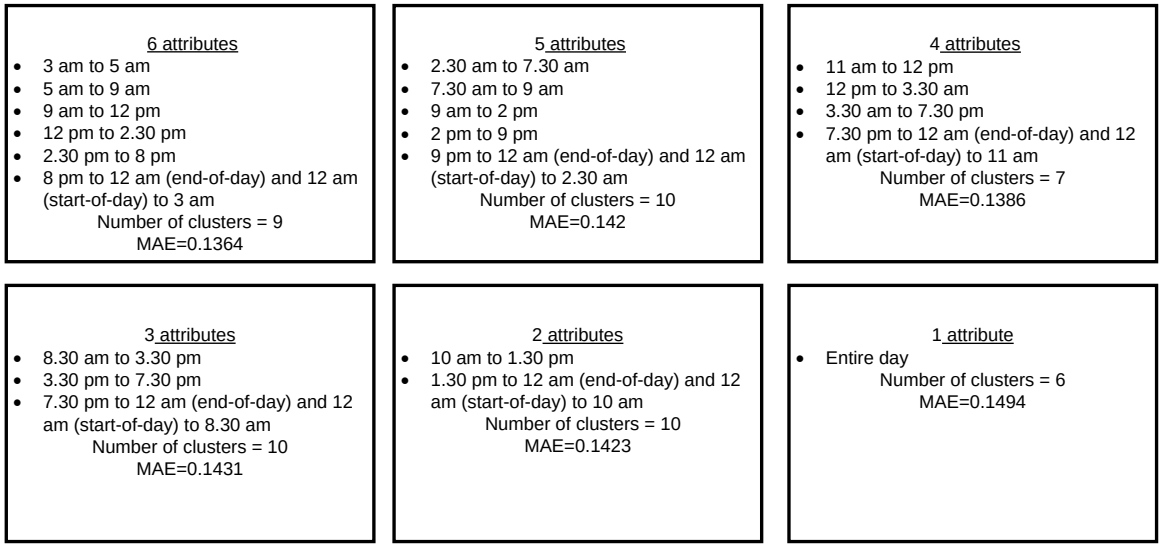

Fig. 2.4 The time periods of the six attribute sets used for clustering electrical demand, which are optimised over a year using GA.

PV and electrical demand models are benchmarked using kernel estimates obtained without clustering. As mentioned earlier, the PV output and electrical demand data are available for three years, so the first two years of data are used for learning and the third year for validation.

2.4.1 Attributes and the number of clusters

The first task is to optimise and compare six attribute sets for the electrical demand and two attribute sets for the PV output. The GA is use to minimise the MAE of the forecasts over a year and the maximum number of clusters is set to ten. Here GA is used as it is computationally intensive to find the exact solutions using other methods and a near optimal solution is enough for our optimisation problem.

The optimised time periods of the six attribute sets for electrical demand are in Fig. 2.4. Note that the 6^{th} attribute set has six time periods, which is referred to as having six attributes. The rest of the attribute sets follow the same pattern. Two attribute sets are used for the PV output: (1) the total daily PV output and (2) the total morning and evening PV output. The time-step that separates morning and evening is 12.30 pm, which is optimised using a GA. In Fig. 2.5, we use the optimised time periods of the attributes and investigate the MAE and *root-mean-square error* (RMSE) with respect to the number of clusters that ranges between 1 to 20. We investigate up to 20 clusters to see how RMSE and MAE behave as we continue to increase the number of clusters, however, we believe a maximum of ten clusters is reasonable in practical applications.

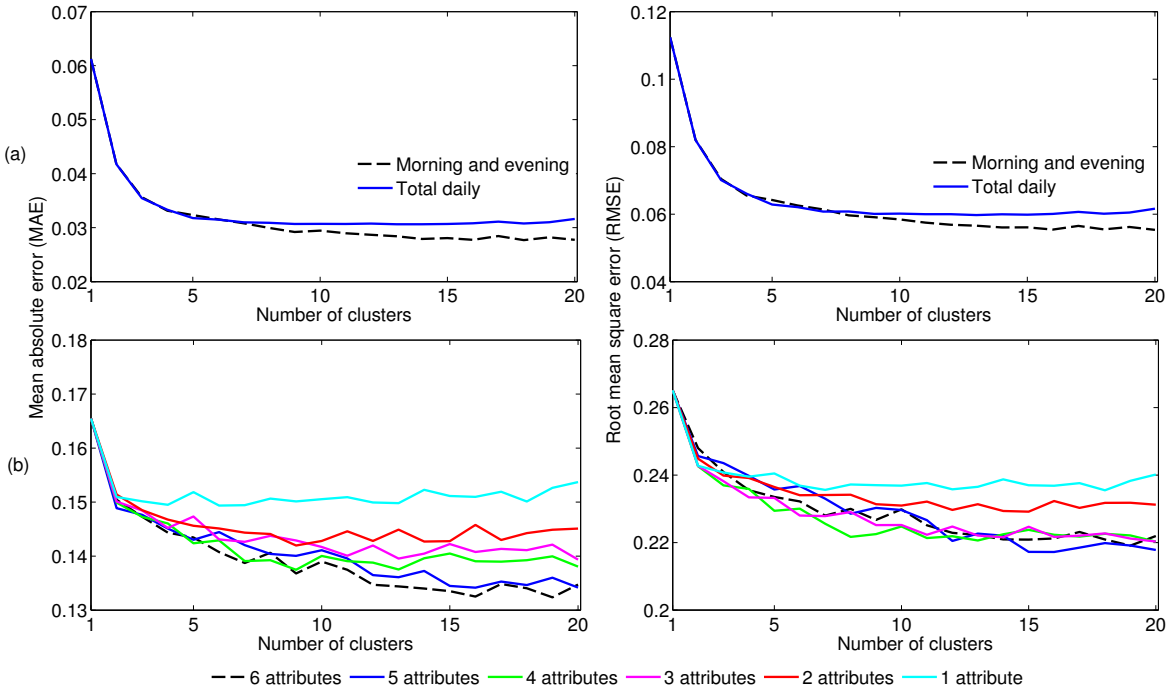

Fig. 2.5 MAE and RMSE vs. the number of clusters for (a) PV output and (b) electrical demand. The two attributes of the PV output are the total daily and total morning and evening PV outputs (separated at 12.30 pm) while the time periods of the six attributes used for the electrical demand are in Fig. 2.4.

The exact number of clusters and attributes for electrical demand will vary depending on the inhabitants knowledge in practical applications so we present a range of suitable attributes and the corresponding number of clusters in Fig. 2.4. However, for the simulation purposes, we use six attributes and nine clusters as it results in the lowest MAE as depicted in Fig. 2.4 from GA results and in Fig. 2.5. In Fig. 2.5, the RMSE is similar for three to six attributes because we optimised the time-periods using the MAE. Even though we use six attributes in the simulations, our results suggest that having two to six attributes and nine or ten clusters is a good estimate.

This thesis use five clusters for the PV output because the MAE and the RMSE of the PV output predictions decreases exponentially as the number of clusters increases up to five and then continues to decrease at a lesser rate as depicted in Fig. 2.5(a). Moreover, having a large number of clusters is not possible in practical applications as it requires a higher user interaction. The MAE and the RMSE of the PV output predictions using both of the attribute sets are approximately the same up to seven clusters and then having two attributes for morning and evening is slightly better. Given this, the number of attributes has little or no impact when we are using five clusters.

2.4.2 PV and electrical demand models

The actual and the predicted values of the PV output and electrical demand obtained from the proposed hierarchical approach for different scenarios are in Fig. 2.6, Fig. 2.8, Fig. 2.10 and Fig. 2.12 for residential building A; and Fig. 2.14, Fig. 2.16, Fig. 2.18 and Fig. 2.20 for residential building B. The corresponding benchmark profiles without clustering are in Fig. 2.7, Fig. 2.9, Fig. 2.11 and Fig. 2.13 for residential building A; and Fig. 2.15, Fig. 2.17, Fig. 2.19 and Fig. 2.21 for residential building B. The predicted values are the median, with the 10^{th} and 90^{th} percentiles shown as error bars, of the values in the corresponding cluster. The probability density functions of this variation are estimated using kernel regression.

There are several important observations of our PV and electrical demand models. The probability density functions of the electrical demand is either a skewed unimodal or a bimodal distribution with smaller secondary peaks. These secondary peaks are because of the appliances with different power ratings used at different times of the day. The kernel estimates of the electrical demand are right-skewed when the median values in the cluster underestimate the actual values, which means there is a higher probability of demand increasing than decreasing.

The probability density functions of the PV output follows a skewed unimodal distribution. The RMSE and MAE of the PV output predictions are minimum for sunny days, such as the summer day on January 5^{th}, 2013 for two residential buildings (A.3 and B.3), as depicted in Table 2.2. This means that the PV profiles are smooth, as shown in Fig. 2.10(a) and Fig. 2.18(a). The converse is seen to be happening for cloudy days. In Fig. 2.18(a) (residential building B on a summer day), PV panels generate the maximum output for approximately 4 hours between 12 pm to 4 pm. At these time periods, kernel estimates are skewed left and are limited at the peak, which means there is a probability of going cloudy but zero probability of increasing the PV output further as the generation capacity is reached. For some time-steps probability density functions discontinues after a certain point when there are no data points beyond that point in the corresponding cluster. For example the 8 am PV output probability density function in Fig. 2.8 discontinues at 0.2 kW because the probability of having a high PV output early in the morning is zero.

Our estimated models from the hierarchical approach are mostly better than the kernel estimates that are obtained without clustering, as shown in Table 2.2. However, clustering has no benefits (sometimes slightly worse predictions) when the demand is very low with less variation throughout the day. These scenarios are extremely rare and the resulting prediction error is insignificant compared to the improvements from the other scenarios when clustering. The probability density functions of the PV output can have bimodal distribution when we don't cluster the empirical data, as depicted in Fig. 2.7, Fig. 2.9, Fig. 2.11, Fig. 2.13, Fig. 2.15,

Fig. 2.17, Fig. 2.19, Fig. 2.21. We can overcome this by increasing the bandwidth of the Epanechnikov kernel estimation technique. However, having a larger bandwidth means kernel estimates becomes less accurate. Also, the probability distributions are the same for every day in a particular season when we don't cluster empirical data. This only works in situations where the user behaviour is very regular and predictable.

2.5 Summary

This chapter first presented a general formulation of the sequential stochastic optimisation problem, and then applied it to the SHEMS problem, which consists of PV-storage systems. This formulation is used to model the SHEMS problem as an MDP to solve using DP and ADP in Chapter 3 and 5, respectively; and a mathematical programming problem to solve using MILP in Chapter 3. The characteristics of the controllable devices and electricity price signal presented in Section 2.2 are used for all the subsequent chapters.

An hierarchical approach, which involves first clustering empirical data into day types and second estimating probability distributions using kernel regression, was proposed to estimate stochastic variables models. The results showed that the accuracy of the estimates increases as the number of clusters and attributes increases. This is because the draws from the kernel estimations within a day type are independent so the clustering is needed to capture inter daily variations. These estimations conforms with the MDP construction in Chapter 3 and 5 and in practical applications the user only needs to choose the correct day type instead of having to estimate the entire day's PV output and demand. These stochastic variable models are used in the subsequent chapters.

Table 2.2 The total actual and the predicted electrical demand and PV output with their RMSE and MAE for four days each for two residential buildings. Note that the * corresponds to the benchmark scenarios.

Scenarios	PV output				Electrical demand			
	Actual	Predicted	RMSE	MAE	Actual	Predicted	RMSE	MAE
A.1	7.028	7.703	0.0284	0.0141	21.464	14.812	0.3387	0.2174
A.1*	7.028	7.934	0.0393	0.0189	21.464	9.170	0.5365	0.3453
A.2	11.978	13.34	0.06	0.0284	7.435	5.3230	0.1533	0.086
A.2*	11.978	10.52	0.0726	0.0441	7.435	6.2155	0.1555	0.0964
A.3	13.467	13.0915	0.0208	0.0107	5.521	5.352	0.0811	0.0526
A.3*	13.467	9.76	0.1245	0.0775	5.521	5.755	0.0596	0.0434
A.4	5.5533	6.274	0.1087	0.0567	9.35	5.8865	0.1511	0.0971
A.4*	5.5533	6.622	0.1050	0.0521	9.35	7.743	0.1343	0.0875
B.1	8.921	8.415	0.1679	0.0681	62.377	46.338	1.2595	0.822
B.1*	8.921	10.961	0.1657	0.0773	62.377	33.6235	1.3017	0.8005
B.2	26.772	25.055	0.1617	0.0931	18.022	8.9485	0.5502	0.2363
B.2*	26.772	19.373	0.3120	0.1825	18.022	17.7235	0.4914	0.2309
B.3	32.591	31.046	0.0641	0.0338	63.2270	54.733	0.7489	0.4743
B.3*	32.591	18.833	0.4397	0.2866	63.2270	18.376	1.3980	1.0089
B.4	16.034	14.7145	0.1501	0.0772	17.466	17.429	0.2252	0.1612
B.4*	16.034	9.3495	0.2939	0.1441	17.466	20.3295	0.3051	0.2050

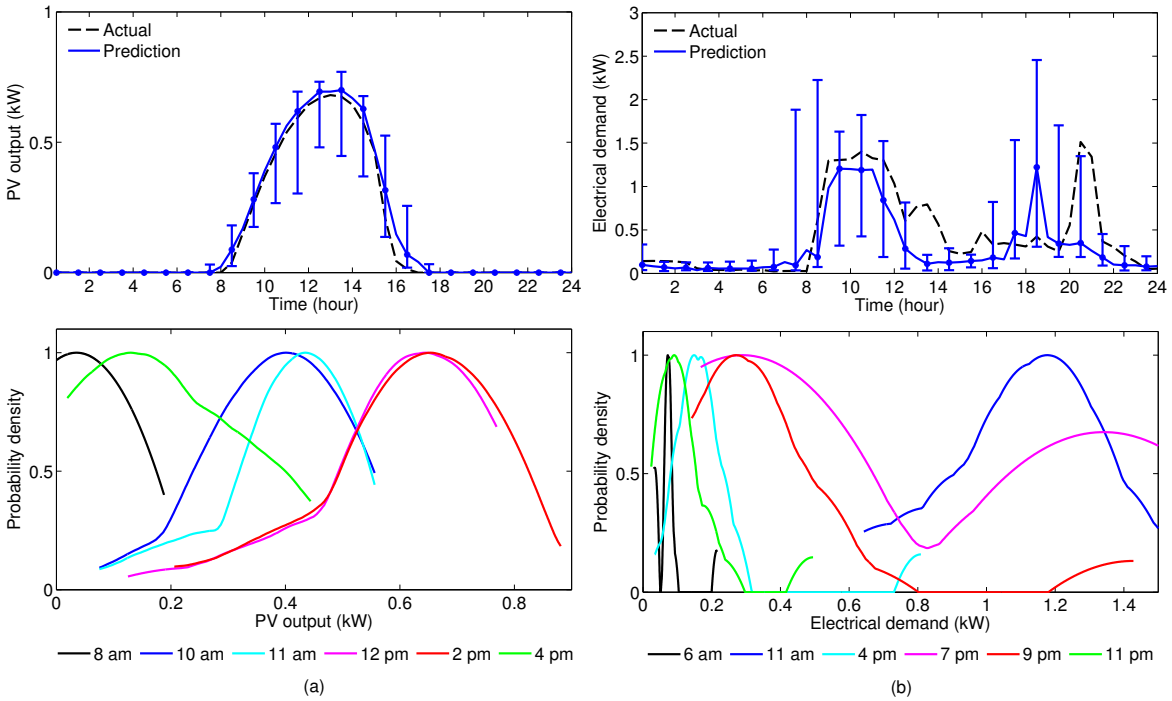

Fig. 2.6 The actual and the prediction along with the probability density functions for (a) PV output and (b) the electrical demand of residential building A on a winter day 15th July, 2012. The prediction is the median values of the cluster while its error bars are for the 10th and 90th percentiles (with clustering).

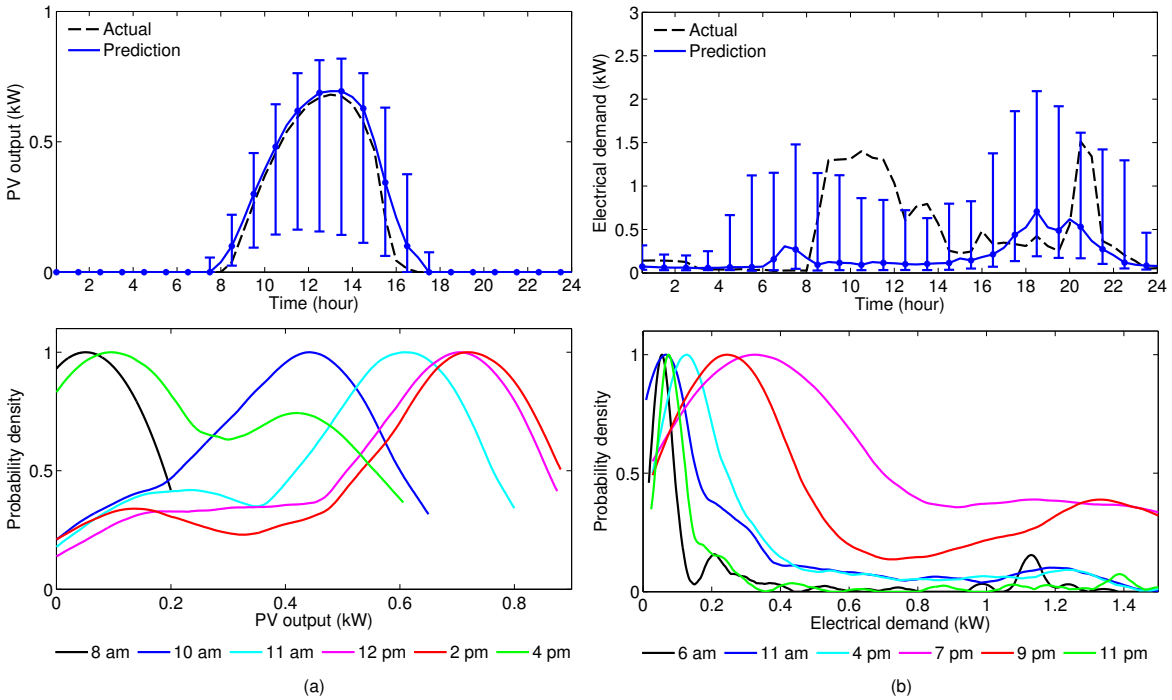

Fig. 2.7 The actual and the prediction along with the probability density functions for (a) PV output and (b) the electrical demand of residential building A on a winter day 15th July, 2012. The prediction is the median values of the cluster while its error bars are for the 10th and 90th percentiles (no clustering).

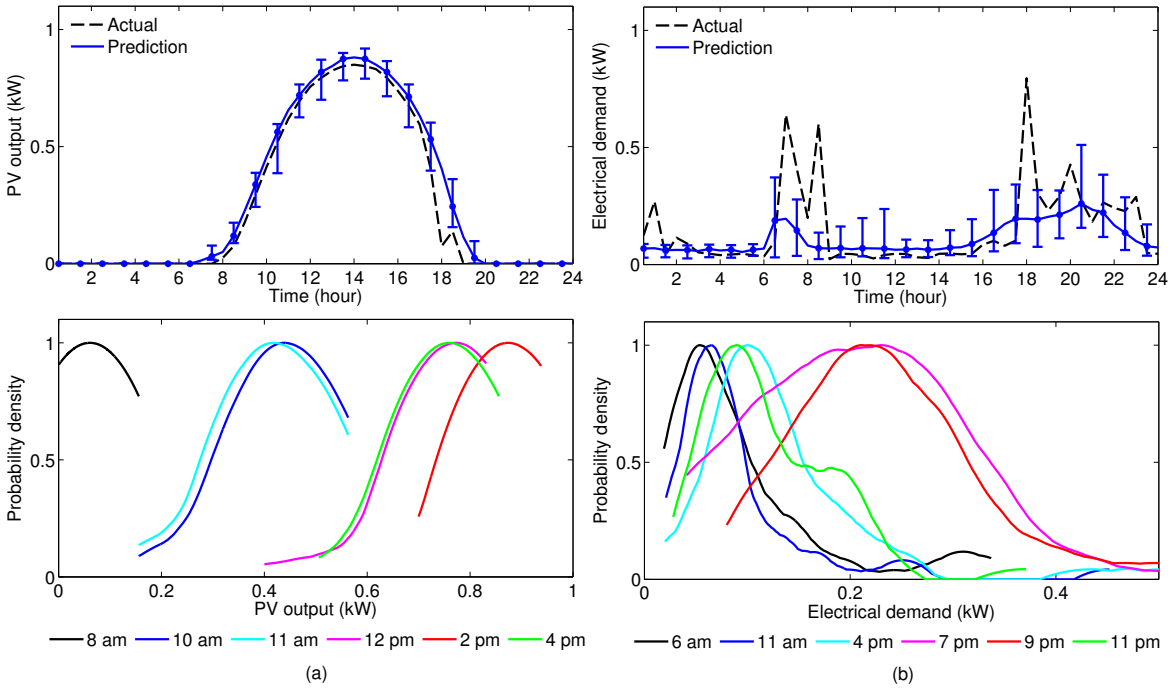

Fig. 2.8 The actual and the prediction along with the probability density functions for (a) PV output and (b) the electrical demand of residential building A on a spring day 10th October, 2012. The prediction is the median values of the cluster while its error bars are for the 10th and 90th percentiles (with clustering).

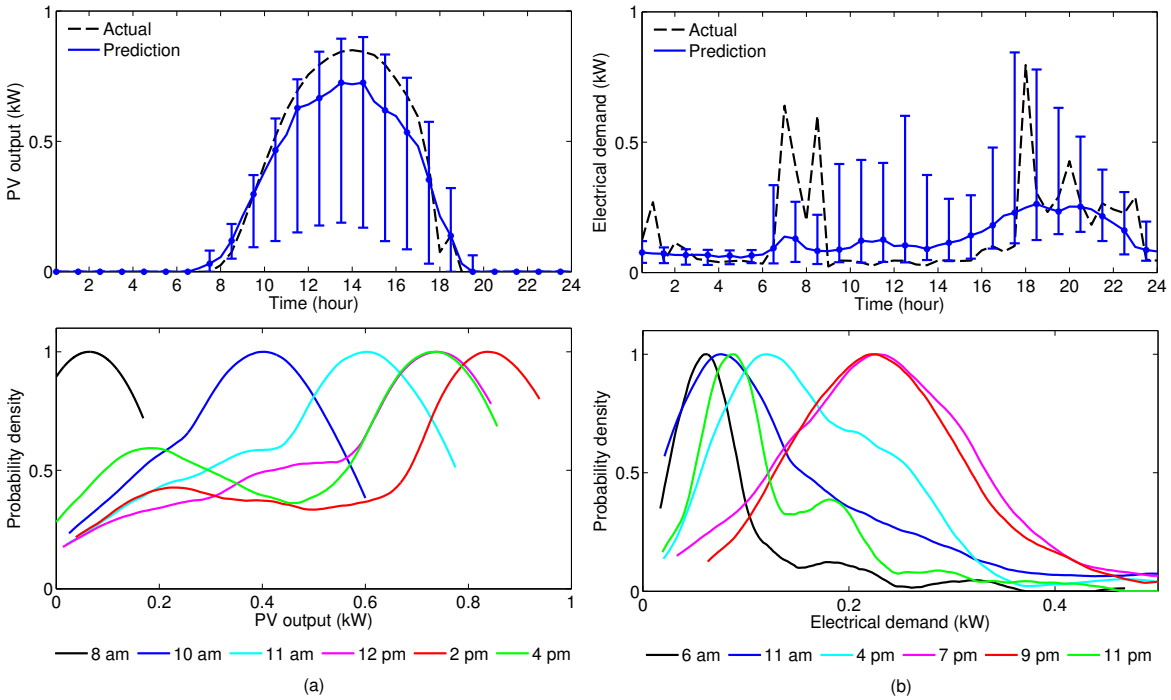

Fig. 2.9 The actual and the prediction along with the probability density functions for (a) PV output and (b) the electrical demand of residential building A on a spring day 10th October, 2012. The prediction is the median values of the cluster while its error bars are for the 10th and 90th percentiles (no clustering).

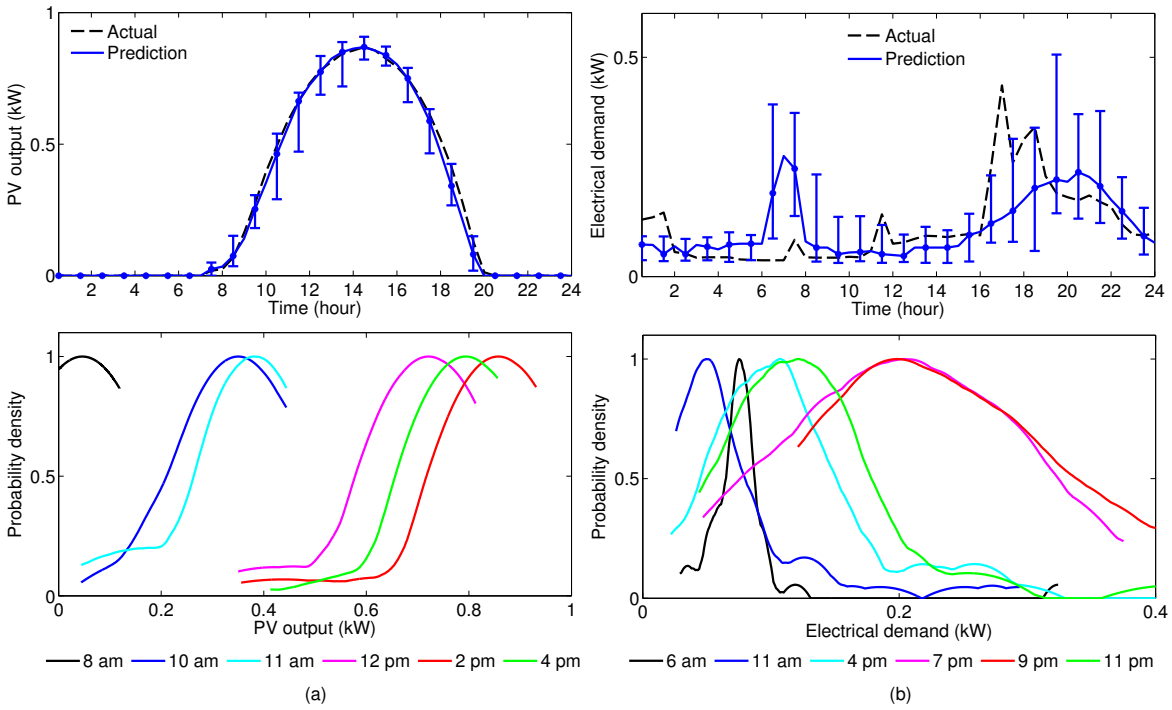

Fig. 2.10 The actual and the prediction along with the probability density functions for (a) PV output and (b) the electrical demand of residential building A on a summer day 5th January, 2013. The prediction is the median values of the cluster while its error bars are for the 10th and 90th percentiles (with clustering).

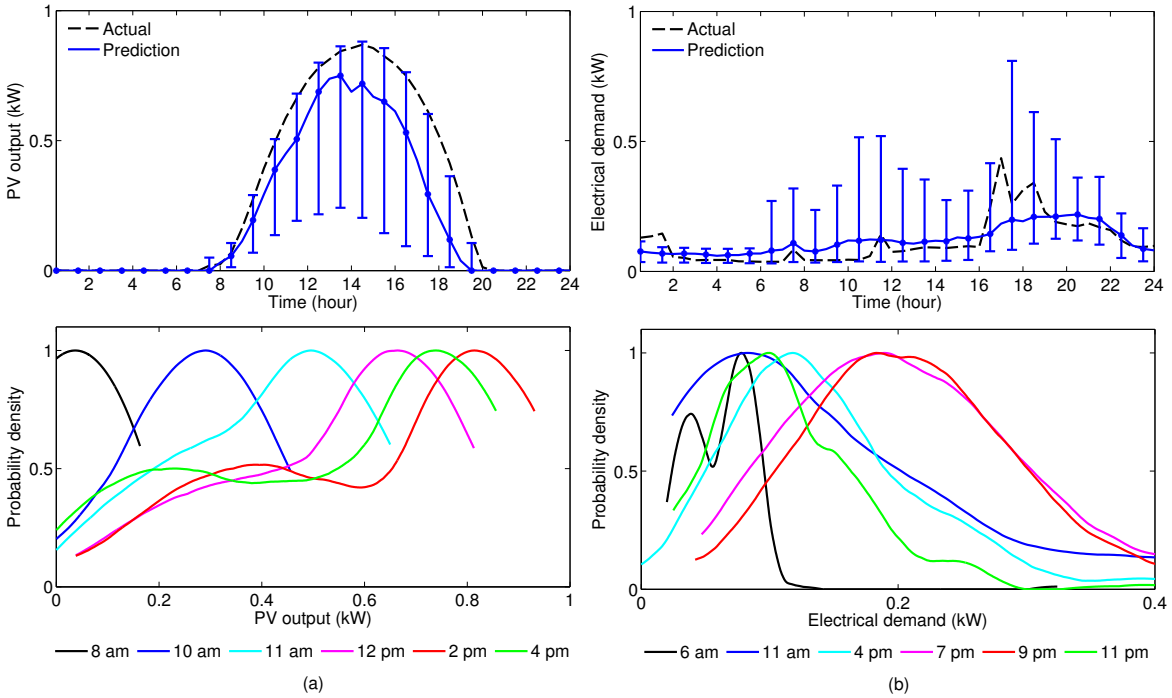

Fig. 2.11 The actual and the prediction along with the probability density functions for (a) PV output and (b) the electrical demand of residential building A on a summer day 5th January, 2013. The prediction is the median values of the cluster while its error bars are for the 10th and 90th percentiles (no clustering).

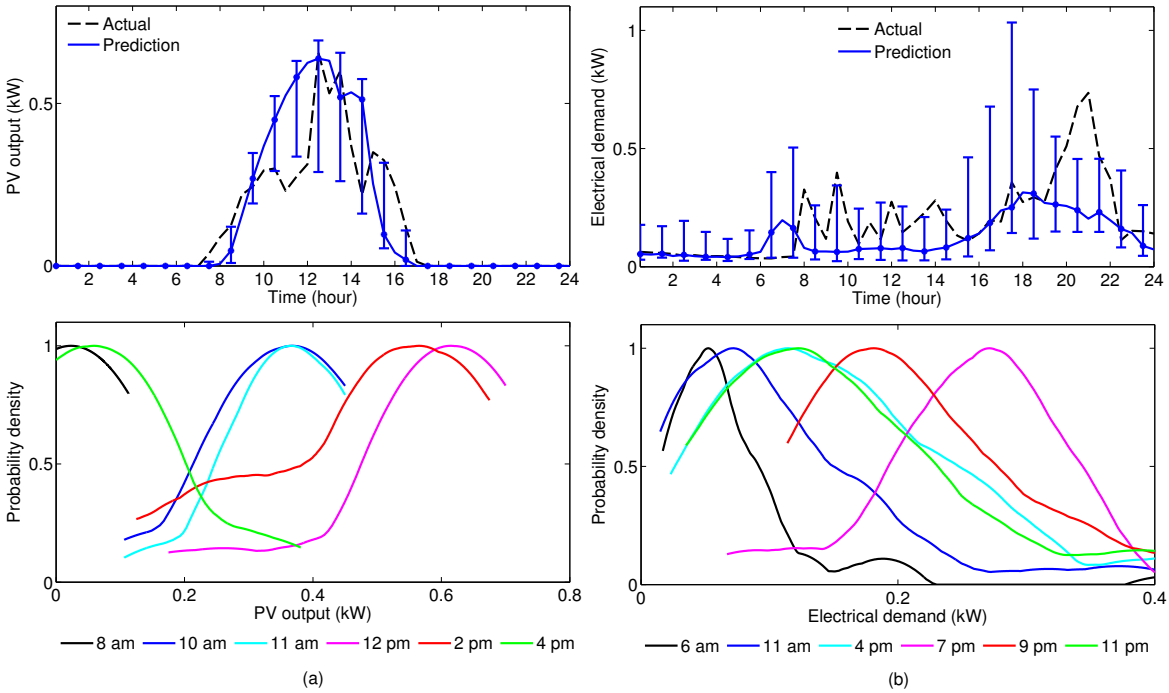

Fig. 2.12 The actual and the prediction along with the probability density functions for (a) PV output and (b) the electrical demand of residential building A on a autumn day 15th April, 2013. The prediction is the median values of the cluster while its error bars are for the 10th and 90th percentiles (with clustering).

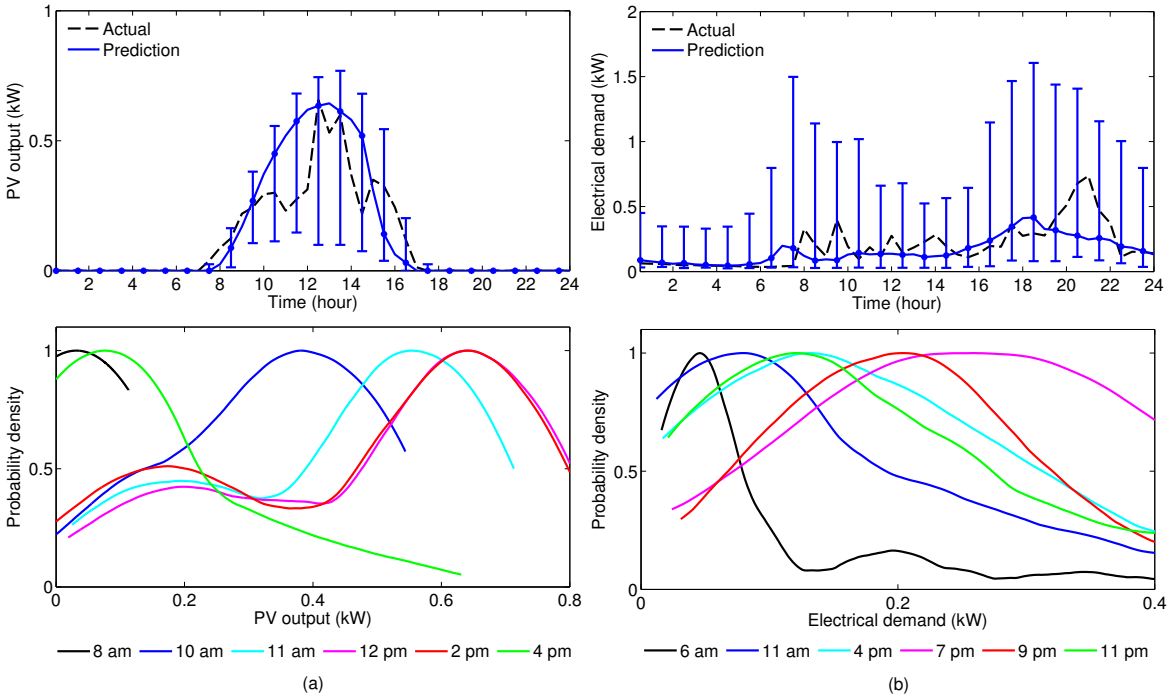

Fig. 2.13 The actual and the prediction along with the probability density functions for (a) PV output and (b) the electrical demand of residential building A on a autumn day 15th April, 2013. The prediction is the median values of the cluster while its error bars are for the 10th and 90th percentiles (no clustering).

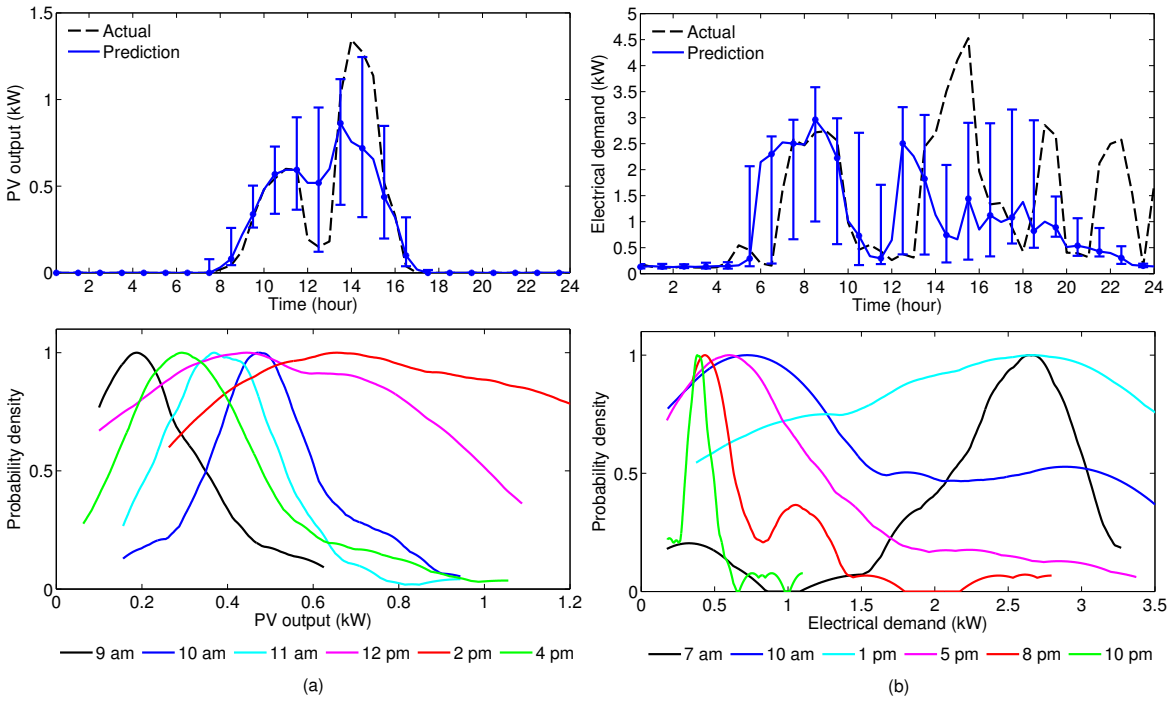

Fig. 2.14 The actual and the prediction along with the probability density functions for (a) PV output and (b) the electrical demand of residential building B on a winter day 15th July, 2012. The prediction is the median values of the cluster while its error bars are for the 10th and 90th percentiles (with clustering).

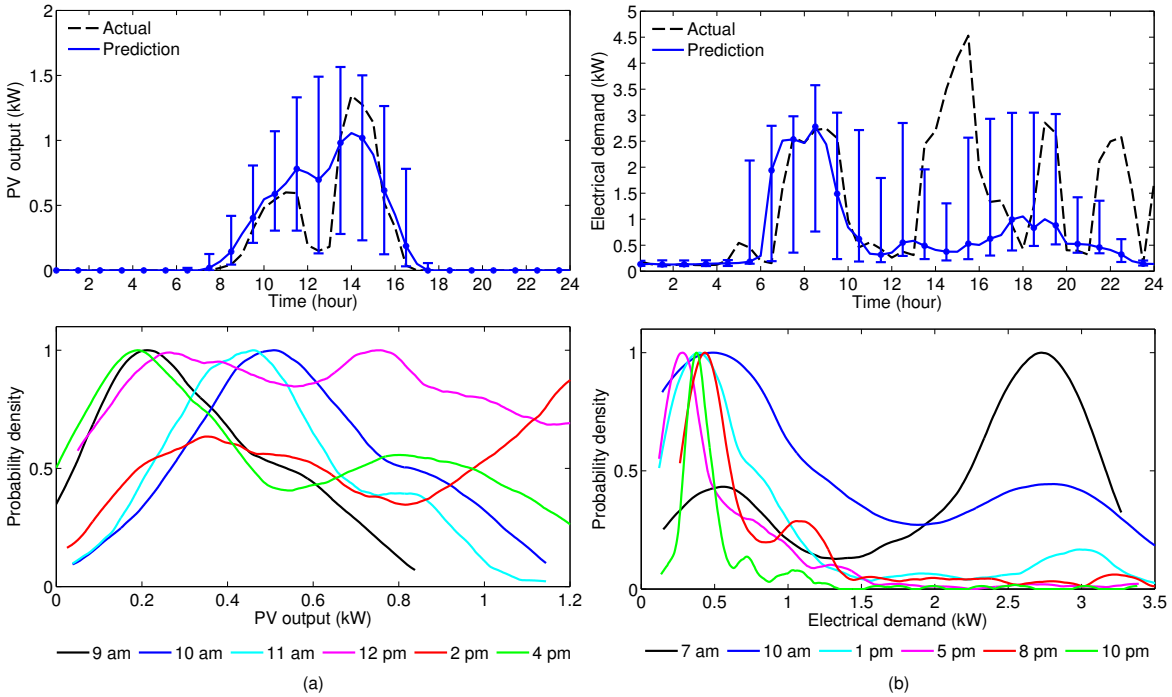

Fig. 2.15 The actual and the prediction along with the probability density functions for (a) PV output and (b) the electrical demand of residential building B on a winter day 15th July, 2012. The prediction is the median values of the cluster while its error bars are for the 10th and 90th percentiles (no clustering).

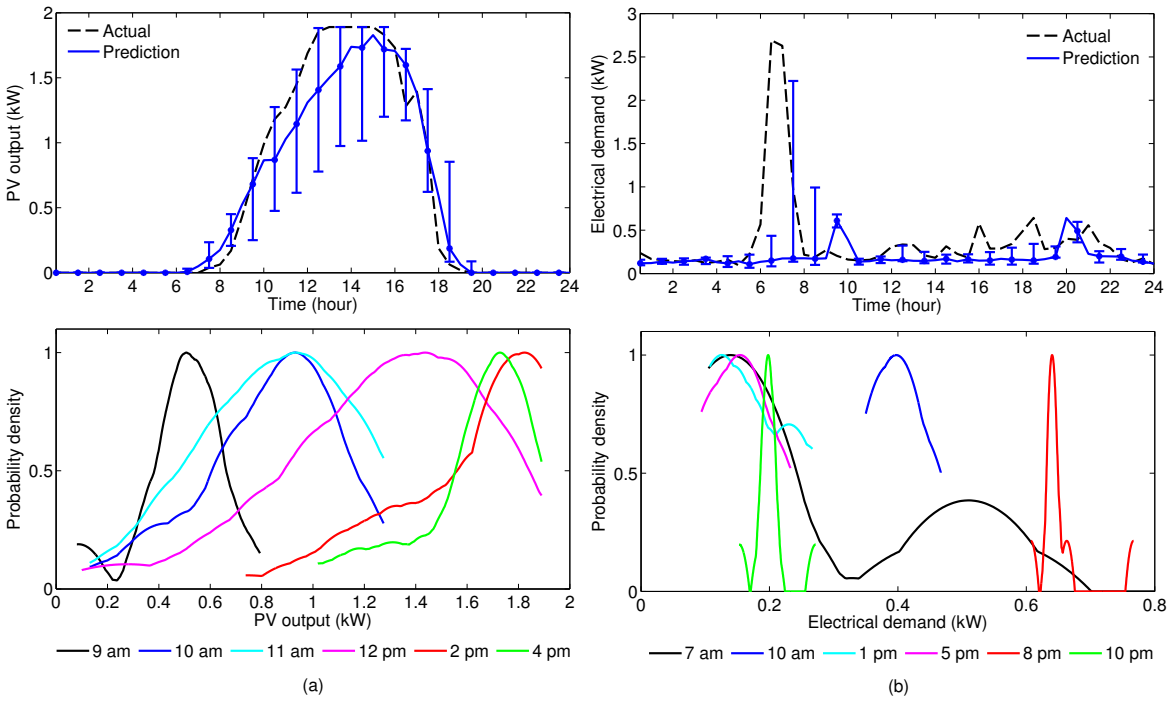

Fig. 2.16 The actual and the prediction along with the probability density functions for (a) PV output and (b) the electrical demand of residential building B on a spring day 10th October, 2012. The prediction is the median values of the cluster while its error bars are for the 10th and 90th percentiles (with clustering).

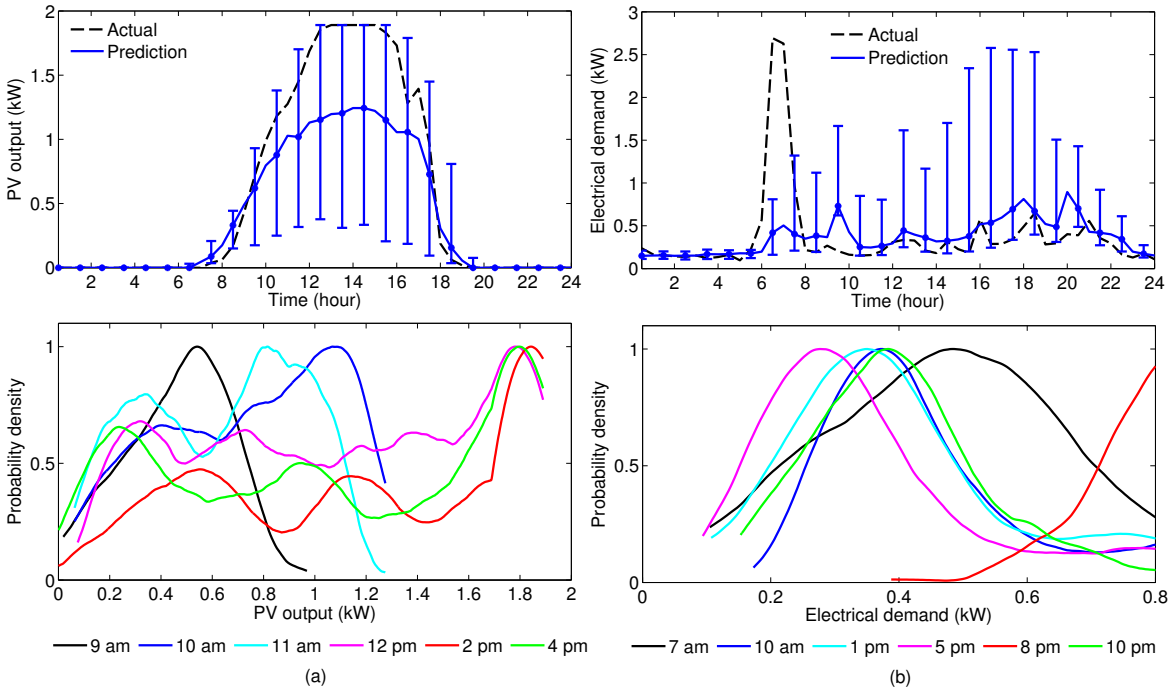

Fig. 2.17 The actual and the prediction along with the probability density functions for (a) PV output and (b) the electrical demand of residential building B on a spring day 10th October, 2012. The prediction is the median values of the cluster while its error bars are for the 10th and 90th percentiles (no clustering).

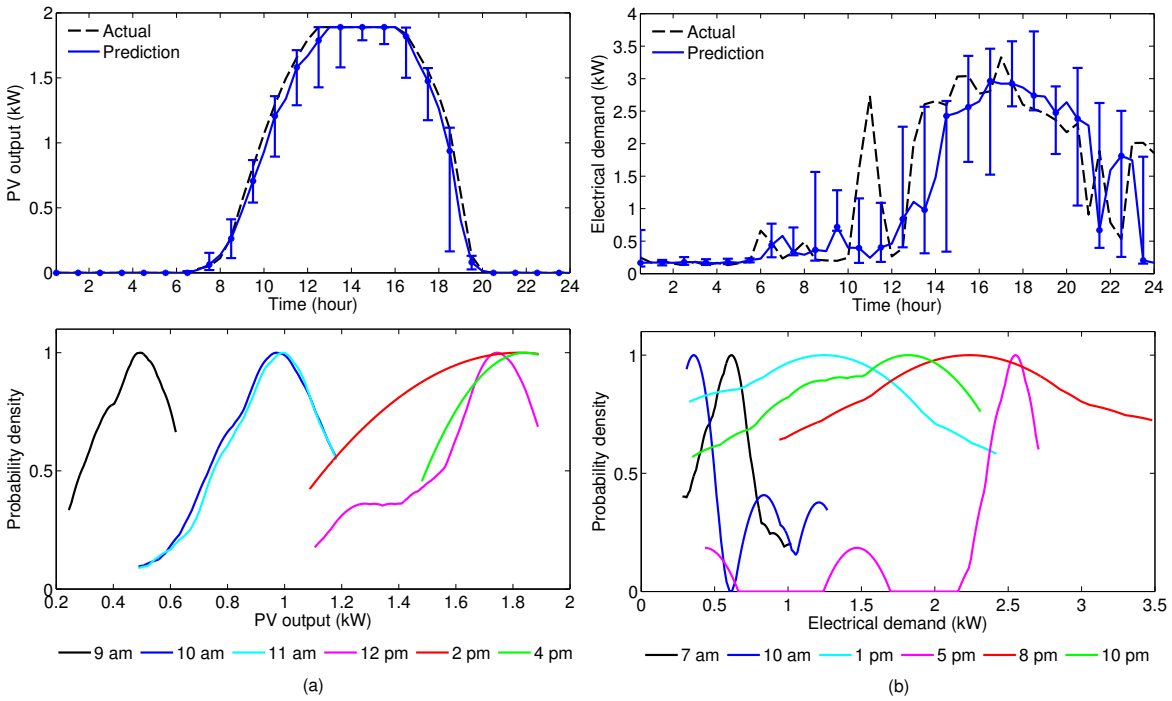

Fig. 2.18 The actual and the prediction along with the probability density functions for (a) PV output and (b) the electrical demand of residential building B on a summer day 5th January, 2013. The prediction is the median values of the cluster while its error bars are for the 10th and 90th percentiles (with clustering).

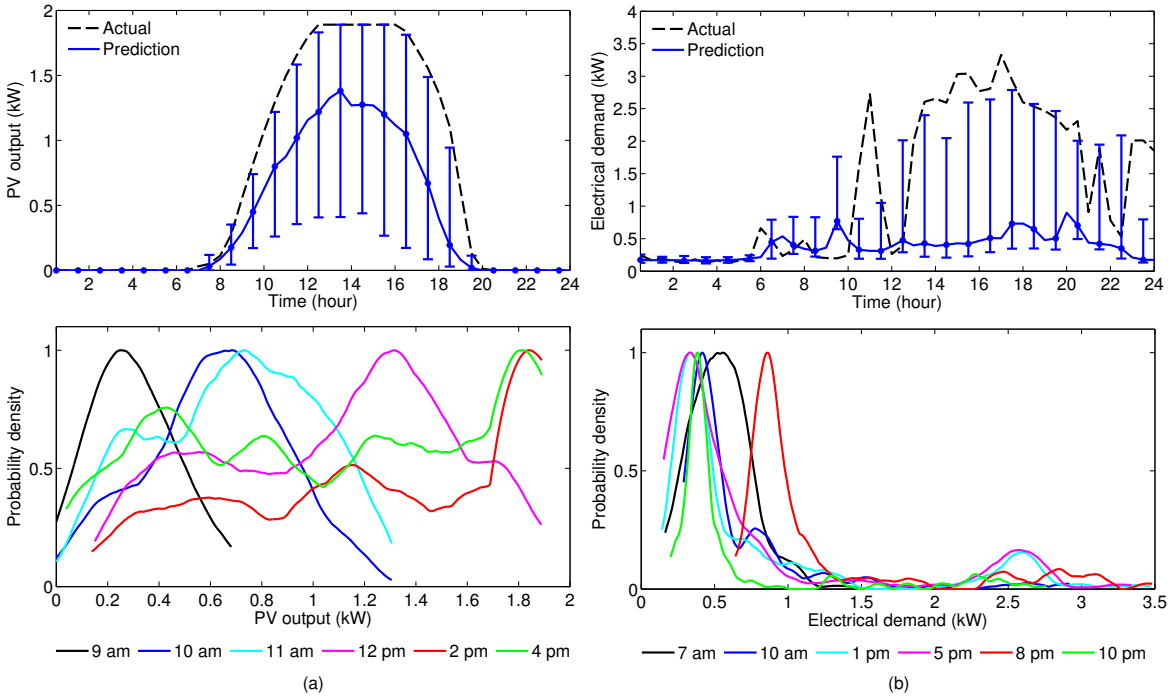

Fig. 2.19 The actual and the prediction along with the probability density functions for (a) PV output and (b) the electrical demand of residential building B on a summer day 5th January, 2013. The prediction is the median values of the cluster while its error bars are for the 10th and 90th percentiles (no clustering).

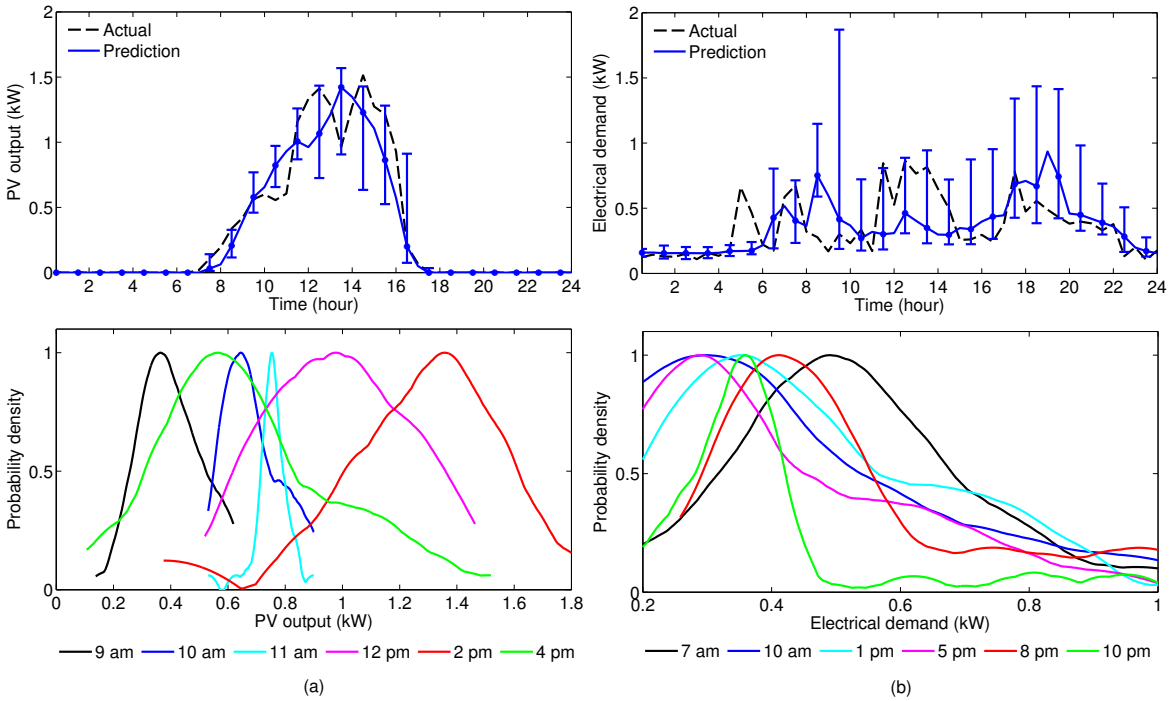

Fig. 2.20 The actual and the prediction along with the probability density functions for (a) PV output and (b) the electrical demand of residential building B on a autumn day 15th April, 2013. The prediction is the median values of the cluster while its error bars are for the 10th and 90th percentiles (with clustering).

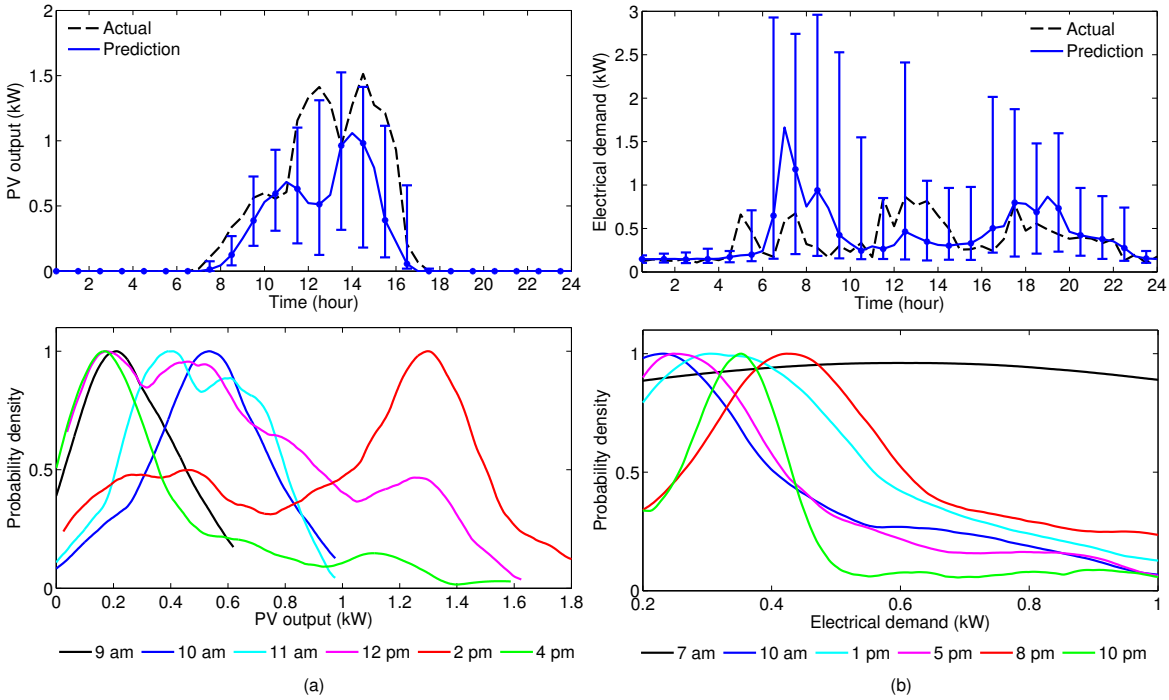

Fig. 2.21 The actual and the prediction along with the probability density functions for (a) PV output and (b) the electrical demand of residential building B on a autumn day 15th April, 2013. The prediction is the median values of the cluster while its error bars are for the 10th and 90th percentiles (no clustering).

Chapter 3

Comparison of Stochastic MILP and Dynamic Programming

This chapter presents a comparison of two existing solution techniques that can be used to solve the stochastic SHEMS problem. The first method is a scenario-based MILP approach, referred to as *stochastic* MILP in [56]. This technique requires linearised constraints and transition functions, as mentioned in Chapter 2, and models the problem as a mathematical programming problem. The second method is DP, in which the problem is modelled as a Markov decision process (MDP). Although computationally more intensive than MILP, DP enables us to incorporate all the non-linear constraints and transition functions with no additional computational burden over using linear constraints and transition functions.

This chapter is structured as follows: First the deterministic and stochastic versions of the MILP are presented and then the deterministic and stochastic DP are presented. The simulation results and discussion section consists of comparisons of deterministic and stochastic versions of DP and MILP using scenarios with different PV and electrical and thermal demand patterns. These comparisons are used to show the benefits of stochastic DP over stochastic MILP when making decisions under uncertainty, which justifies the use of DP to solve the shorter decision horizon in Chapter 4.

3.1 Stochastic MILP

First describes the deterministic MILP formulation use to solve the SHEMS problem, which assumes a perfect foresight. Then the scenario-based stochastic MILP approach, which is used to incorporate the stochastic variables.

3.1.1 Deterministic MILP

The deterministic version of the SHEMS problem can be solved using a MILP approach, which optimises a linear objective function subject to linear constraints with continuous and integer variables [34]. Note that the transition functions presented in Section 2.2 are considered as constraints in the MILP formulation. The MILP formulation of the optimisation problem is given by:

$$\min_{\mathbf{x}} \sum_{k=1}^{N} \left(s_k^{\mathrm{p,buy}} x_k^{\mathrm{g}+} - s_k^{\mathrm{p,sell}} x_k^{\mathrm{g}-} \right), \tag{3.1}$$

The decision variables in the MILP formulation consists of both the decision and state variables of the controllable devices that are mentioned in Chapter 2 and integer variables, which are used to model power flow directions. Note that the non-controllable inputs such as PV output and electrical and thermal demand are only represented using state variables (no separation into state and random variables). The continuous decision variables are:

$$x_k^{\mathrm{g+}}, x_k^{\mathrm{g\text{-}}}, x_k^{\mathrm{b+}}, x_k^{\mathrm{b\text{-}}}, x_k^{\mathrm{bg}}, x_k^{\mathrm{bd}}, x_k^{\mathrm{wh}}, d_k^{\mathrm{pv}}, s_k^{\mathrm{b}}, s_k^{\mathrm{t}}, \in \mathbb{R}, \tag{3.2}$$

and the binary decision variables are:

$$d_k^{\mathrm{g}}, d_k^{\mathrm{b}}. \tag{3.3}$$

In detail, the decision vector $\mathbf{x} = \left[x_k^{\mathrm{g+}}, x_k^{\mathrm{g\text{-}}}, x_k^{\mathrm{b+}}, x_k^{\mathrm{b\text{-}}}, x_k^{\mathrm{bg}}, x_k^{\mathrm{bd}}, x_k^{\mathrm{wh}}, d_k^{\mathrm{pv}}, s_k^{\mathrm{b}}, s_k^{\mathrm{t}}, d_k^{\mathrm{g}}, d_k^{\mathrm{b}} \right]$ consists of:

- $x_k^{\mathrm{g}+/-}$: electrical power flowing from/to grid,
- $x_k^{\mathrm{b}+/-}$ battery charge/discharge power,
- x_k^{bg} power flowing from battery to grid,
- x_k^{bd} power flowing from battery to demand,
- x_k^{wh} electric water heater input,
- $d_k^{\mathrm{g}} \in \{0,1\}$ is the direction of grid power flow (0: demand $\rightarrow$ grid, 1: grid $\rightarrow$ demand),
- $d_k^{\mathrm{pv}} \in [0,1]$: proportion of PV power flow (0: all PV power flows to grid, 1: all PV power flows to demand),
- $d_k^{\mathrm{b}} \in \{0,1\}$: battery charging status (0: discharge, 1: charge),

- s_k^{b}: battery SOC,

- s_k^{t}: TES SOC.

The constraints are separated into equality and inequality constraints. The equality constraints are:

$$x_k^{\mathrm{g}+} = s_k^{\mathrm{d,e}} - \mu^i(\mu_k^{\mathrm{b}\text{-}} x_k^{\mathrm{bd}} + d_k^{\mathrm{pv}} s_k^{\mathrm{pv}} - x_k^{\mathrm{b}+}) + x_k^{\mathrm{wh}}, \tag{3.4}$$

$$x_k^{\mathrm{g}-} = \mu^i(\mu_k^{\mathrm{b}\text{-}} x_k^{\mathrm{bg}} + (1 - d_k^{\mathrm{pv}}) s_k^{\mathrm{pv}}), \tag{3.5}$$

$$x_k^{\mathrm{b}-} = x_k^{\mathrm{bd}} + x_k^{\mathrm{bg}}, \tag{3.6}$$

$$s_k^{\mathrm{b}} = s_{k-1}^{\mathrm{b}} + x_{k-1}^{\mathrm{b}+} - x_{k-1}^{\mathrm{b}\text{-}}, \tag{3.7}$$

$$s_1^{\mathrm{b}} = s_k^{\mathrm{b,start}}, \tag{3.8}$$

$$s_K^{\mathrm{b}} = s_k^{\mathrm{b,end}}, \tag{3.9}$$

$$s_k^{\mathrm{t}} = s_{k-1}^{\mathrm{t}} + x_{k-1}^{\mathrm{wh}} - s_{k-1}^{\mathrm{d,t}}, \tag{3.10}$$

$$s_1^{\mathrm{t}} = s_k^{\mathrm{t,start}}, \tag{3.11}$$

$$s_K^{\mathrm{t}} = s_k^{\mathrm{t,end}}. \tag{3.12}$$

Inequality constraints are:

$$x_k^{\mathrm{g}+} \leq \gamma^{\mathrm{g}} d_k^{\mathrm{g}} \tag{3.13}$$

$$x_k^{\mathrm{g}-} \leq \gamma^{\mathrm{g}} (1 - d_k^{\mathrm{g}}) \tag{3.14}$$

$$x_k^{\mathrm{b}+} \leq \gamma^{\mathrm{b}+} d_k^{\mathrm{b}} \tag{3.15}$$

$$x_k^{\mathrm{b}-} \leq \gamma^{\mathrm{b}-} (1 - d_k^{\mathrm{b}}) \tag{3.16}$$

Upper and lower limits of the variables are:

$$0 \leq x_k^{\mathrm{g}+} \leq \gamma^{\mathrm{g}}, \tag{3.17}$$

$$0 \leq x_k^{\mathrm{g}-} \leq \gamma^{\mathrm{g}}, \tag{3.18}$$

$$0 \leq x_k^{\mathrm{b}+} \leq \gamma^{\mathrm{c}}, \tag{3.19}$$

$$0 \leq x_k^{\mathrm{b}-} \leq \gamma^{\mathrm{d}}, \tag{3.20}$$

$$0 \leq x_k^{\mathrm{bd}} \leq \gamma^{\mathrm{d}}, \tag{3.21}$$

$$0 \leq x_k^{\mathrm{bg}} \leq \gamma^{\mathrm{d}}, \tag{3.22}$$

$$0 \leq x_k^{\mathrm{wh}} \leq \gamma^{\mathrm{wh}}, \tag{3.23}$$

$$0 \leq d_k^{\mathrm{pv}} \leq 1 \tag{3.24}$$

$$s^{\mathrm{b,min}} \leq s_k^{\mathrm{b}} \leq s^{\mathrm{b,max}}, \tag{3.25}$$

$$s^{\mathrm{t,req}} \leq s_k^{\mathrm{t}} \leq s^{\mathrm{t,max}}, \tag{3.26}$$

Integer variables are:

$$d_k^{\mathrm{g}}, d_k^{\mathrm{b}} \in \{0, 1\}. \tag{3.27}$$

The above formulated optimisation problem is solved for the whole horizon at once using a standard MILP solver. Here CPLEX is used, however, all commercial solvers gives similar quality solutions. In general, the solutions are of lower quality because of the linear approximations made and the inability to incorporate the probability distributions.

3.1.2 Scenario-based approach

The above deterministic MILP approach can be applied to a stochastic optimisation problem by using a *scenario-based* approach, which is referred to as *stochastic* MILP.

This approach is implemented as follows: First a large set of scenarios are generated by sampling from all combined realisations of the stochastic variables mentioned in Chapter 2. A larger number of scenarios should improve the solutions generated by better incorporating the stochastic variables, but this imposes a greater computational burden. Therefore, heuristic scenario reduction techniques, such as (a) *backward scenario reduction* and (b) *forward scenario selection* are typically employed to obtain a scenario set of size N, which can be solved within a given time with a reasonable accuracy [48].

In this thesis, the backward scenario reduction technique is used to remove scenarios with small probabilities that are similar to scenarios with higher probabilities. The detail steps are described below:

1. Initially N consists of all the scenarios. Let $\mathcal{E}$ be the set of deleted scenarios, which is empty at the start;

2. Compute the distances between all scenario pairs in N;

3. For each scenario $\mathbf{s}^{j,n}$, find the scenario $\mathbf{s}^{j,n,c}$ that is closest to it, and calculate the utility $U(\mathbf{s}^{j,n})$ using:

$$U(\mathbf{s}^{j,n}) = P(\mathbf{s}^{j,n})D(\mathbf{s}^{j,n},\mathbf{s}^{j,n,c}), \tag{3.28}$$

   where $D(\mathbf{s}^{j,n},\mathbf{s}^{j,n,c})$ is the distance between them, given by:

$$D(\mathbf{s}^{j,n},\mathbf{s}^{j,n,c}) = \sqrt{\sum_{k=1}^{K}\left(\mathbf{s}_k^{j,n}-\mathbf{s}_k^{j,n,c}\right)^2}. \tag{3.29}$$

   Note that $P(\mathbf{s}^{j,n})$ is the probability that corresponds to scenario $\mathbf{s}^{j,n}$.

4. Remove the scenario $\mathbf{s}^{j,n}$ with the smallest utility value from N and add it to E;

5. Update the probability of the closest scenario $\mathbf{s}^{j,n,c}$ using:

$$P(\mathbf{s}^{j,n,c}) = P(\mathbf{s}^{j,n,c}) + P(\mathbf{s}^{j,n}). \tag{3.30}$$

6. Repeat steps 3, 4 and 5 until we find the desired number of scenarios, that can quickly solve the SHEMS problem with a reasonable accuracy.

Given this, a scenario-based stochastic MILP formulation of the problem is described by:

$$\min \sum_{n=1}^{N} P_n(\mathbf{s}^{j,n}) \sum_{k=1}^{K} \left(s_k^{\text{p,buy}} x_k^{\text{g+}} - s_k^{\text{p,sell}} x_k^{\text{g-}} \right), \tag{3.31}$$

where $P_n(\mathbf{s}^{j,n})$ is the probability of a particular scenario n corresponding to realizations of stochastic variables $\mathbf{s}^j$, subject to $\sum_{n=1}^{N} P_n(\mathbf{s}^{j,n}) = 1$. These probabilities are from the kernel estimations in Chapter 2.

The solution time of stochastic MILP grows exponentially with the length of the decision horizon because the deterministic problem is solved for the whole horizon at once and the number of scenarios increases as the length of the horizon increases. As such, in the existing literature, a one day optimisation horizon is typically assumed. Moreover, it is computationally difficult to solve the SHEMS problem at every time-step using existing smart meters. Given this, the solutions from stochastic MILP are of lower quality because of the linear approximations made and the inability to incorporate all the probability distributions [56]. In response to these limitations, DP is used to solve the SHEMS problem, which is expected to improve the solution quality.

3.2 Dynamic Programming

DP is an optimisation approach that transforms a complex problem into a sequence of simpler problems; its essential characteristic is the multi-stage nature of the optimisation problem. The problem in (2.7) is easily cast as an MDP due to the separable objective function and Markov property of the transition functions. Given this, DP solves the MDP form of (2.7) by computing a value function $V^{\pi}(\mathbf{s}_k)$. This is the expected future cost of following a policy, π, starting in state, $\mathbf{s}_k$, and is given by:

$$V^{\pi}(\mathbf{s}_k) = \sum_{\mathbf{s}' \in \mathcal{S}} \mathbb{P}(\mathbf{s}' | \mathbf{s}_k, \pi(\mathbf{s}_k), \omega_k) \left[C(\mathbf{s}_k, \pi(\mathbf{s}_k), \mathbf{s}') + V^{\pi}(\mathbf{s}') \right]. \tag{3.32}$$

Algorithm 1 : Value iteration using DP

```
1: Initialise V_k,    k ∈ K,
2: for k = K,...,1 do
3:     for b = 1,...,B do
4:         Set s_k.
5:         for r = 1,...,R do
6:             Calculate the future value (3.33).
7:         end for
8:         Compute the expected future value from s_k (3.32).
9:     end for
10: end for
```

An optimal policy, π^*, is one that minimises (3.32), and which also satisfies Bellman's optimality condition:

$$V_k^{\pi^*}(\mathbf{s}_k) = \min_{\pi^*} \left(C_k(\mathbf{s}_k, \pi(\mathbf{s}_k)) + \mathbb{E}\left\{ V_{k+1}^{\pi^*}(\mathbf{s}') | \mathbf{s}_k \right\} \right). \tag{3.33}$$

The expression in (3.33) is typically computed using backward induction, a procedure called *value iteration*, and then an optimal policy is extracted from the value function by selecting a minimum value action for each state. The pseudo-code of the value iteration algorithm is given in Algorithm 1.

In detail, Algorithm 1 proceeds as follows:

1. Set initial value functions to zero. In order to control the end-of-day states, we have to penalise all the undesired states or provide a benefit for the desired states in the value function at $K+1$ (line 1).

2. Loop over all the possible combinations of the state variables of different controllable devices, where b is a particular combination of state variables and B is the total (lines 3-9).

3. Loop over all the possible combinations of non-controllable inputs, where r is a particular combination and R is the total. Calculate the future cost from the state we are at $\mathbf{s}_k$ using (3.33). Here the contribution function is calculated using the current combination of the non-controllable inputs (lines 5-7).

4. Calculate the expected future cost from $\mathbf{s}_k$ using (3.32). The probabilities are from the kernel estimations in Chapter 2 (line 8).

An illustration of a deterministic DP using a simplified model of a battery storage is shown in Fig. 3.1. The difference here from the stochastic problem is that we don't have to

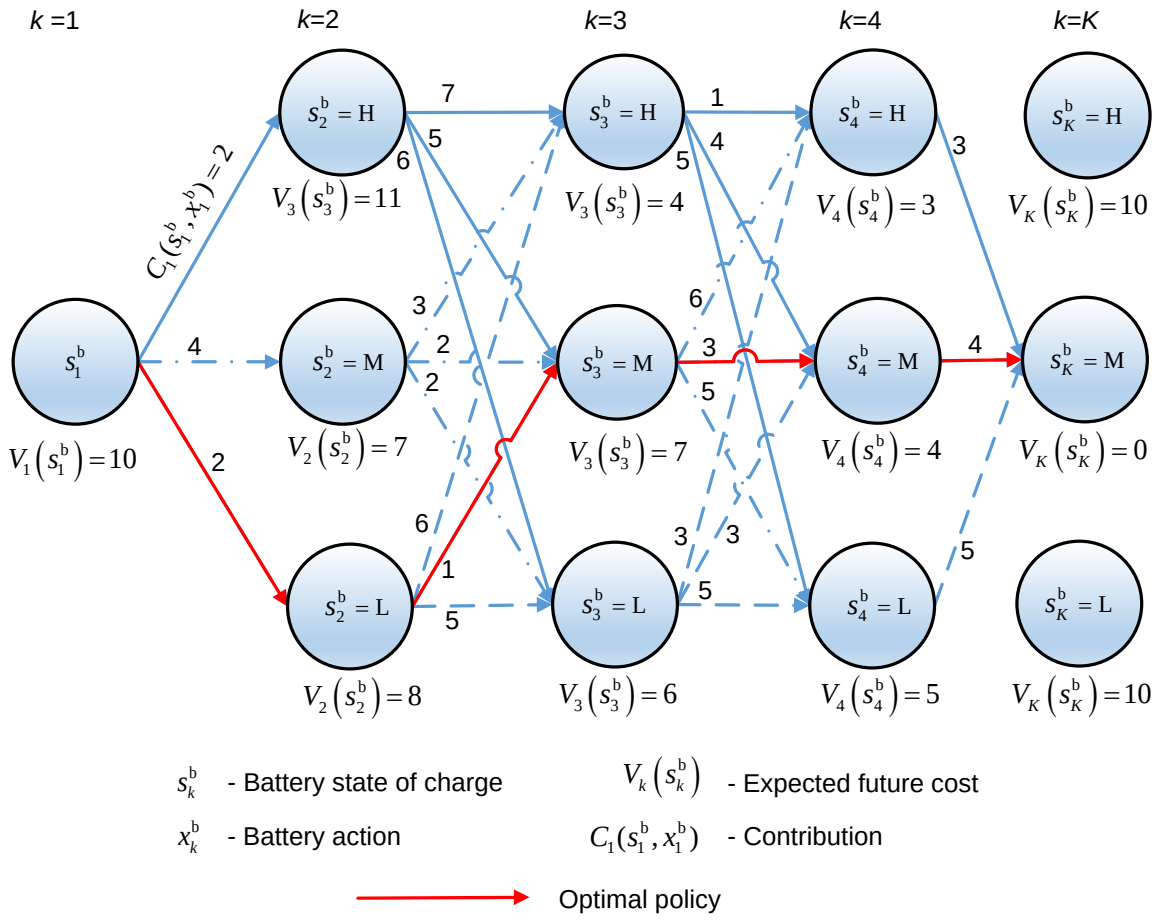

Fig. 3.1 A deterministic DP example using a battery storage, where expected future cost is calculated using (3.33). The instantaneous contributions from the battery decisions are on the edges of the lines while the expected future cost is below the states. The optimal policy satisfies (2.7), which is obtained using (3.33).

loop over all the possible combinations of the non-controllable inputs, as in Algorithm 1. At every time-step, there are three battery SOC states (i.e. highest, middle, and lowest) and three possible battery actions that results in different instantaneous costs. At the last time-step, $k = K$, the expected future cost from the desired state, s_k= M, is zero, while the other two states are penalised with a large cost. This is an important step that allows us to control the end-of-day battery SOC (helpful in Chapter 4). The expected future cost at every possible state is calculated using (3.33), which is the minimum of the combined instantaneous cost that results from the decision that we take and the expected future cost from the state we end up at the next time-step. In Fig 3.1, instantaneous cost is on the edges of the lines while the expected future cost is below the states. Note that a value function at a given time-step consists of the expected future cost from all the states.

Table 3.1 Daily simulation results from deterministic optimisations

Total daily:	Scenario 1	Scenario 2
PV output (kWh)	9.27	6.05
Electrical demand (kWh)	24.72	64.75
Thermal demand (kWh)	10.42	19.1
Benchmark ($)	6.13	10.5
DP ($)	3.16	8.04
MILP ($)	3.22	8.14

An optimal policy is extracted from the value functions by selecting a minimum value action for each state using (3.33). For example, from s_1^{b}, if we take the optimal decision to go to s_2^{b}= L then the total combined cost of 10 consists of an instantaneous cost of 2 and an expected future cost of 8. Even though the expected future cost of 7 from s_2^{b}= M is lower than the expected future cost from s_2^{b}= L, the instantaneous cost that takes us there is 4 so the total combined cost is 11. Given this, the expected future cost of following the optimal policy from s_1^{b} is 10 and at time-step 2 we will be at s_2^{b}= L.

Now we compare deterministic and stochastic optimisations using DP and MILP.

3.3 Simulation Results and Discussion

There are two sets of comparisons. The first is a comparison of deterministic optimisations using DP and MILP, assuming a perfect foresight for PV output and electrical and thermal demand. The second is a comparison of stochastic and deterministic optimisations using DP and MILP under uncertainty. For illustration purposes of each of the comparisons, we consider two scenarios that are on 2$^{\mathrm{nd}}$ July, 2012 and 20$^{\mathrm{th}}$ August, 2012 for a residential building in Central Coast, NSW, Australia with a 2.22 kWp PV system. All the device parameters are in Fig 2.3 and Table 2.1 of Chapter 2. The ToUP signal is in Fig. 2.2.

3.3.1 Deterministic optimisations using DP and MILP

The schedules from deterministic MILP and DP approaches are shown in Fig. 3.2 and Fig 3.3 for the two scenarios. Here we consider PV, battery, and TES units and assume a perfect foresight so the actual and the estimated values of the PV output and electrical and thermal demand are the same. Note that this is difficult to achieve in practice so these simulations are only carried out to give the reader an understanding of an ideal scenario and to highlight the benefits of DP over MILP.

The benchmark electricity cost in Table 3.1 is the combined electricity cost when there is no PV-battery system (entire electrical demand is supplied by the grid) and the TES is controlled by a dummy mechanism. The dummy control system always keeps the TES SOC at the minimum required TES SOC. Note that the TES SOC in both Fig. 3.2 and Fig. 3.3 is shown after the thermal demand is supplied to the household so the TES SOC can sometimes be less than the minimum required TES SOC. From the dummy control system, the electric water heater will have to be used a lot during the peak periods (2.30 pm to 8pm), as shown in Fig. 3.2(d) and Fig 3.3(d). On the other hand, electric water heater input and the electrical grid power from DP and MILP based SHEMSs are minimised during peak periods. This is because the DP and MILP approaches charges the battery and the TES up to a certain level before the beginning of peak-periods, as depicted in Fig. 3.2(c) and (e) and Fig 3.3(c) and (e), respectively.

The DP approach results in lower electricity cost for both Scenario 1 and Scenario 2 compared to MILP, as shown in Table 3.1. In more detail, the DP based SHEMS reduces the total electricity cost by 48.45% and 23.43% for Scenarios 1 and 2, respectively, while MILP only reduces it by 47.47% and 22.48%. The reason is that DP properly incorporates non-linear constraints, as explained in Chapter 2, such as the battery discharge and inverter efficiencies, maximum charge rate of the battery, and battery and TES losses. Note that these benefits are only over a day so add up to a significant impact on the household's yearly costs (see more in Chapter 5 and 6). The deterministic MILP only takes seconds to compute a solution while DP takes approximately 26 minutes as we have to loop over all the possible combinations of battery and TES SOC states.

3.3.2 Optimisation under uncertainty

Here we consider a PV-battery system. The PV and electrical demand models are estimated according to Chapter 2. The yearly optimisation results from stochastic and deterministic DP and stochastic MILP is given in Table 3.2 for two smart homes:

1. Central coast, NSW, Australia based residential building with a 2.22 kWp PV system;
2. Sydney, NSW, Australia based residential building with a 3.78 kWp PV system.

In practical applications, the accuracy of the estimates depends on the user's (or the prediction algorithm's) ability to correctly determine the PV and electrical demand clusters. Given this, two sets of comparisons are given for (A) reasonably good estimates (five PV clusters and nine electrical demand clusters with six attributes); and (B) estimates with the minimum expected quality (three clusters for PV output and one cluster for electrical demand).

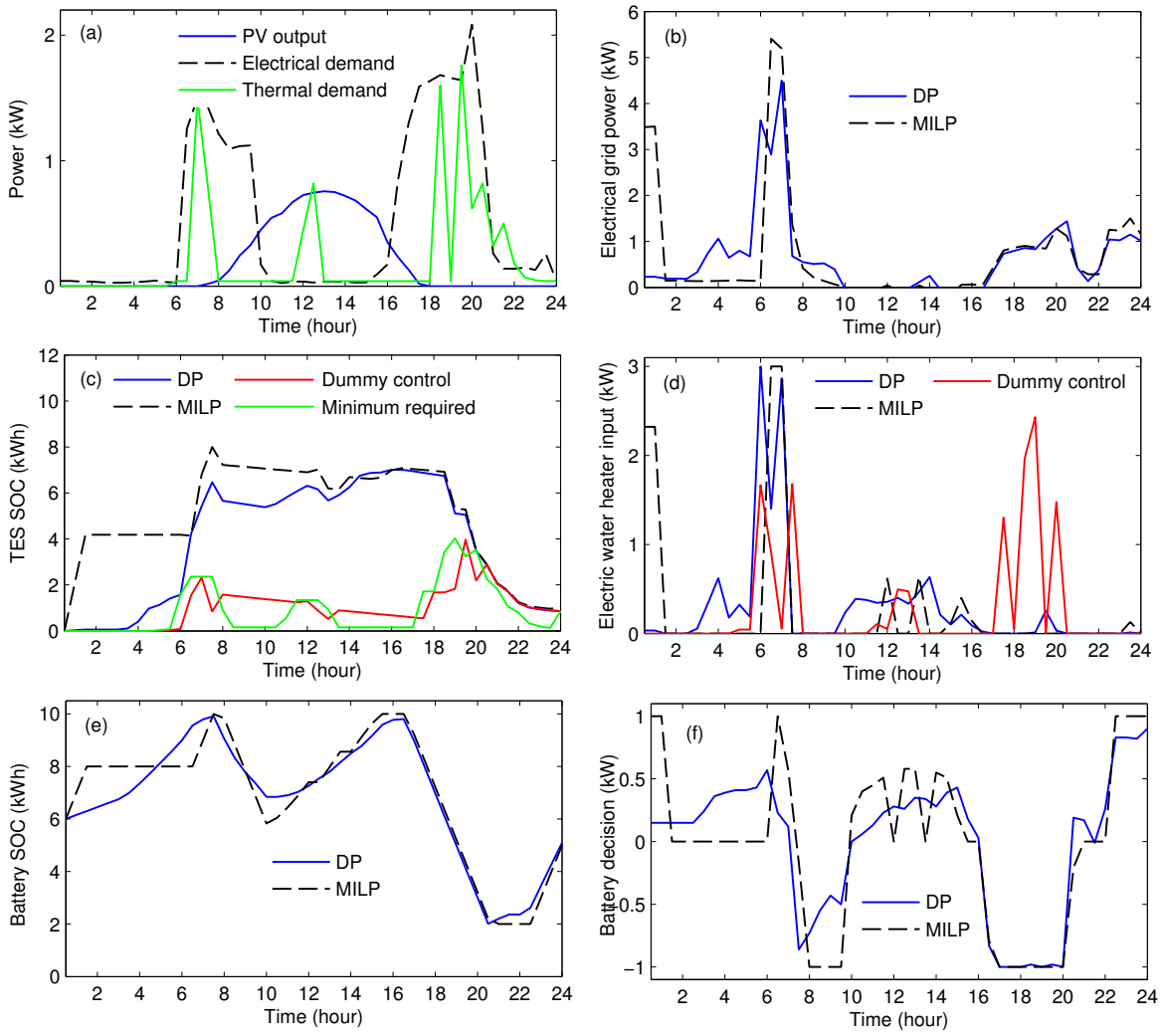

Fig. 3.2 A comparison of deterministic DP and MILP for Scenario 1: (a) PV output, electrical and thermal demand; (b) electrical grid power; (c) TES SOC; (d) electric water heater input; (e) battery SOC; and (f) battery decisions.

Our results shows that stochastic DP results in better quality solutions for all the cases followed by deterministic DP and then stochastic MILP. We noticed that for the lower quality estimates, stochastic DP will result in 5.13% and 3.37% improvement in electrical cost over deterministic DP for smart homes 1 and 2 respectively. The improvement is only 0.13% and 1.07% for smart homes 1 and 2, respectively, when the estimates are accurate. In summary, we need to use a stochastic optimisation approach because the estimates of the electrical demand and PV output are not always accurate as they depend on the user's ability to choose the correct cluster. However, the computational time of DP increases exponentially when we loop over all the possible outcome spaces (i.e. on top of the computational burden from

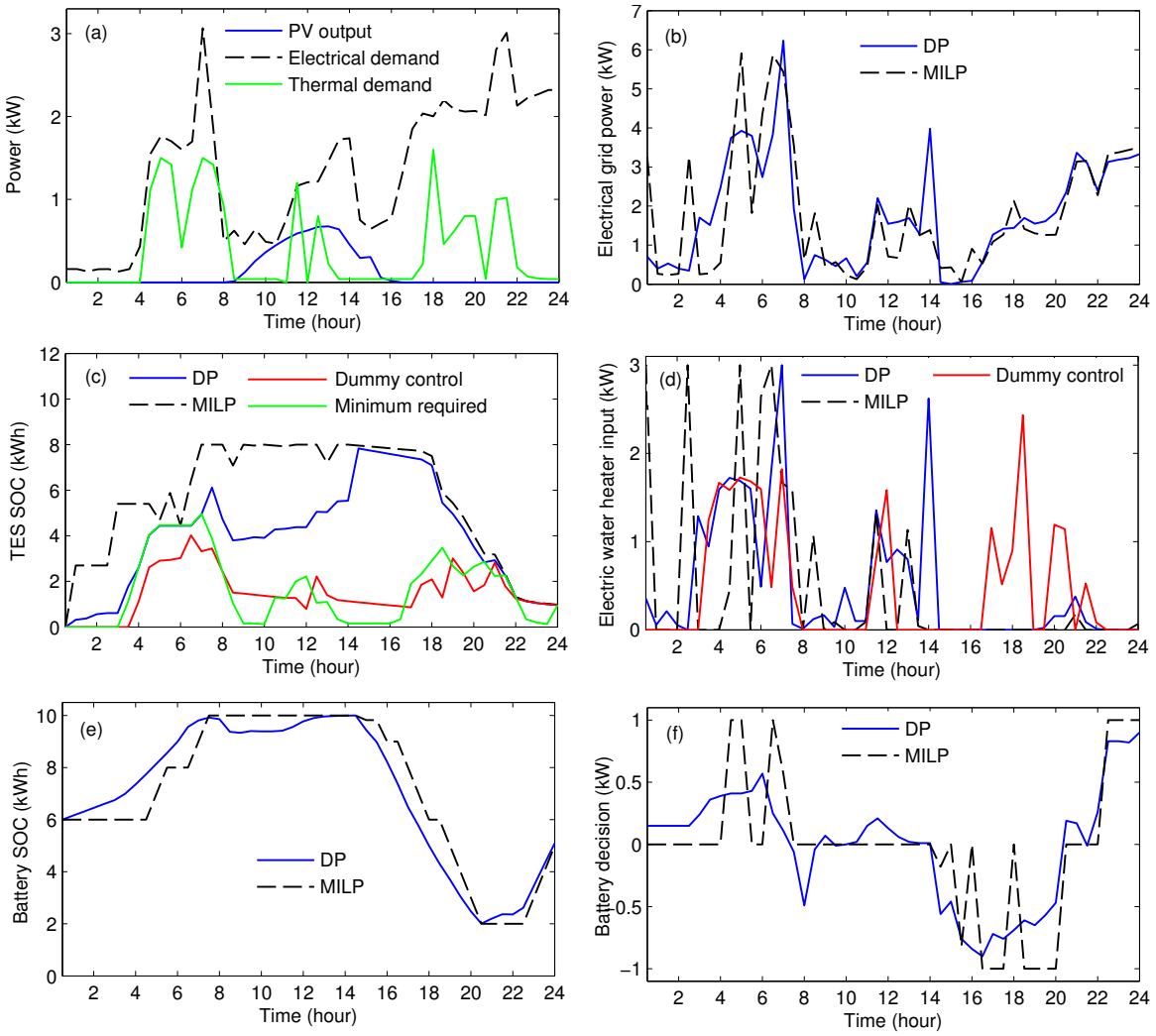

Fig. 3.3 A comparison of deterministic DP and MILP for Scenario 2: (a) PV output, electrical and thermal demand; (b) electrical grid power; (c) TES SOC; (d) electric water heater input; (e) battery SOC; and (f) battery decisions.

deterministic DP). Given this, our aim is to obtain a solution technique that can consider the stochastic nature without a noticeable increase in the computational burden (see Chapter 5).

For illustration purposes, we compare the daily schedules from stochastic and deterministic DP and stochastic MILP in Fig. 3.4 and Fig. 3.5; and a summary of their results are in Table 3.3. Important observations are as follows: the stochastic MILP approach charges the battery unnecessarily in both cases as the expected PV output is higher than the actual values. On the other hand, both the DP approaches charges battery up to a minimum required level before the peak period and recharges the battery after 10 pm (off-peak) with the highest possible charge rate to meet the end-of-day battery SOC constraint. The only difference is

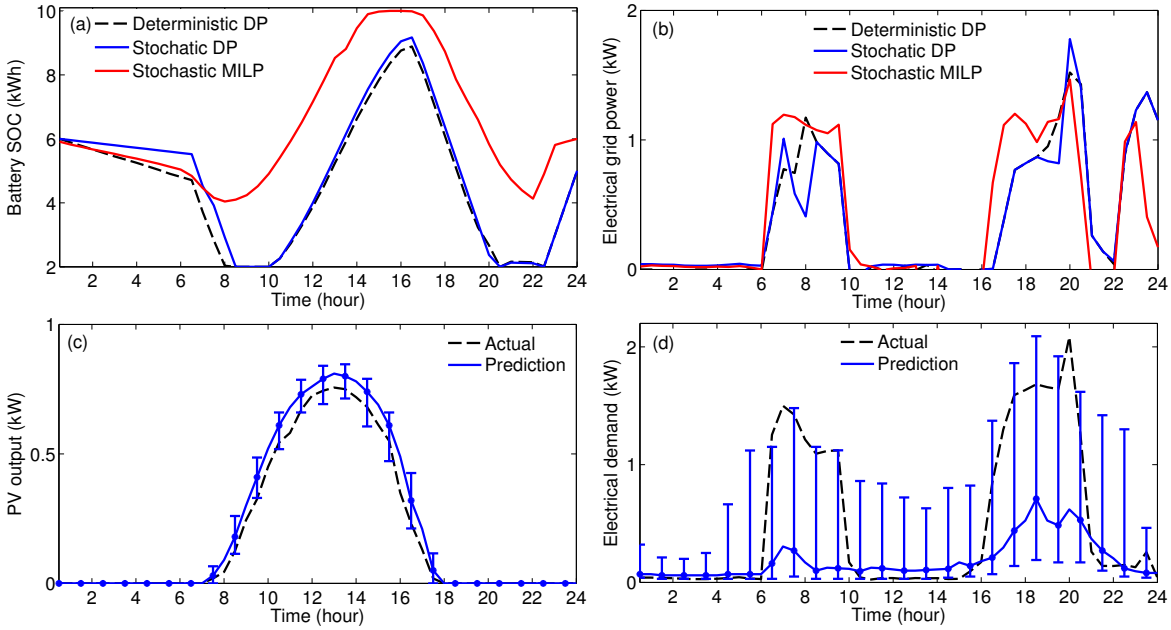

Fig. 3.4 A comparison of deterministic DP, stochastic DP and stochastic MILP for Scenario 1 (under uncertainty): (a) battery SOC; (b) electrical grid power; actual and estimated (c) PV output; and (d) electrical demand (3 PV and 1 demand clusters).

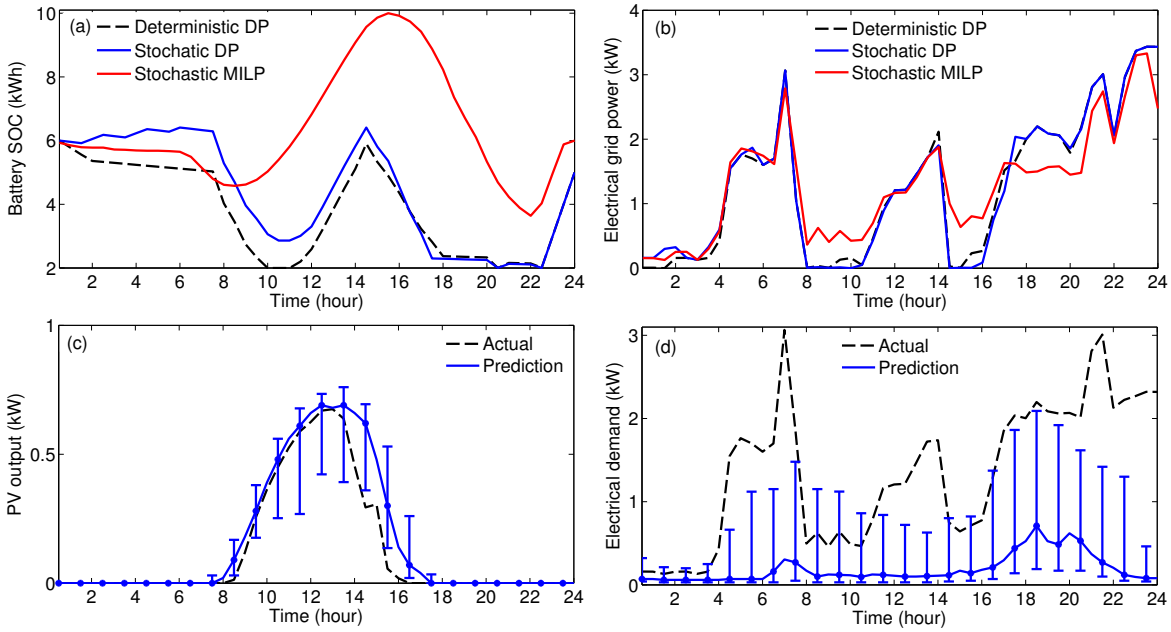

Fig. 3.5 A comparison of deterministic DP, stochastic DP and stochastic MILP for Scenario 2 (under uncertainty): (a) battery SOC; (b) electrical grid power; actual and estimated (c) PV output; and (d) electrical demand (3 PV and 1 demand clusters).

that stochastic DP expects a high demand and have a higher battery SOC at the beginning of peak periods compared to deterministic DP.

Table 3.2 Year-long simulation results

Total yearly:	Household 1	Household 2
PV output (MWh)	2.91	5.99
Electrical demand (MWh)	4.29	9.82
Benchmark ($)	568.094	1208.3
PV (no storage) ($)	440.52	821.7
Stochastic DP (A) ($)	253.62	546.86
Deterministic DP (A) ($)	253.95	552.75
Stochastic DP (B) ($)	258.59	588.76
Deterministic DP (B) ($)	267.62	620.6
Stochastic MILP ($)	369.8	700.14

Table 3.3 Daily simulation results for two scenarios under uncertainty (PV-battery systems)

Total daily:	Scenario 1	Scenario 2
PV output (kWh)	9.27	6.05
Electrical demand (kWh)	24.72	64.75
Benchmark ($)	4.00	7.94
Stochastic DP ($)	2.40	6.81
Deterministic DP	2.49	6.89
MILP ($)	3.01	7.15

3.4 Summary

This chapter compared stochastic and deterministic versions of the DP and MILP using scenarios with different PV and demand profiles. Our simulation results showed that stochastic DP performs better than both deterministic DP and stochastic MILP. We also noted that benefits from the stochastic optimisation is higher when the error between the actual and the kernel estimated PV and electrical demand is high.

There are several reasons to prefer DP over MILP. First, DP produces close-to-optimal solutions when the value functions obtained during the offline planning phase are from finely discretised state, action and outcome spaces. Second, in practical applications, the SHEMS can make real-time decisions using the policy implied by (3.33). This means that at each time-step, the optimal decision from the current state can be executed. Note that (3.33) is a simple linear program at each time-step so is computationally feasible using existing smart meters. This stands in contrast to a stochastic MILP formulation, which would involve solving the entire stochastic MILP program, which is computationally difficult even for the offline planning. Third, we can always obtain a solution with DP regardless of the constraints and the inputs while MILP fails to find a solution when the constraints are not satisfied. From our experience, MILP fails to find a solution when the end-of-day TES SOC is fixed, because the energy out of the TES unit can not be controlled, which is the thermal demand of the household. We can overcome this by either removing the end-of-day TES constraint or by having a range of values. However, this means we end up with a sub optimal level of TES SOC at the end of the day or require user interaction to adjust the TES SOC, which we should avoid in practical applications.

Given these insights, DP is the better solution technique in terms of the solution quality. However, the required computation to generate value functions using DP grows exponentially with the size of the state, action and outcome spaces. One way of overcoming this problem is to approximate the value function, while maintaining the benefits of DP (see proposed ADP approach in Chapter 5). Before that, Chapter 4, identifies the benefits of extending the decision horizon by proposing a multi-stage stochastic optimisation framework. This is a longer-horizon solver using deterministic MILP (computationally fast) and a more detail shorter-horizon solver using DP (better quality solutions).

Chapter 4

Evaluation of a Multi-stage Stochastic Optimisation Framework

This chapter identifies the benefits of PV-battery systems coupled with a SHEMS that considers uncertainties over several days. To illustrate the benefits, consider a few sunny days with low demand (e.g. a weekend) followed by a few cloudy days with high demand; in anticipation of this, the SHEMS may adjust the end-of day battery SOC to reap significant financial benefits. The uncertainties over several days can be considered by extending the decision horizon of the SHEMS. However, increasing the decision horizon is difficult because of the computational burden associated with the currently proposed solution techniques such as DP and stochastic MILP.

Given these insights, this chapter evaluates the benefits of increasing the SHEMS decision horizon by using a multi-stage stochastic optimisation framework. This is a two-stage lookahead optimisation, which extracts the end-of-day one battery SOC from a longer-horizon solver that uses MILP and is used in daily horizon solver that uses DP. In doing so, this chapter also identifies the benefits of residential PV-battery systems coupled with an SHEMS. Note that this two-stage lookahead falls into the second of the four classes of policies explained in Chapter 1.

This chapter is structured as follows: First, implementation details of the two-stage lookahead is presented. The simulation results section presents comparisons of the two-stage lookahead and a daily DP method for four households. Finally, the conclusions section summarises the benefits and the drawbacks of the two-stage lookahead, which is used as a motivation for the proposed ADP approach in Chapter 5.

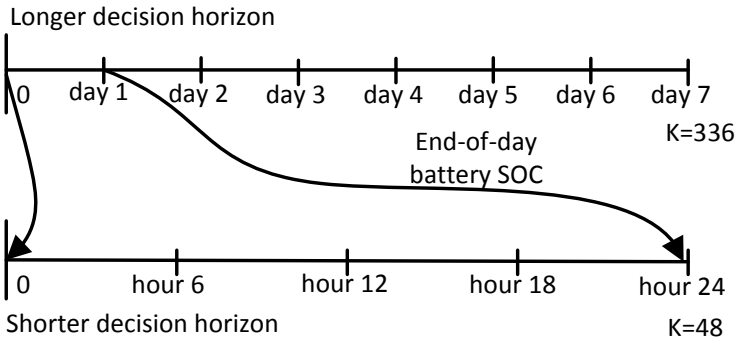

Fig. 4.1 Illustration of a two-stage lookahead optimisation, where the end-of-day battery SOC for the shorter decision horizon optimisation is extracted from the longer decision horizon optimisation.

4.1 Implementation

The residential building considered in this chapter consists of a PV system and a battery storage system. A comparison is made of two approaches to optimising the operation of this PV-battery system: (i) a one-stage daily DP method with a fixed end-of-day SOC constraint, and (ii) a two-stage method, considering the SHEMS problem over a week-long decision horizon, which is solved using deterministic MILP, and which is used to set the end-of-day battery SOC constraint for a daily DP method. In a practical implementation, the longer decision horizon optimisation is carried out before the start of each day to approximate its end-of-day battery SOC, which is referred to as a rolling horizon approach. By making the required battery SOC at the end of the day depend on the PV output and the predicted demand of future days, the overall system performance should be improved. For both the one stage and two-stage methods, the daily decision horizon is a 24 hour period, divided into 30 minutes time-steps, giving a total of K=48 time-steps. For the two-stage method, the longer decision horizon is a week, divided into 30 minutes time-steps, giving a total of K=336 time-steps. These are illustrated in Fig 4.1. The SHEMSs using DP and MILP are implemented according to Chapter 3. To recap, the SHEMS is operating according to the following:

- The battery is charged with the highest possible charge rate if the power generated from the PV system is greater than the household demand.
- Send electrical power back to the grid if the power generated by the PV system is greater than the electrical demand of the household and the highest possible charge rate of the battery.

Next section compares the two-stage lookahead with a daily DP method.

Table 4.1 A summary of the weekly optimisation results from one-stage and two-stage optimisations

	One-stage ($)	Two-stage ($)
Scenario 1 (Household 3 Week 1)	0.33	0.18
Scenario 2 (Household 3 Week 2)	6.37	6.23
Scenario 3 (Household 3 Week 3)	1.67	1.54
Scenario 4 (Household 3 Week 4)	2.42	2.25
Scenario 5 (Household 4 Week 1)	0.33	0.28
Scenario 6 (Household 4 Week 2)	8.56	8.19
Scenario 7 (Household 4 Week 3)	5.79	5.74
Scenario 8 (Household 4 Week 4)	7.08	6.67

4.2 Simulation Results

The simulations are carried out using the two-stage lookahead and a one-stage daily DP over a year for four residential buildings:

1. Central coast, NSW, Australia based residential building with a 2.22 kWp PV system;
2. Sydney, NSW, Australia based residential building with a 3.78 kWp PV system;
3. Residential building based in Central coast and has a 2.04 kWp PV system;
4. Residential building based in Sydney and has a 4.04 kWp PV system.

Then the simulation results are given in three sections. The first section illustrates weekly simulation results for four scenarios each for residential buildings 3 and 4. The second section presents the simulation results for all four households over a year. The third section identifies the benefits of extending the decision horizon of a one-stage optimisation using DP. The stochastic variables are according to Chapter 2; the device characteristics are in Fig 2.3 and Table 2.1; and the ToUP signal is in Fig. 2.2.

4.2.1 Weekly optimisation

The simulation results are illustrated for the following four weeks:

1. The first week of January, 2013;
2. The first week of July, 2012;
3. From 10^{th} to 16^{th} October, 2012;

4. From April 10^{th} to 16^{th}, 2013.

The Scenarios 1-4 are for residential building 3 and Scenarios 5-8 are for residential building 4. The Fig. 4.3, Fig. 4.4, Fig. 4.5, and Fig. 4.6 show the PV output, electrical demand, battery SOC and electricity cost for Scenarios 1-4. As expected, the PV output and electrical demand varies over the week. The start-of-day and end-of-day battery SOC from the one-stage optimisation are the same ($s_1^{\mathrm{b}} = s_K^{\mathrm{b}} = 6$ kWh) for all the days. In most of the scenarios the start-of-day battery from the one-stage and two-stage optimisations are not the same because these illustrations are taken from the yearly optimisation results. This also applies for the end-of-day battery SOC.

The total electricity cost is reduced by 45%, 2.2%, 7.78%, 7.02%, 15.15%, 4.32%, 0.86%, 5.8% for Scenarios 1 to 8, respectively, by using the two-stage optimisation, as shown in Table 4.1. This is because the end-of-day battery SOC is controlled using the two-stage optimisation compared to having a fixed end-of-day battery SOC with one-stage daily optimisation. The important observations are as follows: In Scenario 1 (Fig. 4.3), for the first two days, there is an electricity cost from two-stage optimisation compared to having no cost from the one-stage optimisation. This is because the start-of-day battery SOC is lower for the two-stage optimisation, which means electricity cost from the previous week has been reduced significantly. For the rest of the week, electricity cost is lower for the two-stage optimisation. In Scenario 2 (Fig. 4.4), everyday in the week have a high evening demand and day 6 also has a high morning demand. The PV output is similar throughout the week with not much variation (winter week). In response to this, the two-stage minimised the end-of-day SOC except for the end-of-day SOC of day five as we are expecting a high morning demand on day 6. In Scenario 3, electricity cost for day one is higher for two-stage lookahead because the two-stage started the day at 4 kWh and ended at 10 kWh while the both start and end values for one-stage are 6 kWh. The day two is cloudy and has a high demand so having the maximum battery at the end of the day is the best thing to do. In Scenario 4, days 3-5 and 7 are sunny compared to cloudy day 6. In anticipation of this, the two-stage lookahead gives a higher start-of-day battery SOC and lower end-of-day battery SOC for day 6 compared to the one-stage optimisation.

4.2.2 Year-long simulation

The summary of the yearly simulation results are given in Table 4.2 for four households. The results showed that the yearly electricity cost can be saved by 4.16%, 0.93%, 8.54% and 3.88% for Households 1, 2, 3 and 4, respectively by using a two-stage lookahead optimisation. However, these benefits decreases to 2.1%, -3.9%, 5.78% and 3.06% when the quality of

the PV output and electrical demand estimates reduces. The reason is that the two-stage lookahead had to resort to deterministic MILP to solve the longer decision horizon so fixing the end-of-day battery SOC in the daily horizon estimate begins to have negative influence when the forecasts becomes inaccurate. For example, if we are expecting a low morning demand in the next day, the end-of-of day battery SOC of the current day will be minimised, however, this has negative influence if the next days actual morning demand goes high. Also, fixing the end-of-day SOC has negative effects if the current day's actual PV output and electrical demand deviates from the estimates. Although there are still considerable amounts of electricity cost savings, they can further decrease if the forecasts become more inaccurate. Therefore, it is difficult to exactly obtain the end-of-day battery SOC to capture future variations in PV and demand under uncertainty. Given this, the next section explores the benefits of extending the decision horizon of a one-stage optimisation using DP. Note that this is only for simulation purposes as it requires high computational power to solve the SHEMS problem using DP beyond one day.

4.2.3 Effects of extending the decision horizon

Extending the decision horizon of the one-stage optimisation beyond one day to consider inter-daily variations in PV output and electrical demand results in significant benefits, as depicted in Fig. 4.2, which shows the normalised electricity cost vs. length of the decision horizon. Note that the benefits of extending the decision horizon varies depending on the household, which is discussed in the next chapter. The results show that increasing the decision horizon beyond two days has no significant benefits on average. However, increasing the decision horizon up to one week is beneficial in some situations, e.g. off-the-grid systems and if there are high variations in PV output and demand. These results are obtained using a DP based SHEMS for ten households over two months. Here DP is used to obtain the exact solution, however in practical implementations, extending the decision horizon with DP is difficult as the computational power is limited in existing smart meters. Given these insights, the next chapter proposes an ADP approach to extend the decision horizon with low computational burden.

4.3 Summary

This chapter proposed a two-stage look-ahead optimisation for considering uncertainties over several days. Here a longer decision horizon solver that uses deterministic MILP is used to capture future information in the end-of-day battery SOC, which is used to solve a

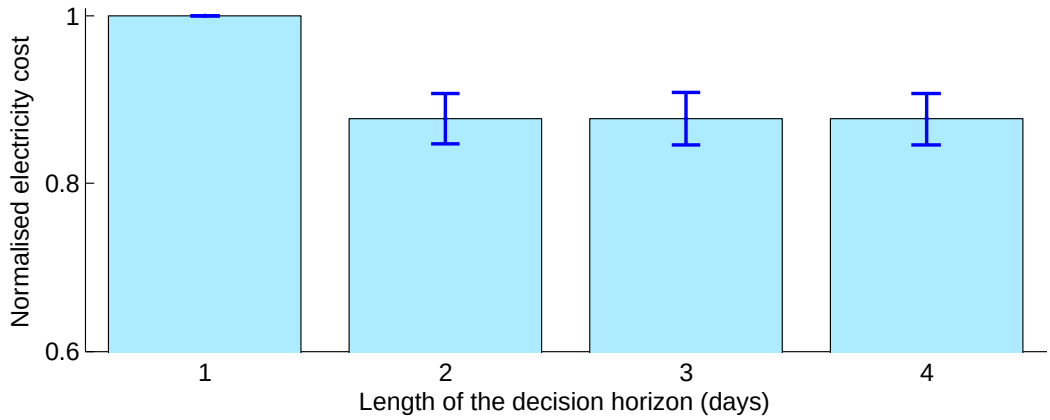

Fig. 4.2 The benefits of extending the decision horizon of a one-stege optimisation using DP.

daily optimisation problem using DP. The two-stage optimisation results in financial benefits compared to a daily DP method with a fixed end-of-day battery SOC constraint. However, the amount of cost savings depends on the accuracy of the forecasts because the longer decision horizon is solved using deterministic MILP and the end-of-day SOC of the daily horizon is fixed regardless of what happened in the current day. Given this, the benefits of extending the decision horizon is investigated using a one-stage DP based SHEMS. The results showed that there are significant benefits when considering uncertainties over two-days and beyond that no significant benefits on average.

Given these findings, when making decisions under uncertainty, the end-of-day battery SOC has to be flexible and should depend on the future information as well what actually happened in the current day. Moreover, the length of the decision horizon should be at least two-days. As such, the aim of Chapter 5 is to propose an ADP approach that can extend the decision horizon of the SHEMS problem with low computational burden. ADP will always be used over two-days compared to DP and stochastic MILP. Note that when extending the decision horizon over two-days, the end-of-day battery SOC will be flexible depending on what actually happened in the current day.

Table 4.2 Year-long simulation results from two-stage lookahead and daily DP

Total yearly:	Household 1	Household 2	Household 3	Household 4
PV output (MWh)	2.91	5.99	2.87	5.28
Electrical demand (MWh)	4.29	9.82	3.23	5.77
Benchmark ($)	568.094	1208.3	389.4	686.4
PV (no storage) ($)	440.52	821.7	268.54	509.8
One-stage DP (accurate)	238.771	527.51	102.35	271.92
Two-stage lookahead (accurate)	228.83	522.6	93.614	261.37
One-stage DP (less accurate)	253.62	546.86	112.71	284.75
Two-stage lookahead (less accurate)	248.34	567.36	106.195	276.05

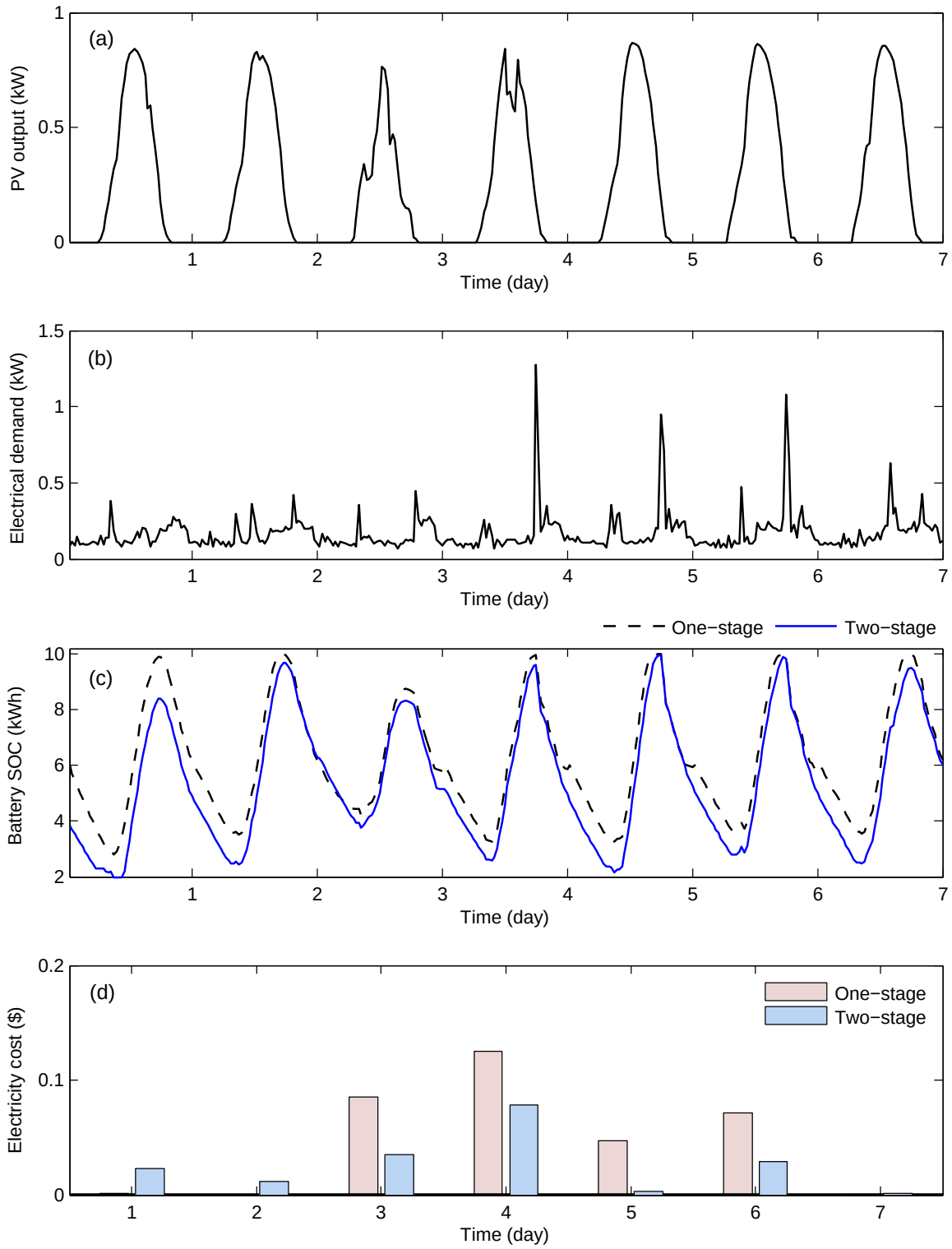

Fig. 4.3 Optimisation results for Scenario 1 from one-stage and two-stage lookahead: (a) PV output; (b) electrical demand; (c) battery SOC; and (d) electricity cost.

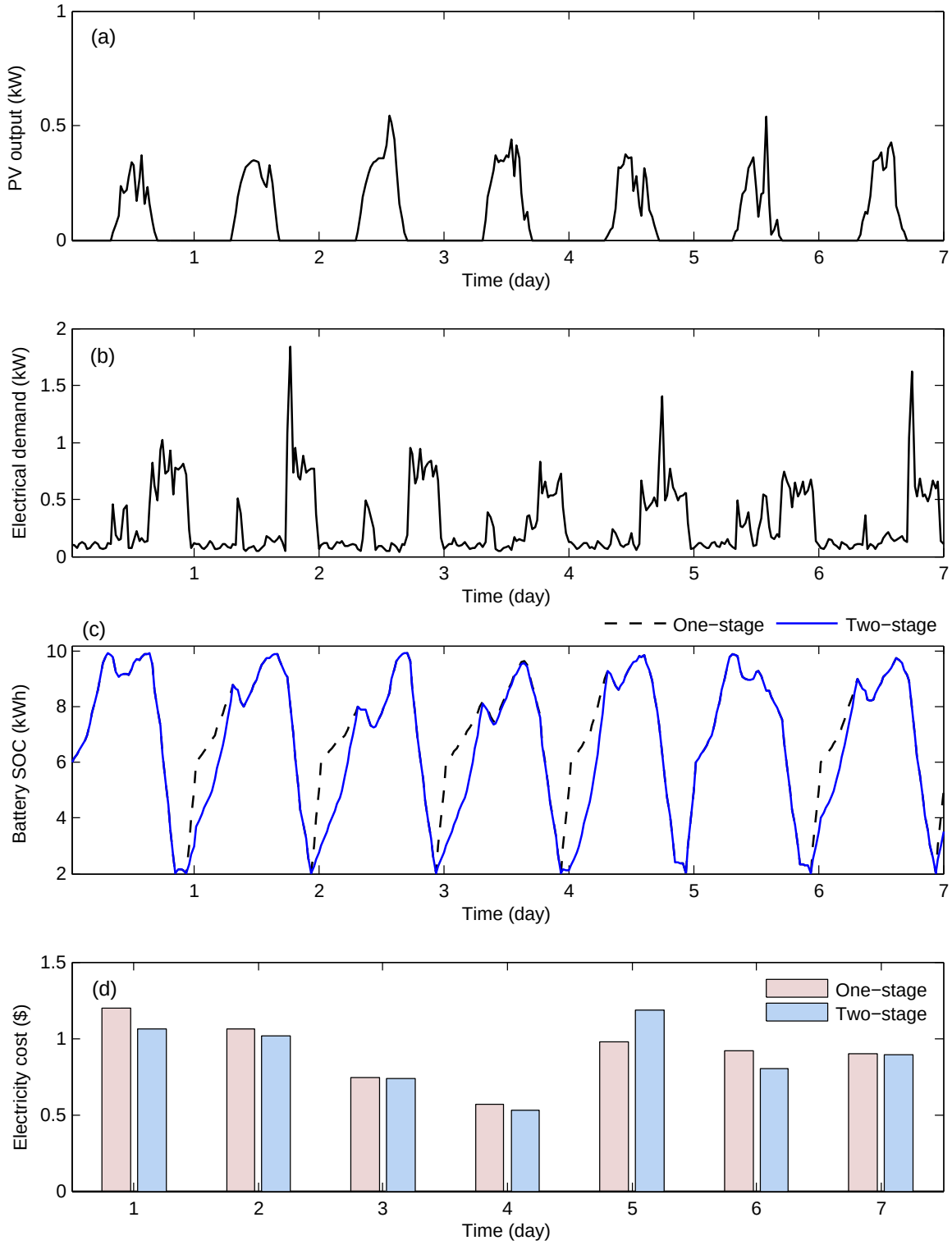

Fig. 4.4 Optimisation results for Scenario 2 from one-stage and two-stage lookahead: (a) PV output; (b) electrical demand; (c) battery SOC; and (d) electricity cost.

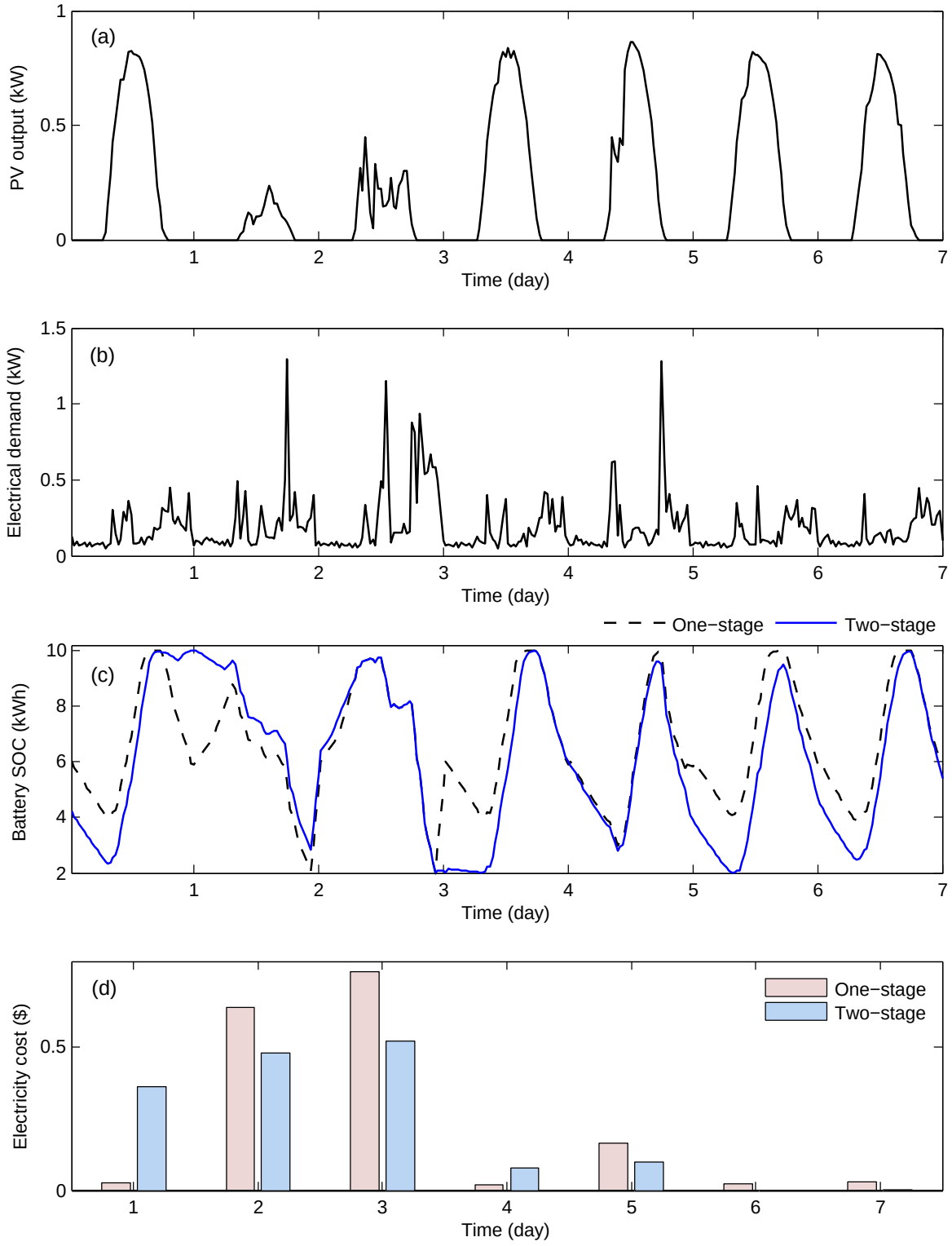

Fig. 4.5 Optimisation results for Scenario 3 from one-stage and two-stage lookahead: (a) PV output; (b) electrical demand; (c) battery SOC; and (d) electricity cost.

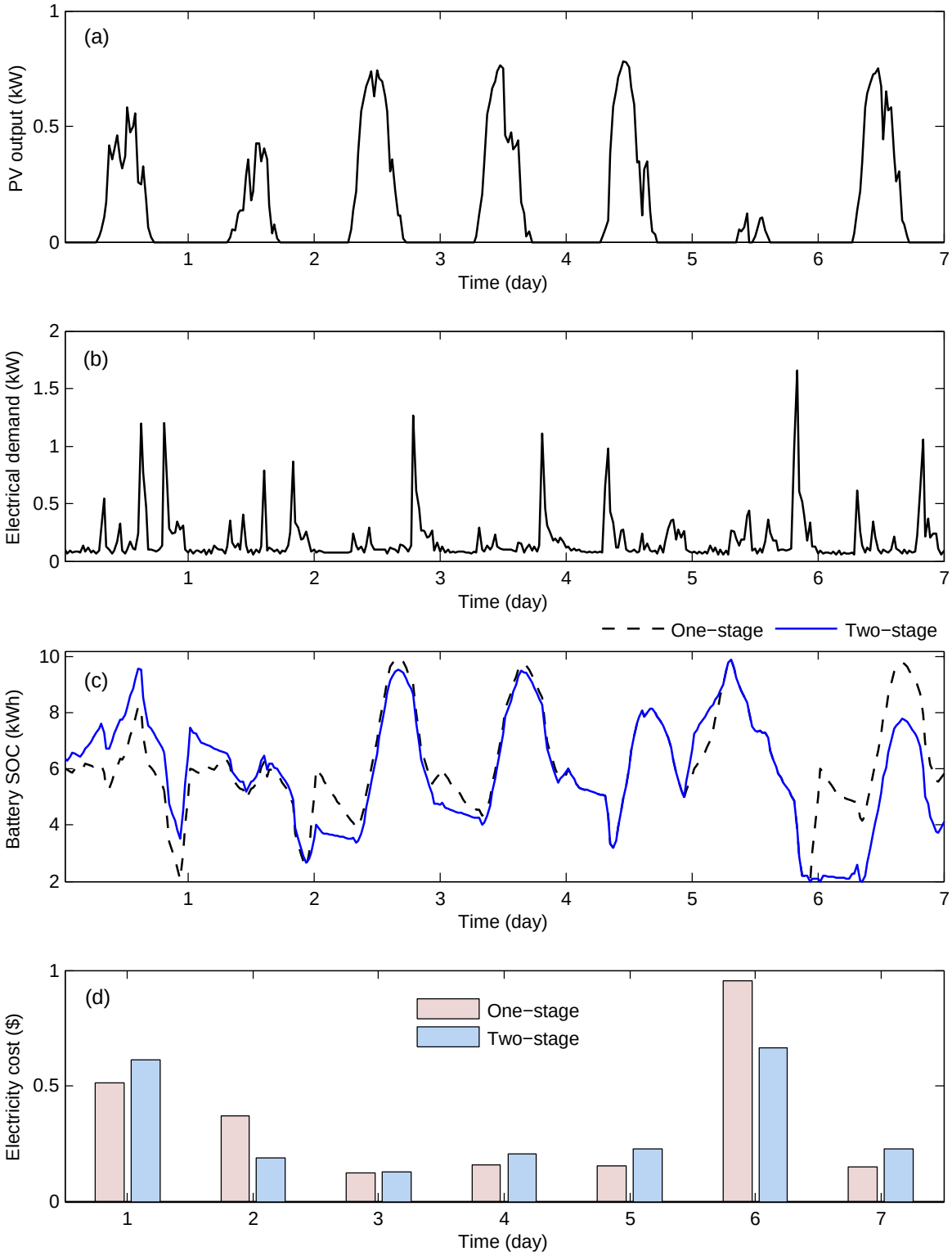

Fig. 4.6 Optimisation results for Scenario 4 from one-stage and two-stage lookahead: (a) PV output; (b) electrical demand; (c) battery SOC; and (d) electricity cost.

Chapter 5

Approximate Dynamic Programming

This chapter presents an ADP approach with *temporal difference learning* to implement a computationally efficient SHEMS. This ADP method produces solutions of a similar quality to DP but with much less computation. ADP, also known as *forward DP*, is an algorithmic strategy for approximating a value function, which steps forward in time, compared to backward induction used in *value iteration*. Similar to DP, the VFAs are obtained during an off-line planning phase, so that fast real-time decisions can be made using the Bellman optimality condition, which is a simple linear problem. Like DP, ADP also operates on an MDP formulation of the problem, so all the non-linear constraints and transition functions in Section 2.2 can be directly incorporated with the same computational burden as modelling linear transition functions and constraints.

ADP is an anytime optimisation solution technique, which is an algorithm that returns a feasible solution even if it is interrupted prematurely. The quality of the solution, however, improves if the algorithm is allowed to run until the desired convergence. Similar to DP, we can always obtain a solution with ADP regardless of the constraints and the inputs.

Specifically, ADP enables us to:

- incorporate stochastic nature of the input variables with no additional computational burden;
- extend the decision horizon with less computational burden to consider uncertainties over several days, which results in significant financial benefits;
- enable integration of multiple controllable devices with less computational burden;
- integrate the SHEMS into an existing smart meter as it needs less computational power compared to existing methods.

Algorithm 2 : ADP using Temporal Difference Learning TD(1)

Initialize $\bar{V}_k^0, \quad k \in K$,
Set $r = 1$ and $k = 1$,
Set $\mathbf{s}_1$.
while $r \leq R$ **do**
    Choose a sample path ω^r.
    for $k = 0, \ldots, K$ **do**
        Solve the deterministic problem (5.8).
        for $i = 1, \ldots, I$ **do**
            Find right and left marginal contributions (5.9).
        end for
        if $k < K$ **then**
            Find the post decision states (5.2) and the next pre decision states (5.3).
        end if
    end for
    for $k = K, \ldots, 0$ **do**
        Calculate the marginal values (5.10).
        Update the estimates of the marginal values (5.11).
        Update the VFAs using CAVE algorithm.
        Combine value functions of each controllable device (5.7)
    end for
    $r = r + 1$.
end while
Return the value function approximations $\bar{V}_k^R \quad \forall k$.

This chapter is structured as follows: First, the ADP approach is presented along with the practical guidelines for its implementation (Section 5.1). The simulation results section consists of comparisons of the solution quality and computational time of the proposed ADP approach, DP and stochastic MILP (Section 5.2). Finally the conclusions in Section 5.3.

5.1 ADP using Temporal Difference Learning

ADP generates VFAs while stepping forward in time. Here VFAs are obtained iteratively and the focus is on approximating the value function around a post decision state vector, $\mathbf{s}_k^x$, which is the state of the system at discrete time, k, soon after making the decisions but before the realisation of any random variables [65]. This is because approximating the expectation within the max or min operator in the Bellman optimality condition (5.1) is difficult in large practical applications as transition probabilities from all the possible states are required. The

Bellman optimality condition, which is defined in Chapter 3 is:

$$V_k^{\pi^*}(\mathbf{s}_k) = \min_{\pi^*} \left(C_k(\mathbf{s}_k, \pi(\mathbf{s}_k)) + \mathbb{E}\left\{ V_{k+1}^{\pi^*}(\mathbf{s}') | \mathbf{s}_k \right\} \right). \tag{5.1}$$

Pseudo-code of the method used to approximate the value function is given in Algorithm 2, which is a double-pass algorithm referred to as *temporal difference learning* with a discount factor $\lambda = 1$ or TD(1).

Given this, the original transition function $\mathbf{s}_{k+1} = \mathbf{s}^M(\mathbf{s}_k, \mathbf{x}_k, \omega_k)$ is divided into a move to the post-decision state:

$$\mathbf{s}_k^x = \mathbf{s}^{M,x}(\mathbf{s}_k, \mathbf{x}_k), \tag{5.2}$$

and then on to the next pre-decision state:

$$\mathbf{s}_{k+1} = \mathbf{s}^{M,\omega}(\mathbf{s}_k^x, \omega_k), \tag{5.3}$$

which are used in line 12 of Algorithm 2.

An example of the new modified MDP is illustrated in Fig. 5.1, which uses the mean and variation of the stochastic variables to obtain the post-decision and next pre-decision states, respectively. In more detail, at $\mathbf{s}_1$, there are three possible decisions that takes us to three post-decision states, which correspond to high, middle and lowest states. However, the next pre decision state $\mathbf{s}_2$ depends on the random variables ω_1.

Given this, a new form of the value function can be written as:

$$\bar{V}_k^{\pi}(\mathbf{s}_k) = \max_{\mathbf{x}_k} \left(C_k(\mathbf{s}_k, \mathbf{x}_k) + \bar{V}_k^{\pi,x}(\mathbf{s}_k^x) \right), \tag{5.4}$$

where $\bar{V}_k^{\pi,x}(\mathbf{s}_k^x)$ is the value function approximation around the post-decision state $\mathbf{s}_k^x$, given by:

$$\bar{V}_k^{\pi,x}(\mathbf{s}_k^x) = \mathbb{E}\left\{ V_{k+1}^{\pi}(\mathbf{s}_{k+1}) | \mathbf{s}_k^x \right\}. \tag{5.5}$$

This method is computationally feasible because $\mathbb{E}\left\{ V_{k+1}^{\pi}(\mathbf{s}_{k+1}) | \mathbf{s}_k^x \right\}$ is a function of the post-decision state $\mathbf{s}_k^x$, that is a deterministic function of $\mathbf{x}_k$. However, in order to solve (5.4), we still need to calculate the value functions in (5.5) for every possible state $\mathbf{s}_k^x$for all k. This can be computationally difficult since $\mathbf{s}_k^x$ is continuous and multidimensional, so we approximate (5.5).

Two strategies are employed. First, we construct lookup tables for VFAs in (5.5) that are concave and piecewise linear in the resource dimension of all the state variables of

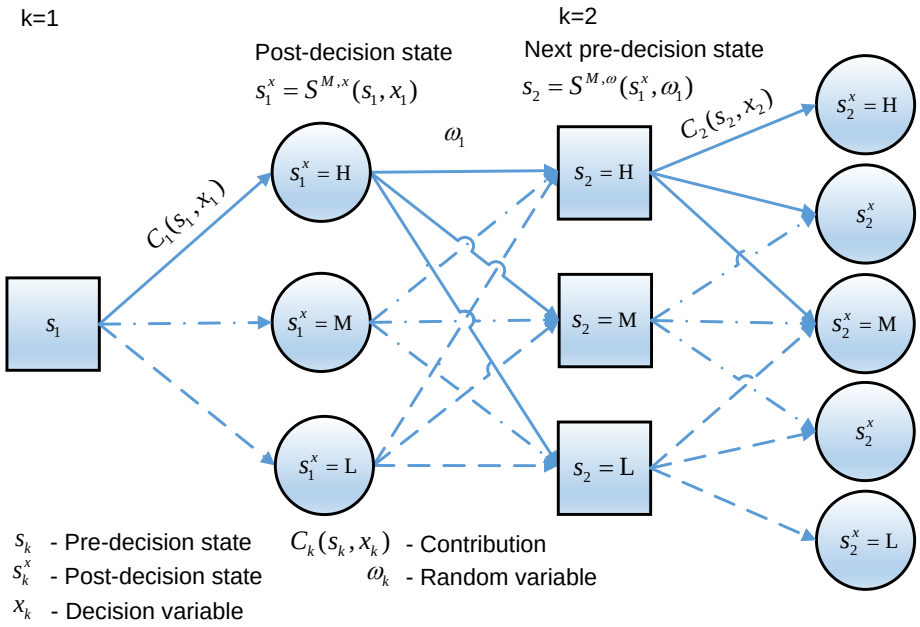

Fig. 5.1 Illustration of the modified Markov decision process, which separates the state variables into post decision states and pre-decision states.

controllable devices [62]. For example, in the VFA for $k = 49$, which is depicted in Fig. 5.2(a), the expected future rewards stay the same after approximately 7 kWh, so if we are at 7 kWh in the time-step $k = 48$, charging the battery further will have no future rewards and will only incur an instantaneous cost if the electricity has to come from the grid. However, if the electricity price or demand is high then we can probably discharge the battery as the expected future rewards will only decrease slightly. Given this, we never charge the storage when there is no marginal value so the slopes of the VFA are always greater than or equal to zero. Accordingly, the VFA is given by:

$$\bar{V}_k^i(s_k^{i,x}) = \sum_{a=1}^{A_k} \bar{v}_{ka} z_{ka}, \tag{5.6}$$

where $\sum_a z_{ka} = s_k^{i,x}$ and $0 \leq z_{ka} \leq \bar{z}_{ka}$ for all a. The resource coordinate variable z_{ka} for segment $a \in (1 \ldots A_k)$, $A_k \in \mathcal{A}$, $\bar{z}_{ka}$ is the capacity of the segment and $\bar{v}_{ka}$ is the slope. Other strategies that could be used for this step are parametric and non-parametric approximations of the value functions [65]. However, in the context of SHEMSs, these strategies are more suited for PFAs, which is our focus in Chapter 6.

Second, we handle the multidimensional state space by generating independent VFAs for each controllable device, which are then combined to obtain the optimum policy. The

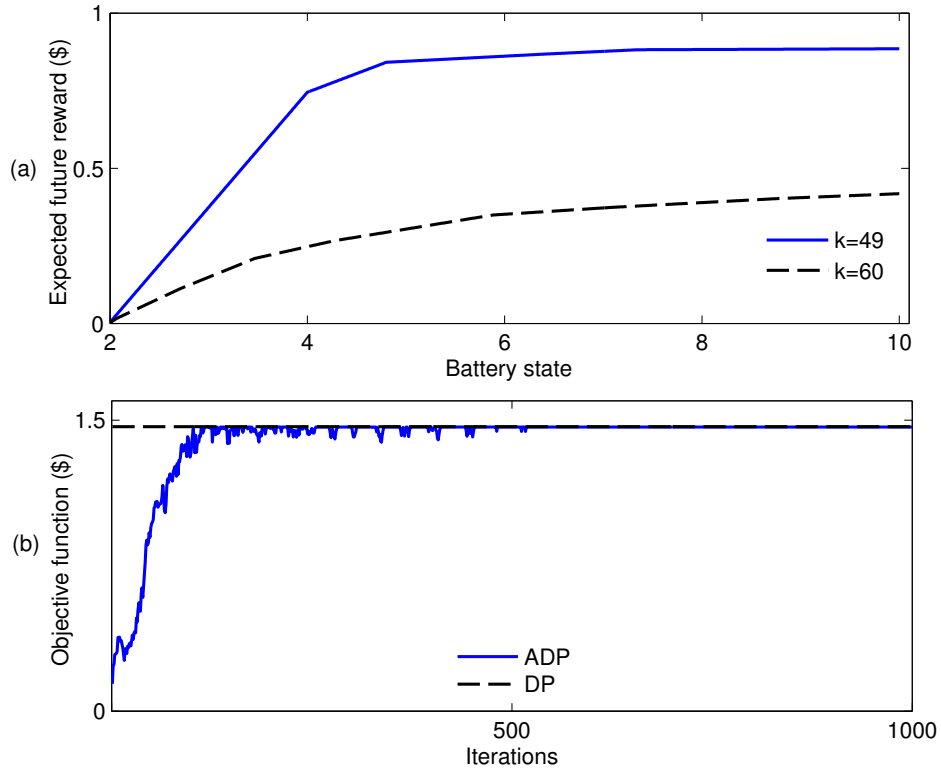

Fig. 5.2 (a) Expected future reward or VFA (5.5) for following the optimal policy vs. state of the battery for time-steps $k = 49$ and $k = 60$, and (b) value of the objective function (i.e. reward) vs. iterations for ADP approach and the expected value from DP.

separable VFA is given by:

$$\bar{V}_k(\mathbf{s}_k^x) = \sum_{i=1}^{I} \bar{V}_k^i(s_k^{i,x}). \tag{5.7}$$

It is possible to separate the VFAs for battery and TES because their state transitions are independent as shown in (2.5) and (2.6), respectively. Instead, the inter-device coupling between the battery and the TES only arises through their effect on energy costs, so it is done in the contribution function in (2.8). If the state transition functions of the controllable devices depend on each other, then the VFAs are not separable and we have to use multidimensional value functions. In such situations the number of iterations needed for VFA convergence will increase, and concavity needs to be generalised as well.

In more detail, Algorithm 2 proceeds as follows:

1. Set the initial VFAs to zero (i.e. all the slopes to zero) or to an initial guess to speed up the convergence (lines 1-3). Estimates for the initial VFAs can be obtained by

solving the deterministic problem using MILP. The value of the initial starting state s_1^i is assumed.

2. For each realisation of random variables, step forward in time by solving the following deterministic problem (line 7) using the VFA from the previous iteration:

$$\begin{aligned}\mathbf{x}_k^r =& \arg\max_{\mathbf{x}_k \in X_k} \left(C(\mathbf{s}_k^r, \mathbf{x}_k) + \bar{V}_k^{r-1}(\mathbf{s}_k^{x,r})\right), \\ =& \arg\max_{\mathbf{x}_k \in X_k} \left(C(\mathbf{s}_k^r, \mathbf{x}_k) + \sum_{a=1}^{A_k^{r-1}} \bar{v}_{ka}^{r-1} z_{ka}\right). \end{aligned} \tag{5.8}$$

3. Determine the positive and the negative marginal contributions $\hat{c}_k^{r,i+}(s_k^{r,i})$ and $\hat{c}_k^{r,i-}(s_k^{r,i})$, respectively (line 9) for each controllable device, using:

$$\begin{aligned}\hat{c}_k^{r,i+}(s_k^{r,i}) &= \frac{c_k^{r,i+}(s_k^{r,i+}, x_k^{r,i+}) - c_k^{r,i}(s_k^{r,i}, x_k^{r,i})}{\delta s}, \\ \hat{c}_k^{r,i-}(s_k^{r,i}) &= \frac{c_k^{r,i}(s_k^{r,i}, x_k^{r,i}) - c_{ki}^{r,i-}(s_k^{r,i-}, x_k^{r,i-})}{\delta s}, \end{aligned} \tag{5.9}$$

where $s_k^{r,i+} = \left(s_k^{r,i} + \delta s\right)$, $x_k^{r,i+} = \mathcal{X}_k^{\pi}\left(s_k^{r,i+}\right)$, and δs is the mesh size of the state space. We do this similarly for $s_k^{r,i-}$ and $x_k^{r,i-}$.

4. Find the post-decision and the next pre-decision states using (5.2) and (5.3), respectively. Transition functions of the controllable devices can be non-linear (line 12).

5. Starting from K, step backward in time to compute the slopes, $\hat{v}_k^{r,i+}$, which are then used to update the VFA (line 16). Compute $\hat{v}_k^{r,i+}$:

$$\hat{v}_k^{r,i+}(s_k^{r,i}) = \begin{cases} \hat{c}_K^{r,i+}(s_K^{r,i}), & \text{if } k = N \\ \hat{c}_k^{r,i+}(s_k^{r,i}) + & \\ \Delta_k^{r,i+} \hat{v}_{k+1}^{r,i+}(s_{k+1}^{r,i}) & \text{otherwise} \end{cases}, \tag{5.10}$$

where $\Delta_k^{r,i+} = \frac{1}{\delta s} S^M(x_k^{r,i} - x_k^{r,i+})$ is the marginal flow (i.e. whether or not there is a change in energy in the storage as a result of the perturbation). We do this similarly for $\hat{v}_k^{r,i-}(s_k^{r,i})$. Note that we took the power coming out of the storage as negative.

6. Update the estimates of the marginal values [63]:

$$\bar{v}_{k-1}^{r,i+}(s_{k-1}^{x,r,i}) = \left(1-\alpha^{r-1}\right)\bar{v}_{k-1}^{r-1,i+}(s_{k-1}^{x,r,i}) + \alpha^{r-1}\hat{v}_{k}^{r,i+}, \tag{5.11}$$

where α is a "stepsize"; $\alpha \in (0,1]$, and similarly for $\bar{v}_{k-1}^{r,i-}(s_{k-1}^{x,r,i})$ (line 17). In this research, a harmonic step-size formula is used, $\alpha = b/(b+r)$, where b is a constant. This step-size formula satisfies conditions ensuring that the values will converge as $r \to \infty$ [81].

7. Use the concave adaptive value estimation (CAVE) algorithm to update the VFAs [82] (line 18). Note that $\bar{v}_{k-1}^{r,i+}(s_{k-1}^{x,r,i})$ is the slope of the VFA at a particular state, and since this slope is obtained for a given random realization, there is possibility of violating the concavity of the VFA. Given this, we need to define an interval for the new slope obtained in (5.11). This is obtained using:

$$Q = \left[\min\left\{s_{k-1}^{x,r,i} - \varepsilon^{-}, u^{-}\right\}, \max\left\{s_{k-1}^{x,r,i} - \varepsilon^{+}, u^{+}\right\}\right], \tag{5.12}$$

where ε^{-} and ε^{+} are tuning parameters in the CAVE algorithm, which is set to 0.01; u^{-} is the closest state to $s_{k-1}^{x,r,i}$ that has a higher slope than $\bar{v}_{k-1}^{r,i-}(s_{k-1}^{x,r,i})$; and u^{+} is the closest state to $s_{k-1}^{x,r,i}$ that has a lower slope than $\bar{v}_{k-1}^{r,i+}(s_{k-1}^{x,r,i})$.

8. Combine value functions of each device using (5.7).

9. Repeat this procedure over R iterations, which are generated randomly according to the probability distributions of the random variables. We find that $R = 500$ realisations is enough for the objective function to come within an acceptable accuracy even for the worst possible scenario. We investigated a range of scenarios and an example is given in Fig. 5.2(b).

Note that when solving a deterministic SHEMS problem using ADP, the post decision and next pre decision states are the same because the random variables will be zero. However, the remaining steps in Algorithm 2 stay the same. This means, with ADP, there is no noticeable computational burden for considering variation in the stochastic variables compared to solving the deterministic problem. On the other hand, with DP we have to loop over all the possible combinations of realisation of random variables, which significantly increases the computational burden.

5.2 Simulation Results and Discussion

The simulation results are used to show the performance of ADP over DP and stochastic MILP. There are three sets of simulations. The first set consists of discussions about: challenges of estimating the end-of-day battery SOC; benefits of PV-storage systems; quality of the solutions from ADP, DP and stochastic MILP; and the benefits of a stochastic optimisation over a deterministic one (Sections 5.2.1-4). The second set consists of a discussion on the computational aspects of the three solution techniques (Section 5.2.5). The third set consists of the year-long optimisation results (Section 5.2.6). The stochastic variables are according to Chapter 2 and the device characteristics are in Fig 2.3 and Table 2.1. The ToUP signal is in Fig. 2.2.

5.2.1 Challenges of estimating the end-of-day battery SOC

In the first set of simulations, we discuss the challenges of estimating the end-of-day battery SOC (Section 5.2.1), benefits of residential PV-storage systems (Section 5.2.2), the performance of the three SHEMSs over a day (Section 5.2.3) and the benefits of using a stochastic optimisation over a deterministic one (Section 5.2.4). Here we consider four scenarios with PV-battery systems (Scenarios 1-4) and three scenarios with PV, battery and TES units (Scenarios 1-3). Scenarios 1, 2, 3, and 4 are on August 20$^{\text{th}}$, 2012, July 2$^{\text{nd}}$, 2012, January 1$^{\text{st}}$, 2013 and October 1$^{\text{st}}$, 2012, respectively, for a Central Coast, NSW, Australia, based residential building shown in Fig. 5.3. The PV system size is 2.2 kWp.

From our preliminary investigations, and as depicted in Fig 5.2(a), the expected future rewards in the start-of-day two (time-step $k = 49$) only increases slightly after 6 kWh, which suggests that using half of the available battery capacity as the start-of-day and end-of-day battery SOC ($s_1^{\text{b}} = s_K^{\text{b}} = 6$ kWh) in daily optimisations with DP is a valid assumption. However, we observe that on days with a low morning demand, high PV output and medium-high evening demand (see Fig. 5.3(c)), $s_1^{\text{b}} = s_K^{\text{b}} = 2$ kWh gives the best results because the battery can be used to supply the evening demand and there is no need to charge it back. However, the next day's electricity cost can significantly increase if we are anticipating a high morning demand and low-high PV output (see Fig. 5.3(a-b)). Because of such situations, it is beneficial to control the end-of-day battery SOC by considering uncertainties over several days, which is our special focus of attention in this chapter. Note that the two-stage lookahead in Chapter 4 requires us to fix the end-of-day battery SOC so we might end up with increased costs if the current days actual PV output and demand deviates from the predictions. The ADP approach is used over a two-day decision horizon because the simulation results

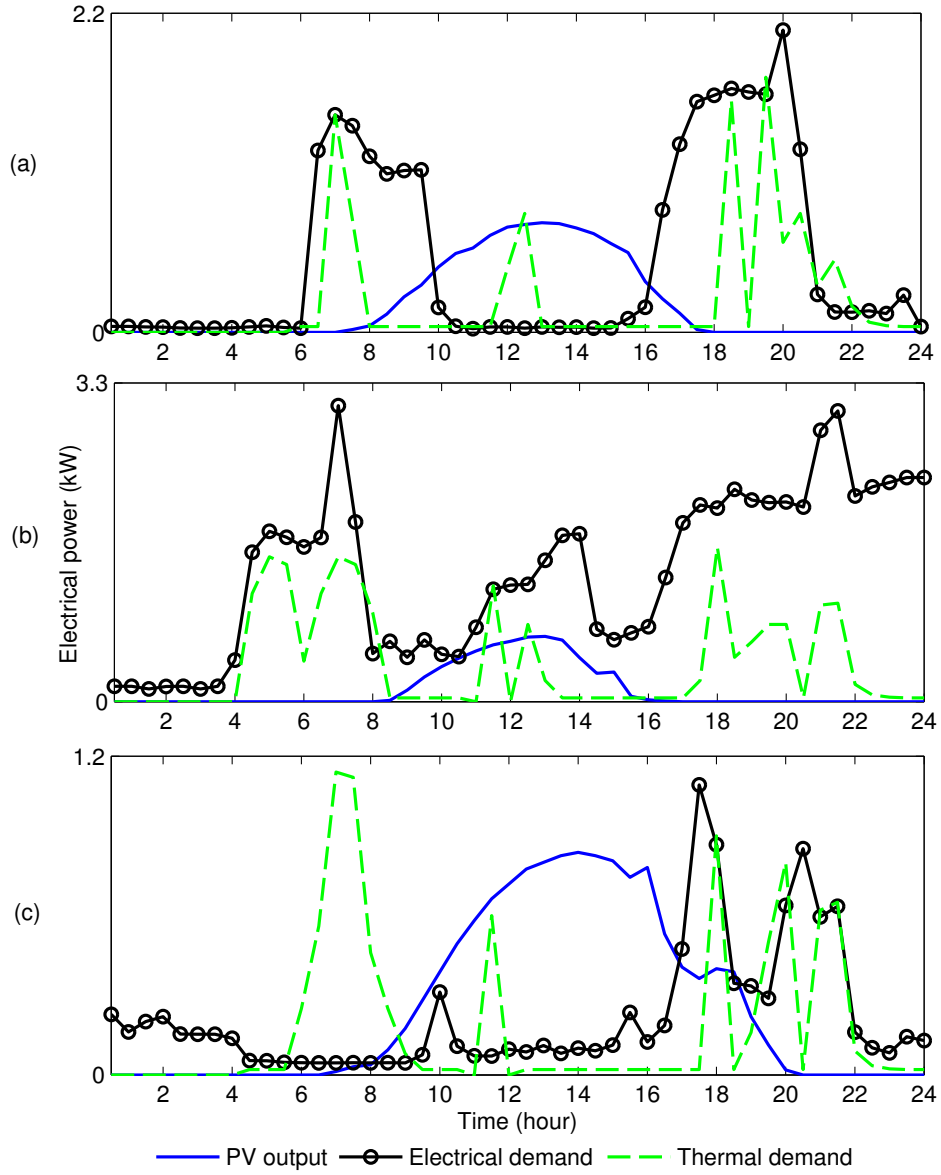

Fig. 5.3 PV output and electrical and thermal demand for (a) Scenario 1, (b) Scenario 2 and (c) Scenario 3.

in Section 4.3 showed that there are no significant benefits when we increase the decision horizon beyond two days.

5.2.2 Benefits of PV-storage systems

Residential PV-storage systems with a SHEMS result in significant financial benefits. This is evident from the electricity cost of the three scenarios in three instances (i.e. benchmark cost with neither PV or storage, cost with PV but no storage and PV-storage system with SHEMSs) in Table. 5.1 and Table. 5.2. First the benefits of PV-battery systems under uncertainty given

Table 5.1 The daily optimisation results for four scenarios with PV-battery systems.

Total daily:	Scenario 1	Scenario 2	Scenario 2	Scenario 4
PV output (kWh)	9.27	6.05	12.31	10.12
Electrical demand (kWh)	24.72	64.75	10.48	10.88
Benchmark ($)	4.00	7.94	0.94	1.87
With PV ($)	3.74	7.29	0.57	0.93
ADP ($)	2.18	6.16	0	0.12
DP ($)	2.14	6.13	0	0.02
Stochastic MILP ($)	2.30	6.36	0.45	0.90
DP ($s_1^b = s_K^b = 6$) ($)	2.36	6.35	0.15	0.23

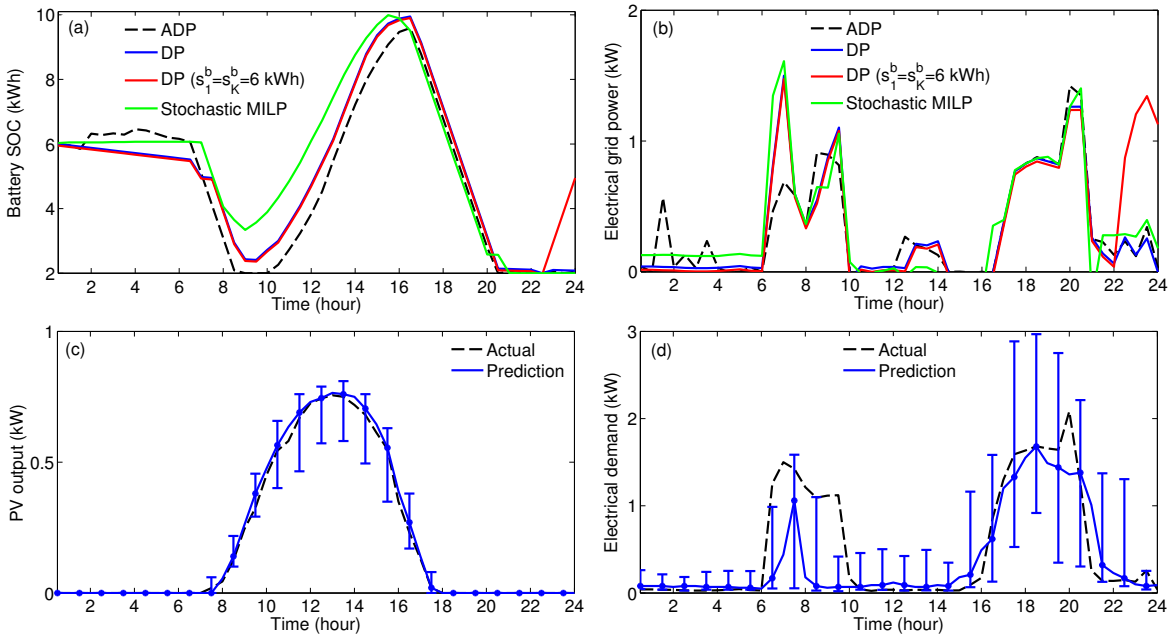

Fig. 5.4 Scenario 1 for a PV-battery system - (a) battery SOC; (b) electrical grid power; and estimated and actual (c) PV output and (d) electrical demand.

in Table. 5.1 are explained. The daily electricity cost can reduce by 6.5%, 8.19%, 39.36% and 50.27% for Scenarios 1, 2, 3 and 4 respectively, if there is only a PV system. We can further improve this by having a battery and effectively controlling its battery SOC using a SHEMS in which the battery is charged to a certain level from solar power and electrical grid before peak periods. A DP based SHEMS constrained to a 60% start-of-day and end-of-day battery SOC reduces the total electricity cost by further 34.5%, 11.84%, 44.68% and 37.43% for Scenarios 1, 2, 3 and 4, respectively. This means a total of 41%, 20%, 84% and 87.7% cost reduction for Scenarios 1, 2, 3 and 4, respectively, by having a PV-battery system. As shown in Fig. 5.3, inhabitants are away during the day for Scenarios 1, 3 and 4, so the extra PV generation is stored in the battery, which shows the benefits of having a storage. In contrast

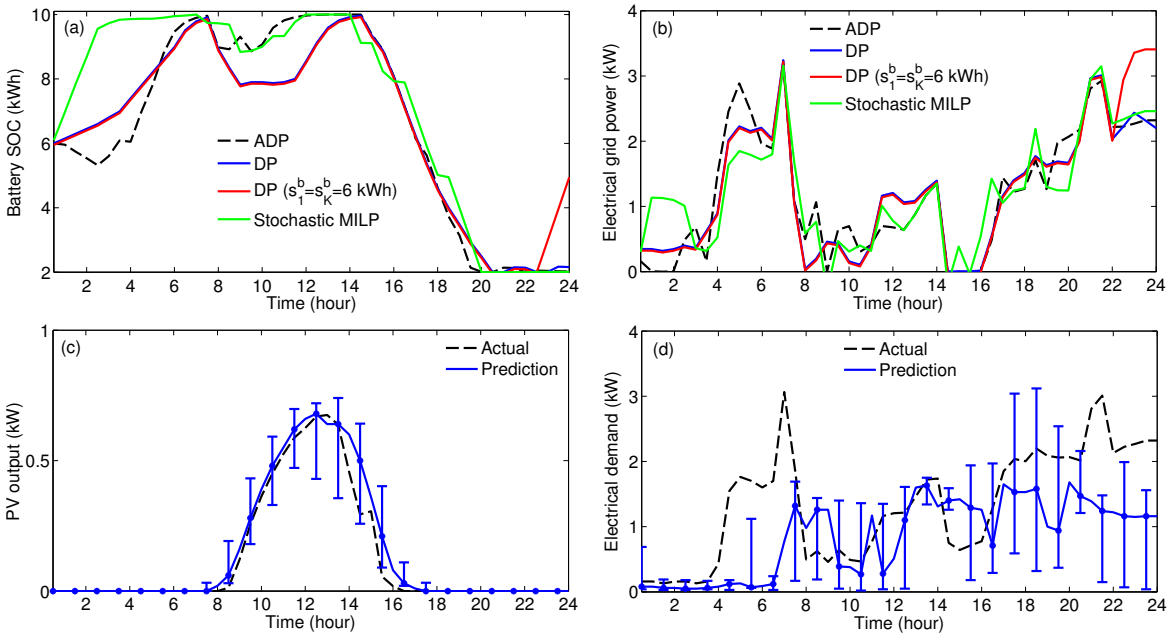

Fig. 5.5 Scenario 2 for a PV-battery system - (a) battery SOC; (b) electrical grid power; and estimated and actual (c) PV output and (d) electrical demand.

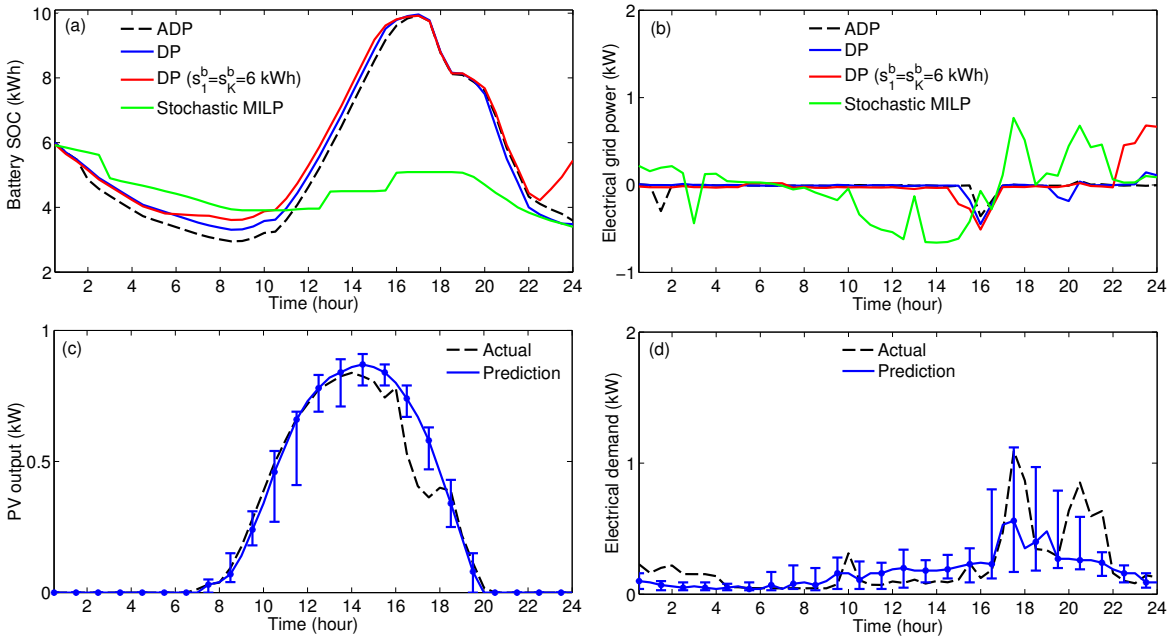

Fig. 5.6 Scenario 3 for a PV-battery system - (a) battery SOC; (b) electrical grid power; and estimated and actual (c) PV output and (d) electrical demand.

to Scenarios 1, 3 and 4, Scenario 2 electrical demand exceeds PV generation so the benefit of battery is minimal.

Second, the benefits of a system with PV, battery and TES units is given in Table. 5.2. The daily electricity cost can reduce by 6.2%, 6.1% and 22.6% for Scenarios 1, 2 and 3,

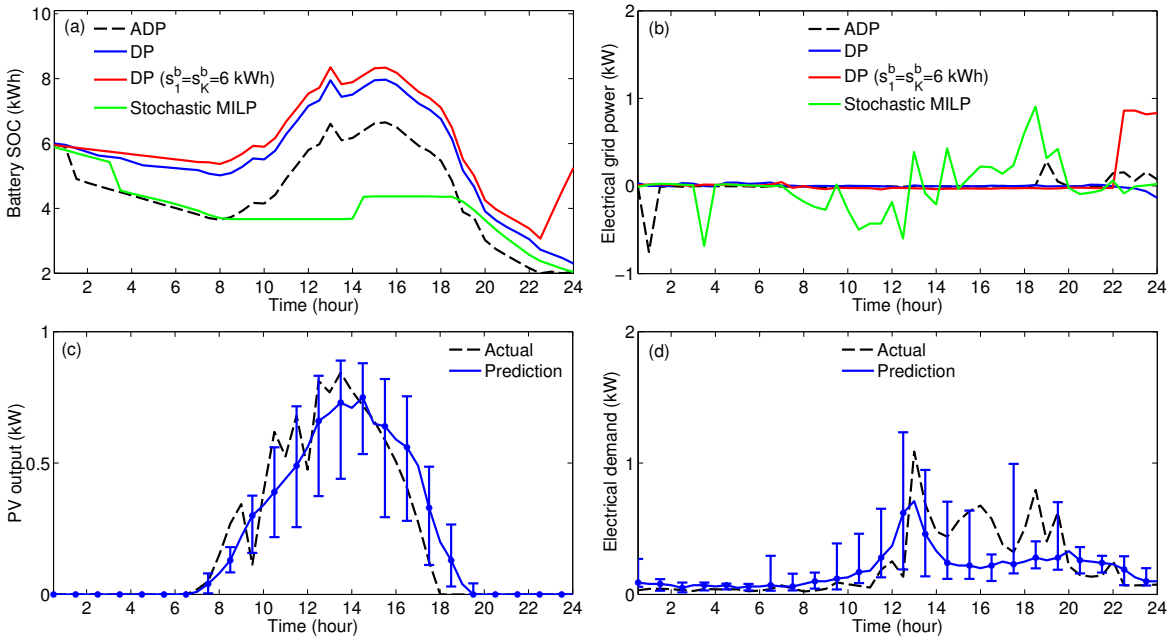

Fig. 5.7 Scenario 4 for a PV-battery system - (a) battery SOC; (b) electrical grid power; and estimated and actual (c) PV output and (d) electrical demand.

respectively, if there is only a PV system. These percentages are lower than the above mentioned percentages (PV-battery) because the total benchmark cost here is higher because of the thermal demand. A DP based SHEMS constrained to a 60% start-of-day and end-of-day battery SOC reduces the total electricity cost by further 42.25%, 17.33% and 36.72% for Scenarios 1, 2, & 3, respectively. That is a total of 48.45%, 23.43% and 59.32% cost reduction for Scenarios 1, 2 and 3, respectively, by controlling both the battery and TES. The electricity cost of controlling the TES in Scenarios 1 and 3 are the lowest because the surplus of solar and battery power is used to charge the TES instead of sending it back to the grid as FiTs are negligible in Australia. Note that we obtain the benchmark cost of the TES by assuming a dummy control system, which operates regardless of the electricity price (same as Chapter 3). The dummy TES control electricity cost varies depending on the time the hot water is used.

5.2.3 Quality of the solutions from ADP, DP and stochastic MILP

ADP and DP result in better quality solutions than stochastic MILP as they both incorporate all the stochastic input variables using appropriate probabilistic models and non-linear constraints [77]. However, ADP results in slightly lower quality schedules compared to the optimal DP solutions in most scenarios because the value functions used are approximations. This is evident in Table. 5.1 and Table. 5.2. In some situations, ADP results in better solutions

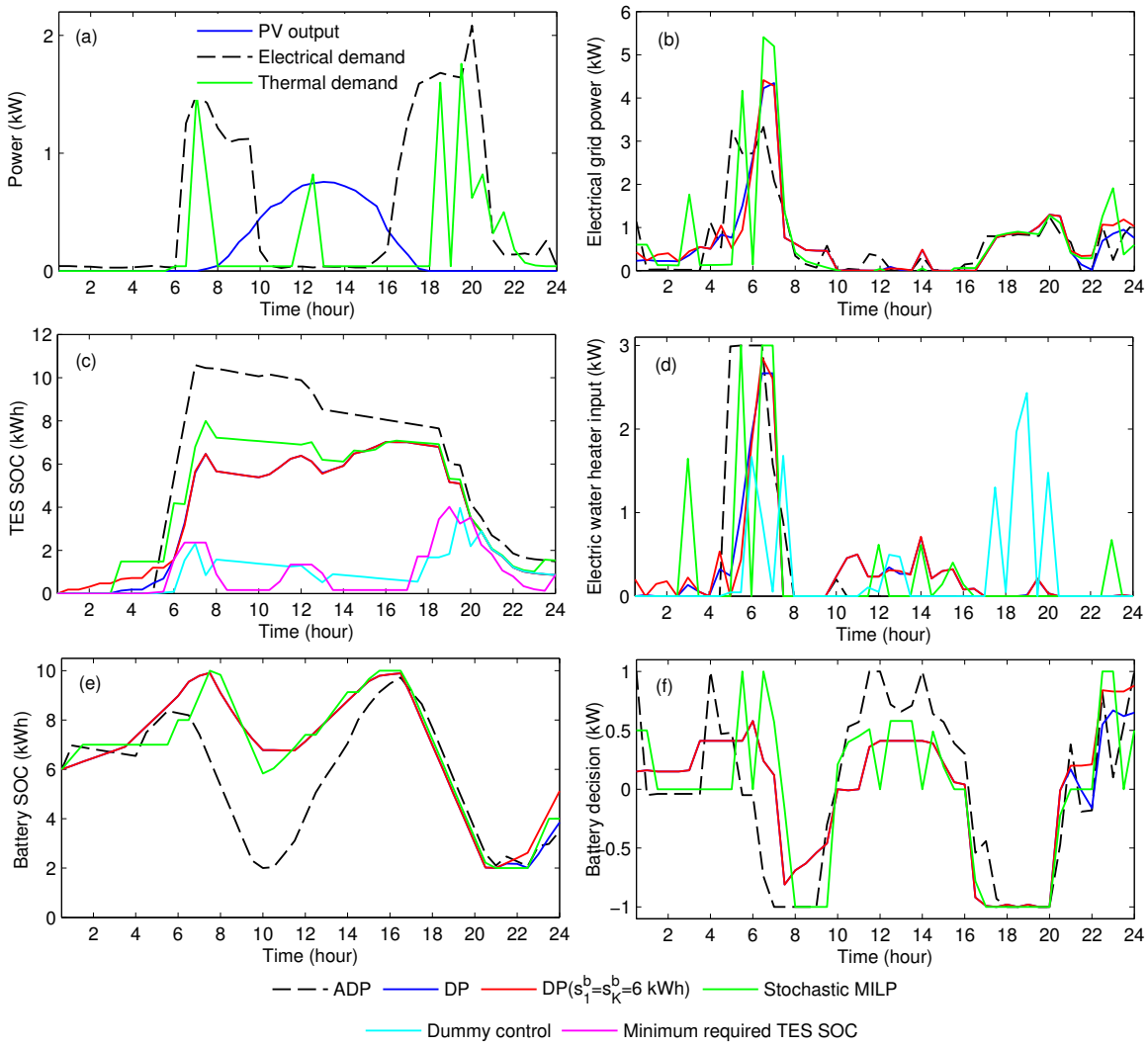

Fig. 5.8 Scenario 1 for a PV-storage system - (a) PV output, electrical and thermal demand; (b) electrical grid power; (c) TES SOC; (d) electric water heater input; (e) battery SOC; and (f) battery decisions.

because we make an approximation to constraint the end-of-day battery SOC using DP. In more detail, ADP uses the transition functions as it is (2.5 and 2.6) while in order to control the end-of-day SOC using DP, the battery and TES losses are included in the contribution function. Note that the DP based SHEMS with two controllable devices (battery and thermal) is computationally intractable to be use in an existing smart meter, and we only use it to compare solutions with ADP.

The quality of the schedules from the three solution techniques are also evident from PV-battery systems' schedules in Fig. 5.4-7 and PV-battery-TES units' schedules in Fig. 5.8-10. First, important observations of the PV-battery systems in Scenarios 1-4 are as follows: Stochastic MILP sends power back to the grid in Scenarios 3 and 4 because the end-the-day battery SOC is fixed and the estimated electrical demand is lower than the actual values, so the

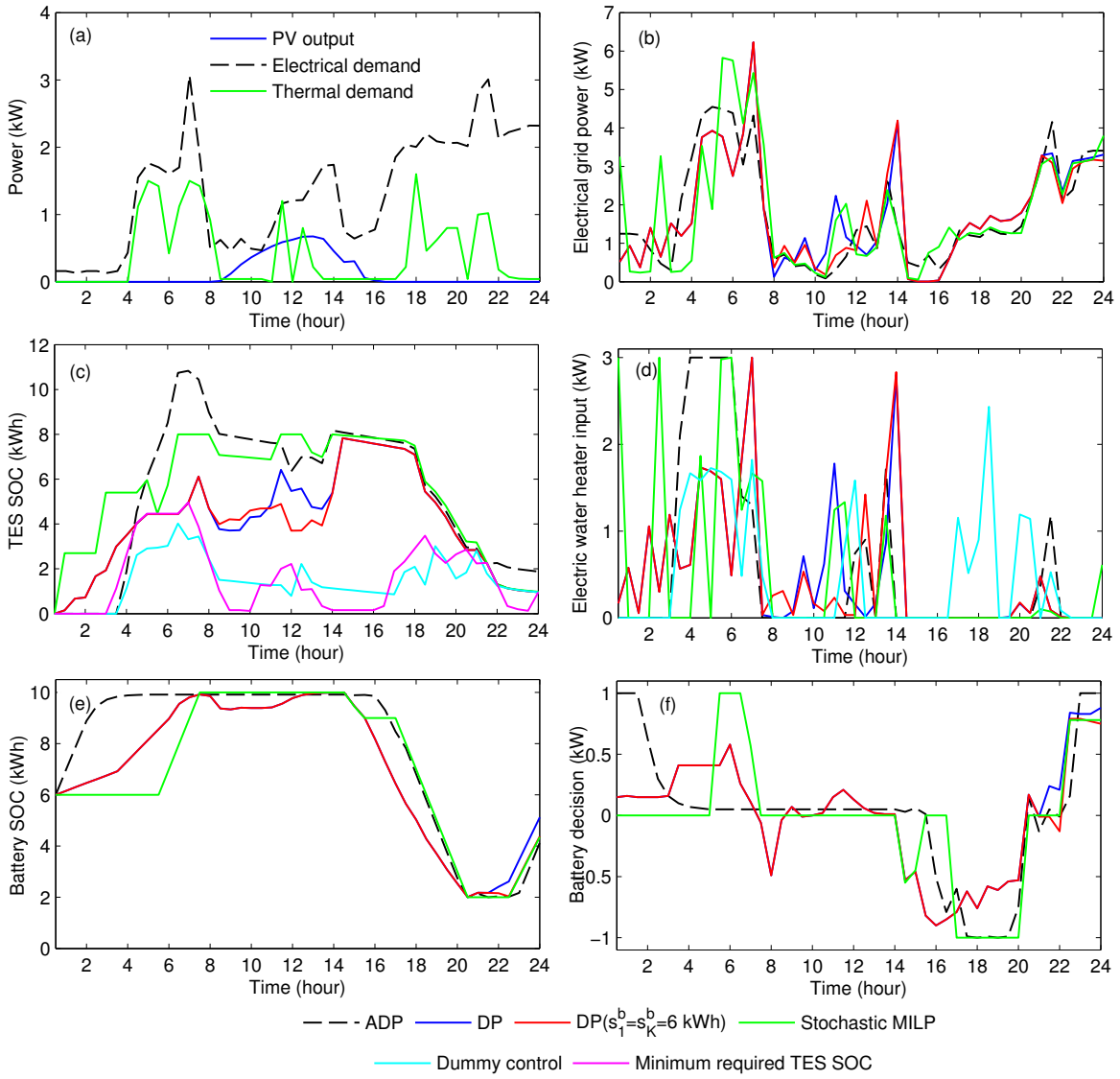

Fig. 5.9 Scenario 2 for a PV-storage system - (a) PV output, electrical and thermal demand; (b) electrical grid power; (c) TES SOC; (d) electric water heater input; (e) battery SOC; and (f) battery decisions.

battery does not charge to the required level. This can be overcome by solving the problem at each time-step, however, we would like to avoid this in practical applications because of the limited computational power and the lack of user interaction (see Chapter 1 and 3). In Scenarios 1 and 2, the battery SOC from all three solution techniques are maximised at the beginning of peak periods starting starting at 29$^{\text{th}}$ time-step. The DP ($s_1^{\text{b}} = s_K^{\text{b}} = 6$) SHEMS has a higher electrical grid power at the last few time-steps compared to other schedules because the battery has to charge back to 6 kWh. Also, note that some times battery SOC does not reach 6 kWh because the end-of-day battery SOC is the next day's start-of-day value.

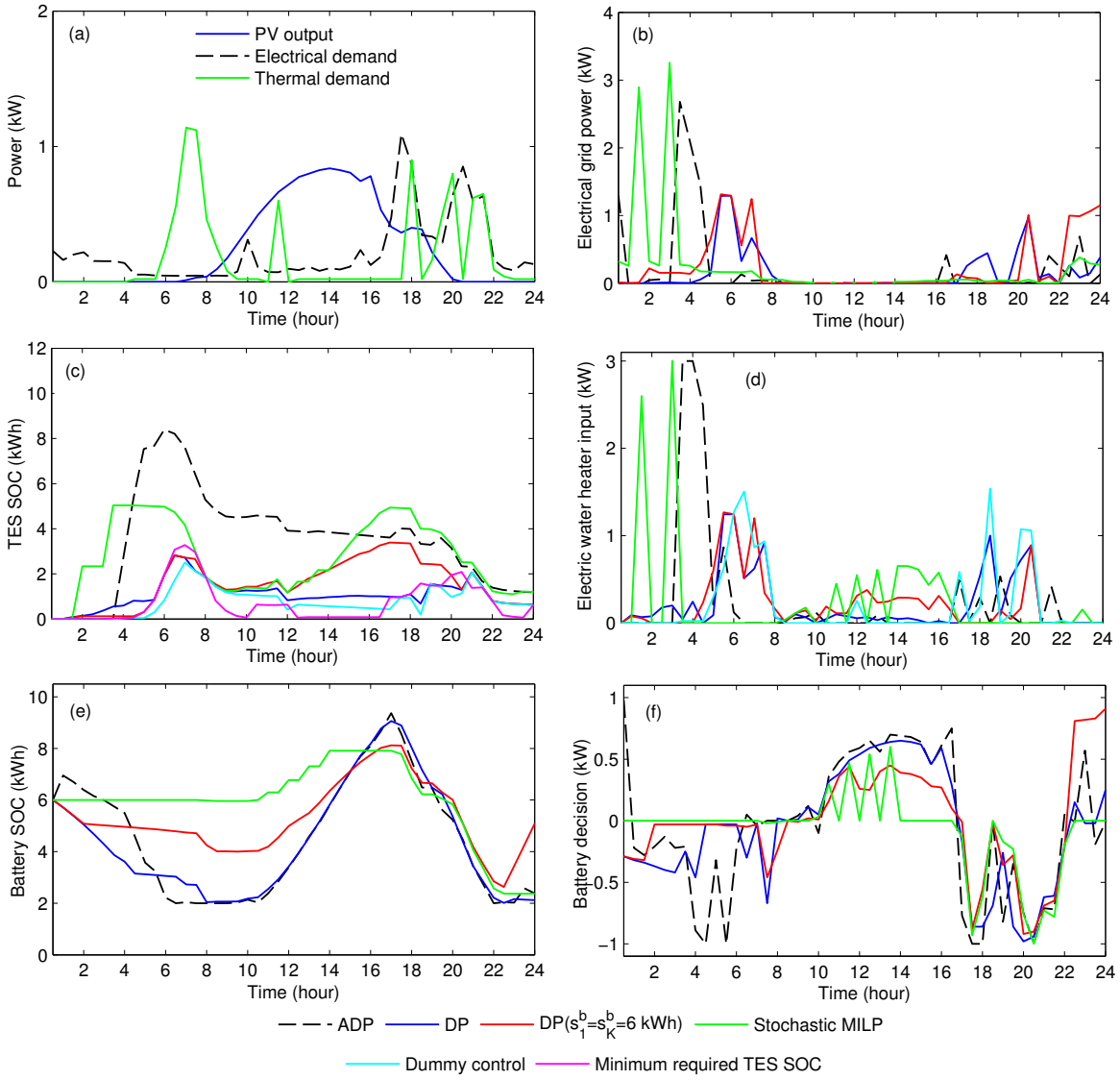

Fig. 5.10 Scenario 3 for a PV-storage system - (a) PV output, electrical and thermal demand; (b) electrical grid power; (c) TES SOC; (d) electric water heater input; (e) battery SOC; and (f) battery decisions.

Second, important observations of the PV-battery-TES systems of Scenarios 1-3 are as follows: The battery and TES SOC are maximised at the beginning of peak periods from solar and electrical grid power. Note that compared to the PV-battery systems above, the solar power is used to charge both the battery and the TES. The dummy control electric water heater is used during peak periods (similar to Chapter 3). The electric water heater controlled using the three SHEMS are never used during peak periods in Scenarios 1 and 2. In Scenario 3, the electric water heater is used during peak periods, however, most of the time electricity came from the battery, which is evident from the zero electric grid power at those time-steps.

Table 5.2 Daily optimisation results for the three scenarios with PV, battery and TES units.

Total daily:	Scenario 1	Scenario 2	Scenario 3
Electrical demand (kWh)	24.72	64.75	10.48
Thermal demand (kWh)	10.42	19.1	8.66
PV generation (kWh)	9.27	6.06	12.31
Benchmark cost ($)	6.13	10.5	1.77
With PV ($)	5.75	9.86	1.37
DP ($s_1^{\mathrm{b}} = s_K^{\mathrm{b}} = 6$) ($)	3.16	8.04	0.72
DP ($)	3.05	7.96	0.59
ADP ($)	3.14	7.79	0.6
Stochastic MILP ($)	3.15	8.11	0.63
Dummy TES control ($)	2.13	2.56	0.83
DP TES control ($)	0.91	1.68	0.58
Marginal value of TES ($)	1.22	0.88	0.25

5.2.4 Benefits of a stochastic optimisation over a deterministic optimisation

In order to evaluate the benefits of a stochastic optimisation over deterministic optimisation, we investigate the following test cases. The Fig. 5.11 is obtained as follows: first we obtain VFAs from both the stochastic and deterministic optimisations using ADP. The stochastic optimisation uses the kernel estimated probability distributions of the PV output and electrical demand while the deterministic ADP only uses the predicted mean PV output and the electrical demand (i.e. all the random variables are zero). Second we obtain the total electricity cost for different possible PV output and demand profiles, which are generated by adding Gaussian noise with varying standard deviation and zero mean to the actual PV output and electrical demand. The mean absolute errors of the actual (i.e. zero Gaussian noise) and predicted mean PV output and demand are 0.238%, 0.696%, and 0.117%, for Scenarios 1, 2, and 3, respectively, which are the initial points. Note that the forecast errors associated with residential electrical demand predictions are typically very high and our aim here is not to minimise forecast errors but to find a suitable stochastic optimisation technique that performs well under uncertainty.

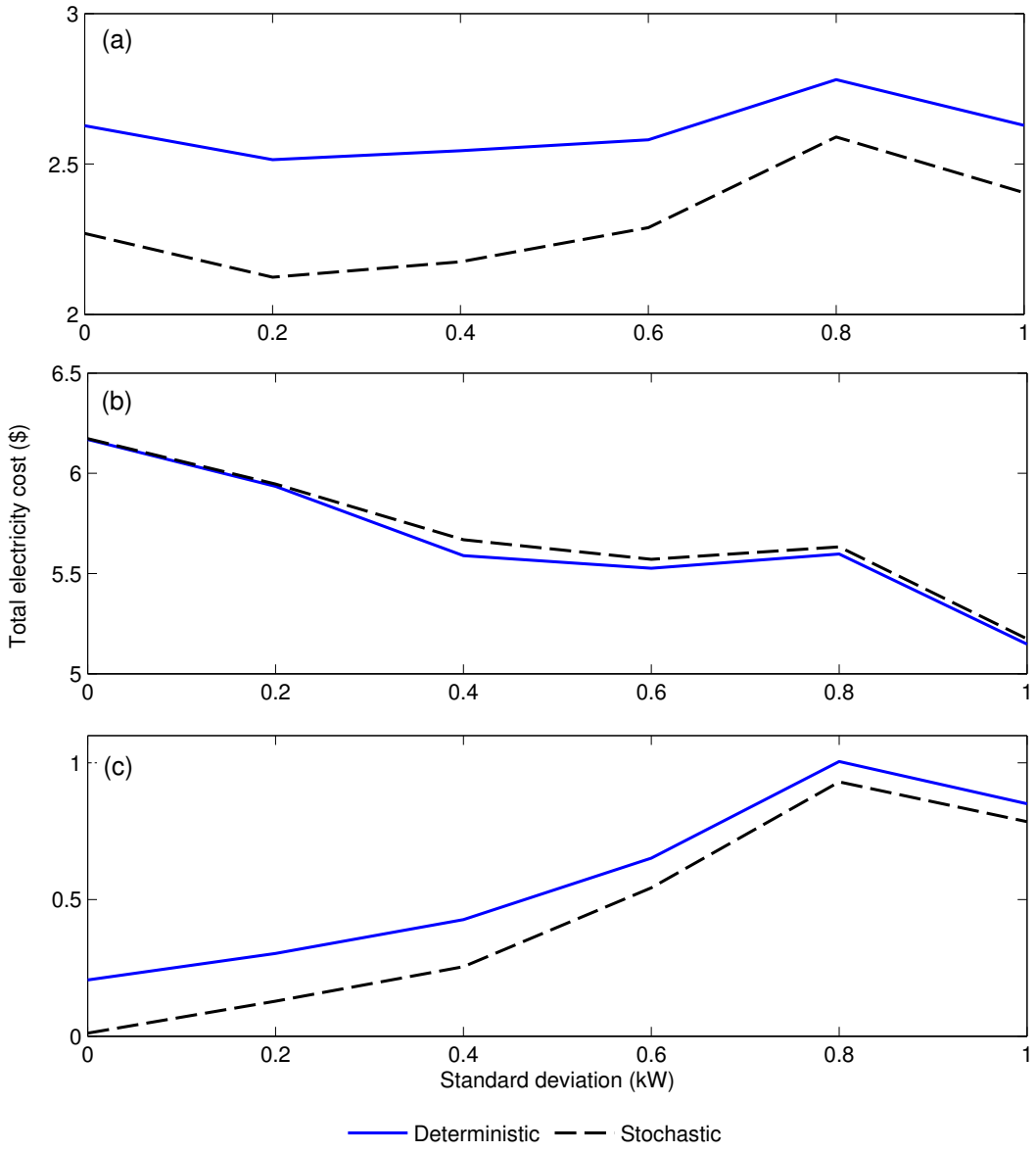

Fig. 5.11 The total electricity cost of PV-battery systems of Scenarios 1-3 from deterministic and stochastic ADP for a range of possible PV output and demand profiles, which are generated by adding Gaussian noise with varying standard deviation and zero mean to the actual PV output and electrical demand.

A stochastic optimisation performs better over a deterministic one when the PV output and electrical demand are estimated from the hierarchical approach in Chapter 2, as shown by the initial points of the Fig. 5.11. An ADP-based stochastic optimisation can reduce the total electricity cost by 13.62%, 0.16%, and 94.67% for Scenarios 1, 2, and 3, respectively, in instances without Gaussian noise. ADP achieved these benefits by incorporating the stochastic input variables without a noticeable increase in the computational effort over a deterministic ADP. Moreover, stochastic ADP requires less computational effort than

deterministic DP. Note that the benefits of a stochastic optimisation for Scenario 3 is very high as a percentage because the stochastic optimisation reduced the electricity cost to almost zero from \$0.21. The benefits from the stochastic optimisation is minimal when the forecast errors are very high (Scenario 2) or very low, which are highly unlikely. The benefits for Scenarios 1 and 3 are noticeable and their forecast errors are what we can expect most of the time [75, 76]. In Scenario 2, the stochastic optimisation gives slightly lower quality results after 0.2 kW standard deviation of Gaussian noise because both the forecast and kernel estimation errors are high. However, these scenarios are highly unlikely and the resulting cost is negligible compared to the benefits from a stochastic optimisation. Moreover, the initial point of Scenario 2 already has a mean absolute error of 0.696, which is highly unlikely to increase any further in a practical scenario. In summary, even though the benefits vary with the scenario and the forecast error, a stochastic optimisation performs better or same as a deterministic one, and ADP provides these benefits without a noticeable increase in the computational effort.

5.2.5 Computational aspects

In our second set of simulation results, we discuss the computational performance of the three solution techniques.

ADP computes a solution much faster than both DP and stochastic MILP and, most importantly, ADP with a two-day decision horizon computes a solution with less than half of the computational time of a daily DP, as depicted in Fig. 5.12. A daily and a weekly optimisation for a residential PV-battery system takes approximately 4 and 28 minutes, respectively, using ADP while DP approach takes approximately 17.1 minutes and 124 minutes, respectively. The computational time of both SHEMSs using ADP and DP increases linearly as we increase the decision horizon, however, ADP has a lesser slope. This linear increase with DP is because the state transitions in this problem are only between two adjacent time-steps, so time does not contribute to an exponential increase in state space size. However, the computational time of DP will increase exponentially when more storage devices are added, where's ADP will have only a linear increase because the state space is factorised. The solution time of stochastic MILP grows exponentially with the length of the horizon because the optimisation problem is solved for the whole horizon at once and the number of possible scenarios increases as the number of time-steps increases [56]. The computational burden can be improved at the expense of solution quality by using scenario reduction techniques. The computational time of ADP with a two-day decision horizon will only increase by 4 minutes when the TES is added while a finely discretised DP based SHEMS takes approximately 2.5 hours. Note that ADP is an anytime optimisation solution

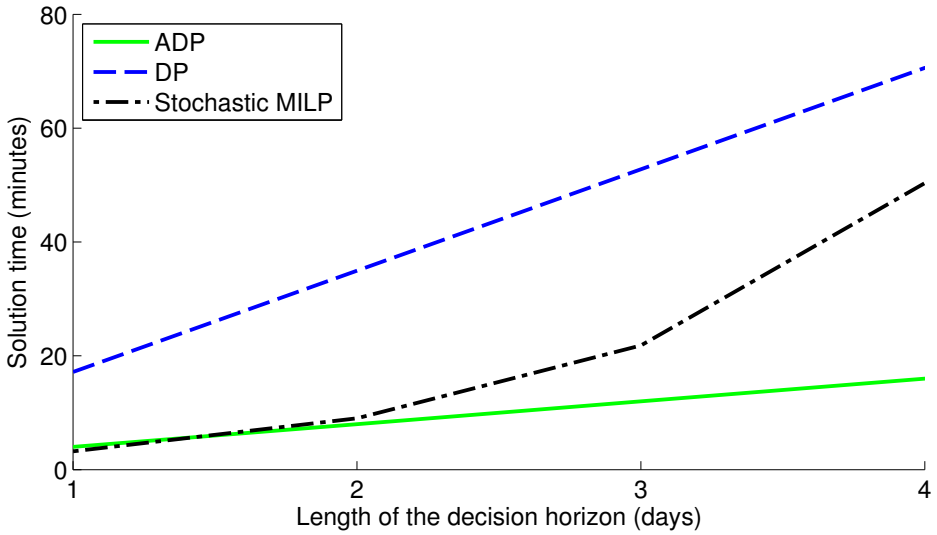

Fig. 5.12 Computational time of ADP, DP and stochastic MILP against the length of the decision horizon.

technique so the computational time will depend on the number of iterations used to achieve the required quality of the solutions.

In summary, we can see that ADP is computationally efficient with good quality solutions. Moreover, we can extend the decision horizon beyond a day and add more storage devices with less computational burden than other approaches. Our simulation results in Chapter 4 indicate that electricity cost can be reduced significantly with a two-day decision horizon, so next section investigates the yearly benefits using an ADP approach with a two-day decision horizon.

5.2.6 Year-long optimisation

In our third set of simulation results, we compare the ADP based SHEMS with a two-day decision horizon to a DP approach with a daily decision horizon over three years for 10 households with PV-battery systems. We omit TES as we already identified its benefits in Section V-B, and moreover, a yearly optimisation using DP with two controllable devices is computationally difficult. The time-periods of the three years are: year 1 from July 1st, 2012 to June 31st, 2013, year 2 is from July 1st, 2011 to June 31st, 2012 and year 3 is from July 1st, 2010 to June 31st, 2011. Electricity cost savings for all the households over three years are given in Fig. 5.13 and in Table 5.3 we demonstrate detailed results of two households in Central Coast (Household 1) and Sydney (Household 2), in NSW, Australia. The PV sizes of the Households 1 & 2 are 2.2 kWp and 3.78 kWp, respectively.

The proposed ADP-based SHEMS implemented using a two-day decision horizon that considers variations in PV output and electrical demand reduces the average yearly electricity

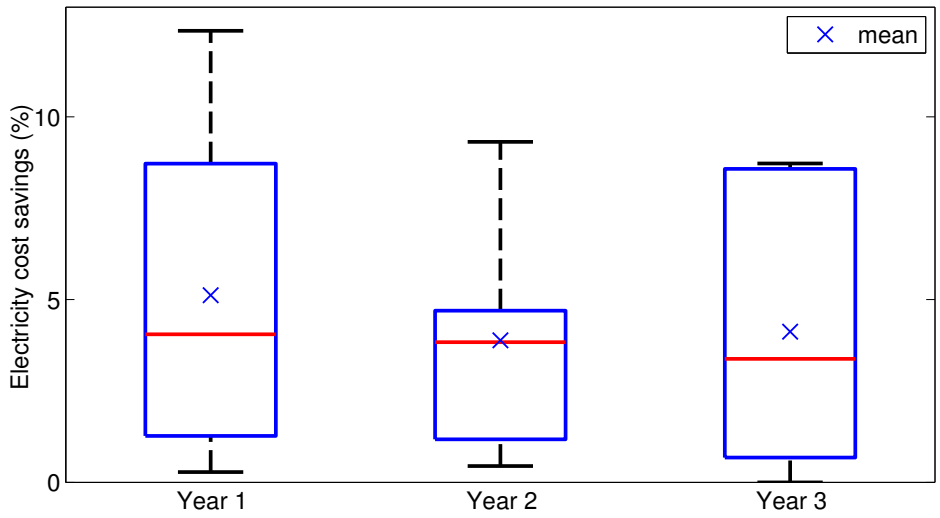

Fig. 5.13 Electricity cost savings over three years for ten households, where blue lines indicate 25th and 75th percentiles and the red lines indicate the median.

cost by 4.63% compared to a daily DP based SHEMS, as depicted in Fig 5.13. We also find that the average yearly savings are 5.12%, 3.89% and 4.95% for years 1-3, respectively. This is because 2013 was a sunny year compared to 2012 and 2011 so the two day optimisation has greater benefits. For example: if we are anticipating a sunny weekend with low demand then we can completely discharge the battery on Friday night. However, if we have a half charged battery on Friday night then we will be wasting most of the free energy as the storage capacity is limited. Our results showed that a daily DP results in a significant cost savings of 12.04% ($107.35) and 1.91% ($39.35) for Households 1 and 2, respectively, compared to a daily stochastic MILP approach. The difference in the savings is because of the following reasons. In scenarios with high demand (i.e. Household 2), most of the time the battery will discharge its maximum possible power to the household during peak periods, so the battery and the inverter will operate in the maximum efficiencies even though MILP solver does not consider the non-linear constraints. The converse is happening for scenarios with low demand (i.e. Household 1).

For demonstration purposes we show optimisation results for two households over three years in Table.2. The average yearly electricity cost for a residential PV-battery system with the proposed ADP based SHEMS can reduce the total electricity cost over 3 years by 57.27% and 50.95% for Households 1 and 2, respectively, compared to the 22.80% and 28.60% improvements by having only a PV system. It is important to note that a DP based SHEMS over a two-day long decision horizon may result in a slightly better solution. However, it is computationally difficult and the computational power available will be limited as it won't

Table 5.3 Yearly optimisation results for two households over three years

Total:	Household 1			Household 2		
	Year 1	Year 2	Year 3	Year 1	Year 2	Year 3
PV output (MWh)	2.91	2.82	2.89	5.99	5.56	5.35
Demand (MWh)	4.29	4.82	4.38	9.82	10.24	12.85
Benchmark cost ($)	568.09	610.6	558	1208.3	1276	1588.2
With PV ($)	440.52	482.5	417.1	821.7	891.4	1194.8
PV-battery DP ($)	248.37	297.55	238.15	534.8	596.25	890.25
PV-battery ADP ($)	232.25	285.63	224.18	526.2	589.23	882.29
PV-battery Stochastic MILP ($)	281.59	333.60	276.23	554.83	599.07	906.75

be worthwhile investing in a specialised equipment to solve this problem given the savings on offer.

5.3 Summary

This chapter shows the benefits of having a SHEMS and presented an ADP approach for implementing a computationally efficient SHEMS with similar quality schedules as with DP. This approach enables us to extend the decision horizon to up to a week with high resolution while considering multiple devices. Our results indicate that these improvements provide financial benefits to households employing them in a SHEMS. Moreover, stochastic ADP performs better over deterministic ADP under uncertainty without a noticeable increase in the computational effort. In practical applications, we can use VFAs generated from ADP during offline planning phase to make faster online solutions. This is not possible with stochastic MILP and generating value functions using DP is computationally difficult.

However, ADP still takes a considerable amount of time to generate VFAs and we need the daily estimated PV output and demand models. Given this, next, in Chapter 6, we derive a method that uses historical results to generate models that map states and decisions so fast online solutions can be made, using learning methods. This proposed approach in Chapter 6 can generate faster offline models, however, the time that takes to make online

solutions is similar to making decision using VFAs. Given the benefits outlined in this chapter, we recommend the use of ADP in SHEMSs when we have enough computational power available for the offline planning phase.

Chapter 6

Policy Function Approximations

This chapter proposes a PFA algorithm to make fast on-line schedules for a SHEMS problem. This is the fourth of the four (meta) classes of policies described in Chapter 1. In detail, PFAs refers to look-up tables, parametric models and/or non-parametric models that return a decision for a given state (more details in Section 6.1).

Until now, all the methods presented to solve the SHEMS problem, such as DP (Chapter 3), stochastic MILP (Chapter 3) and ADP (Chapter 5) are optimisation techniques, which require us to estimate the day ahead PV output and electrical demand models. As such, the quality of the solutions depends on the accuracy of the PV output and electrical demand estimates. The hierarchical approach in Chapter 2 results in good quality estimates but rely on the users' ability to choose the correct day type. Moreover, even though ADP is computationally efficient compared to other methods, it still takes a considerable amount of time to compute VFAs during the off-line planning phase. Note that we can also make fast real-time solutions from VFAs using the Bellman optimality condition.

On the other hand, PFA models can be used over a long period of time (i.e. months) without having to update it and still obtain similar quality solutions. This is a major advantage of PFAs, compared to having to solve an optimisation problem before the start of each day using ADP or DP. However, all the PFA strategies require training data to learn PFA models during the off-line planning phase. The training data set can be generated using a more powerful cloud or home computer (details in Section 6.4). Once we have the training data set, PFA models can be generated within seconds using a low powered device, which can then be used to make fast real-time decisions over a long period of time. Note that ADP is still the preferred optimisation technique when no training data is available.

This chapter is structured as follows: First, the strategies used in PFAs is presented in Section 6.1. This is followed by a review of ELM in Section 6.2 and then the implementation of our proposed PFA algorithm using ELM in Section 6.3. In Section 6.4, simulation results

of the proposed PFA method using ELM (extreme learning machines), ANN (artificial neural networks), FDNNE (fast decorrelated neural network ensembles) and SVM (support vector machine) are compared with DP (Chapter 3), ADP (Chapter 5), stochastic MILP (Chapter 3) and two-stage lookahead (Chapter 4). Finally the conclusions are in Section 6.5.

6.1 Strategies for the PFAs

PFAs refers to functions that return a decision for a given state without having to solve the associated optimisation problem. However, designing specific functions that map a state to a decision is a challenge, which can be overcome by three strategies:

- Rule-based lookup tables;
- Parametric models;
- Non-parametric statistical representations.

These strategies are described below. The first strategy is to use a rule-based lookup table with decisions for each state (if in state s_k^i, then take decision x_k^i). Generating a look up table with decisions to take from every state is computationally challenging in problems that have a large state space such as our SHEMS problem. Moreover, we are not visiting all the states when making daily schedules. Therefore, it is not worthwhile to implement such a lookup table with decisions for each state. Note that in Chapter 5, VFAs obtained using ADP were stored in a matrix, which is a lookup table with a value for each state.

The second strategy is to use parametric models, which are used to obtain a decision at each state depending on different conditions. For example: the battery can be charged if electricity costs are below a certain value and discharge if it is above a certain value. This method is computationally efficient, however, in our problem multiple devices are coupled together so we can only design parametric policy models for a particular scenario.

The third strategy is non-parametric statistical representations used to learn decisions for each state. This is the type of strategy employed in this chapter. The learning methods that are typically used to solve power engineering applications are SVM and ANN that are trained using the *back propagation* (BP) algorithm in conjunction with an optimisation technique such as gradient descent. Even though these techniques result in good quality solutions, they face challenging issues such as intensive human intervention, slow learning speed and poor learning scalability. More details on the drawbacks of the BP algorithm is in [58].

In order to overcome the above difficulties, ELM was proposed in [58] to learn *single hidden layer feedforward networks* (SLFNs). According to [58], ELM is computationally

efficient compared to BP and SVM (i.e. up to thousands of times faster) while obtaining reasonably quality solutions. Another fast algorithm is proposed in [61], which is referred to as FDNNE with random weights. However, the solutions are highly sensitive to the value of the regularizing factor and computational time is high when solving problems that require a large number of random vector functional-link networks with more hidden neurons [61]. Note that the quality of the solutions, difference in learning speeds and the level of human input required from different learning methods varies for different application domains.

Given this, in order to find a suitable learning method for our PFAs, we compare PFAs using ELM, SVM [60], FDNNE and ANN (solved using Levenberg-Marquardt method in MATLAB) [59] with DP, ADP, stochastic MILP and two-stage lookahead solutions. Note that we only give implementation details about ELM (Section 6.2) as it is the fastest algorithm and gives similar quality solutions as FDNNE. The SVM and ANN (using Levenberg-Marquardt) algorithms are already established techniques that have inbuilt MATLAB functions [60, 59]. The Levenberg-Marquardt method is the fastest training algorithm for feedforward neural networks in MATLAB, however, this method tends to be less efficient for large networks with thousands of weights, which is not a concern in this thesis. Our preliminary results indicate that the BP and Levenberg-Marquardt methods result in similar quality solutions.

6.2 Review of Extreme Learning Machines (ELM)

First, a formulation of a single hidden layer feedforward network (SLFN) with random hidden nodes is presented. Second, ELM used to solve SLFNs is presented.

6.2.1 SLFNs with random hidden nodes

A SLFN is an ANN wherein the information only flows in one direction from the inputs to the outputs via a single hidden layer of nodes, as shown in Fig 6.1. In Fig 6.1, there are 4 inputs, $\widetilde{N} = 4$ hidden nodes and 2 outputs. A particular input, hidden node and output is represented using n, q and m, respectively. Every hidden node is connected to every input and output by the weights w_{qn} and β_{qm}, respectively. The input and the output data sets for a given hidden node are $y_q = [y_{q1}, y_{q2}, \ldots y_{qn}] \in \Re^n$ and $t_q = [t_{q1}, t_{q2}, \ldots t_{qm}] \in \Re^m$ respectively. The total number of samples used for training and a particular sample is denoted by N and j, respectively. Given this, the standard SLFNs with the activation function $g(y)$ are

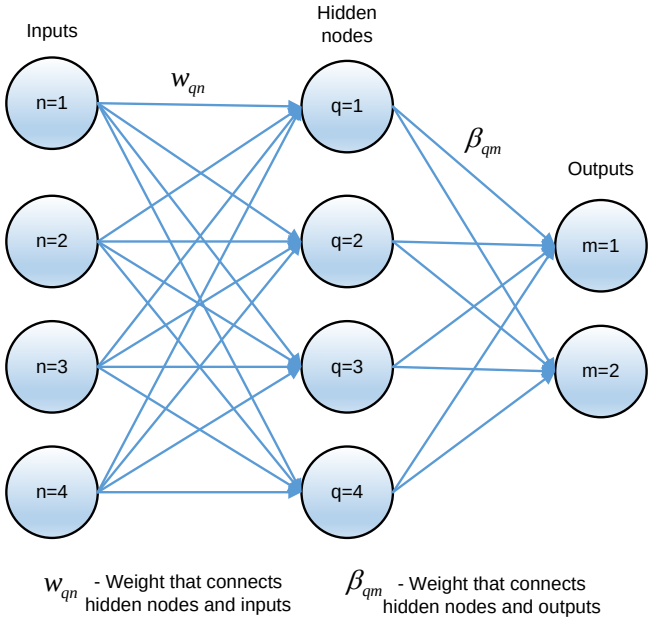

Fig. 6.1 A single hidden layer neural network with four inputs, four hidden nodes and two outputs.

mathematically formulated as:

$$\sum_{q=1}^{\widetilde{N}} \beta_q g_q\left(\mathbf{y}_j\right) = \sum_{q=1}^{\widetilde{N}} \beta_q g_q\left(\mathbf{w}_q \cdot \mathbf{y}_j + b_q\right) = \mathbf{o}_j,$$
$$j = 1, \ldots, N, \tag{6.1}$$

where; $\mathbf{w}_q = [w_{q1}, w_{q2}, \ldots w_{qn}]^{\mathrm{T}}$ is the weight vector that connects a hidden node q and the input node n; $\beta_q = [\beta_{q1}, \beta_{q2}, \ldots \beta_{qm}]^{\mathrm{T}}$ is the weight vector that connects a hidden node q and the output node m; b_q is the threshold of the hidden node q and; $\mathbf{w}_q \cdot \mathbf{y}_q$ is the inner product of $\mathbf{w}_q$ and $\mathbf{y}_q$.

The standard SLFNs with $\widetilde{N}$ hidden nodes and activation function $g(y)$ can approximate N samples with zero error, so $\sum_{j=1}^{N} \left\|\mathbf{o}_j - \mathbf{t}_j\right\| = 0$, which means

$$\sum_{q=1}^{\widetilde{N}} \beta_q g_q\left(\mathbf{w}_q \cdot \mathbf{y}_j + b_q\right) = \mathbf{t}_j,$$
$$j = 1, \ldots, N. \tag{6.2}$$

Now we can write the compact form of the above N equations as:

$$\mathbf{H}\beta = \mathbf{T}, \tag{6.3}$$

Algorithm 3 : ELM for learning SLFNs

1: Initialise training set $\wp = \left\{(\mathbf{y}_q, \mathbf{t}_q)|\mathbf{y}_q \in \Re^n, \mathbf{t}_q \in \Re^m, q = 1,\ldots,\widetilde{N}\right\}$, activation function $g(y)$, and the number of hidden nodes $\widetilde{N}$.
2: Randomly generate $\mathbf{w}_q$ and the threshold $b_q, q = 1,\ldots,\widetilde{N}$.
3: Calculate the hidden layer output matrix $\mathbf{H}$ in (6.4).
4: Calculate the output weight β (6.5).

where,

$$\mathbf{H} = \begin{bmatrix} g(\mathbf{w}_1 \cdot \mathbf{y}_1 + b_1) & \cdots & g(\mathbf{w}_{\widetilde{N}} \cdot \mathbf{y}_1 + b_{\widetilde{N}}) \\ \vdots & \ddots & \vdots \\ g(\mathbf{w}_1 \cdot \mathbf{y}_N + b_1) & \cdots & g(\mathbf{w}_{\widetilde{N}} \cdot \mathbf{y}_N + b_{\widetilde{N}}) \end{bmatrix}_{N \times \widetilde{N}}$$

$$\beta = \begin{bmatrix} \beta_1^{\mathrm{T}} \\ \vdots \\ \beta_{\widetilde{N}}^{\mathrm{T}} \end{bmatrix}_{\widetilde{N} \times m}, \text{ and } \mathbf{T} = \begin{bmatrix} \mathbf{T}_1^{\mathrm{T}} \\ \vdots \\ \mathbf{T}_{\widetilde{N}}^{\mathrm{T}} \end{bmatrix}_{N \times m} \tag{6.4}$$

In [83, 84], $\mathbf{H}$ is called the hidden layer output matrix of the neural network. In more detail, every column of $\mathbf{H}$ corresponds to a particular hidden node output with respect to the inputs $\mathbf{y}_1, \mathbf{y}_2, \ldots, \mathbf{y}_N$.

6.2.2 ELM algorithm

The ELM algorithm used to learn the SLFNs is given in Algorithm 3. In detail, Algorithm 3 proceeds as follows:

1. Load the training data set $\wp = \left\{(\mathbf{y}_q, \mathbf{t}_q)|\mathbf{y}_q \in \Re^n, \mathbf{t}_q \in \Re^m, q = 1,\ldots,N\right\}$, activation function $g(y)$, and the number of hidden nodes $\widetilde{N}$. The training data set consists of inputs $(N \times n)$ and the outputs $(N \times m)$. The activation function has to be infinitely differentiable such as a sigmoidal, sine or hardlim function. If the activation function is infinitely differentiable, then the required number of hidden nodes is $\widetilde{N} \leq N$ [58] (line 1).

2. Randomly generate $\mathbf{w}_q$ and the threshold $b_q, q = 1,\ldots,\widetilde{N}$ (line 2).

3. Calculate the hidden layer output matrix $\mathbf{H}$ in (6.4) (line 3).

Algorithm 4 : PFAs using ELM

1: Separate empirical data into seasons and/or weekdays/weekends.
2: Cluster empirical data into different day types using k-means.
3: Train ELM models for each time-step in every cluster.
4: **for** $k = 1, \ldots, K$ **do**
5: Compute the electrical grid power and electric water heater input using the trained ELM model.
6: Calculate the battery decision that satisfies (2.8).
7: Find the next pre-decision states using (2.5) and (2.6).
8: **end for**

4. Calculate the output weight β using:

$$\beta = \mathbf{H}^{\dagger}\mathbf{T} \tag{6.5}$$

where $\mathbf{T} = [\mathbf{t}_q, \ldots, \mathbf{t}_N]^{\mathrm{T}}$ and $\mathbf{H}^{\dagger}$ is the Moore-Penrose generalised inverse of matrix $\mathbf{H}$ (line 4).

6.3 Implementation

This section presents the implementation details of the proposed PFA algorithm using ELM (Algorithm 4). Here the PFAs are the ELM models that map states (inputs) to decisions (outputs). We can learn these ELM models from empirical data either off-line or online, as it is computationally fast. Once we have the ELM models, fast real-time solutions can be made using the input states while stepping forward in time.

From preliminary simulations, we found that solutions to some scenarios (i.e days) from PFAs using any of the learning methods can be greatly improved by clustering the training data into day types. This means we have to decide the type of day before the start of the decision horizon, which is reasonable compared to having to estimate the entire day's PV and demand models when using DP, ADP or stochastic MILP. However, clustering also has a negative influence on some scenarios if the estimated day types are wrong. This happens when the PV and demand profiles used to train the ELM model of a particular day type is totally different form the actual values. In such situations, solutions can be improved by parametric policy models.

In more detail Algorithm 4 proceeds as follows:

1. Separate empirical data into seasons and weekends/weekdays. This step is only required when we have a large empirical data set or the number of possible clusters (i.e different day types) that customers can choose are less (line 1). The empirical data

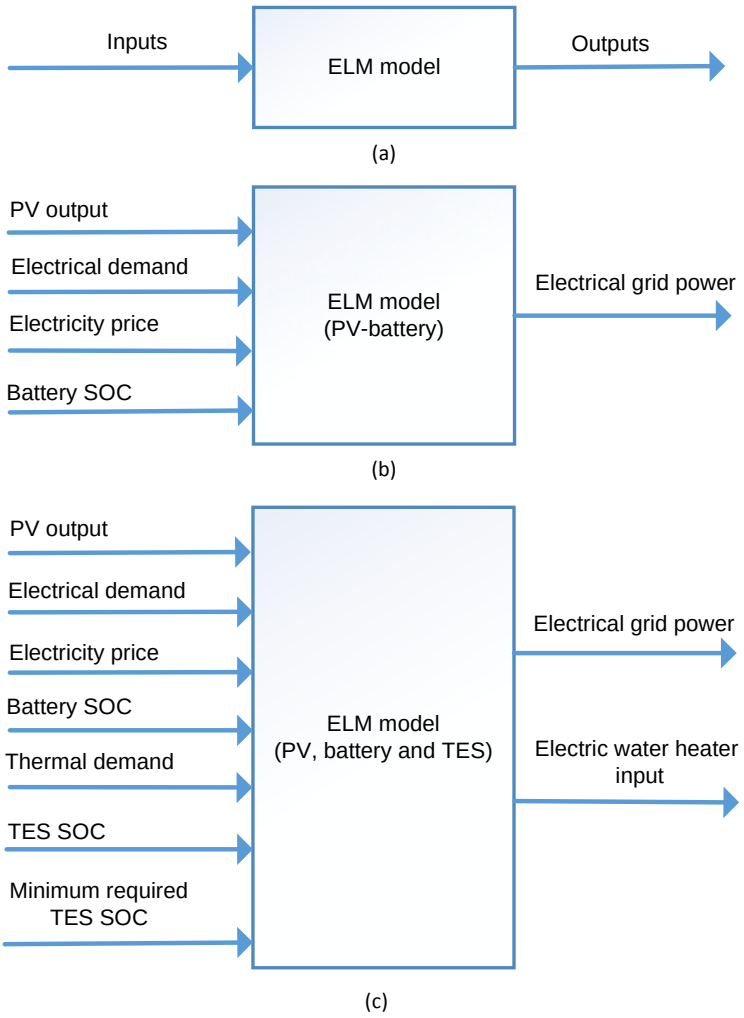

Fig. 6.2 ELM models that map inputs and outputs; (a) basic model, (b) PV-battery system and (c) PV, battery and TES units.

set used to train the ELM model consists of input states, such as battery SOC, TES SOC, minimum required TES SOC, thermal demand, electrical demand, PV output and electricity tariff; and output decisions, such as electrical grid power and electric water heater input, as shown in Fig 6.2.

2. Cluster empirical data into different day types using k-means algorithm. The empirical data is clustered according to the total daily PV output and electrical demand so the resulting clusters correspond to different day types, such as sunny day with low demand, sunny day with high demand, cloudy day with high demand or cloudy day with low demand etc (line 2).

3. Train ELM models for every time-step in every cluster. We can train these ELM models offline or even real time since it is computationally efficient (line 3).

4. In real-time, provide inputs to the trained ELM model to obtain the outputs (line 3). Note that the ELM model is the output weight matrix β calculated in 6.5 and we find H using 6.3 in the same way as for the training set. Outputs are the electrical grid power and the electric water heater input.

5. Calculate the battery decisions that satisfies (2.8). In order to improve the solution quality that arises from bad estimates of the day types, we constrain the policy to stop power flow from battery to grid and grid to battery during peak periods (line 4). In the simulation results section, PFAs with this parametric model is referred to as ELM + parametric policy.

6. Obtain the next pre decision states of the controllable devices using the transition functions (2.5 and 2.6) (line 5).

Next section shows the performance of the PFAs using ELM, SVM, ANN and FDNNE using real-data.

6.4 Simulation Results and Discussion

In this section, we provide simulation results for a PV-battery system. We implement PFAs using ELM, ELM + parametric policy, SVM, FDNNE and ANN and then compare them with ADP, two-stage lookahead, stochastic MILP and DP solutions. For the daily simulation results in Section 6.4.1, we only use DP as a benchmark because we can't control the end-of-day SOC using ADP. Note that for a valid comparison over a day, the end-of-day battery SOC has to be the same from all the solution techniques. We consider four scenarios that consist of two days each for two residential buildings:

1. Central coast, NSW, Australia based residential building with a 2.22 kWp PV system.

2. Sydney, NSW, Australia based residential building with a 3.78 kWp PV system.

The two days are on: July 29th, 2012 and January 1st, 2013. The year-long simulation results in Section 6.4.2 is for the above households. As mentioned in Chapter 2, we have PV output and electrical demand data for three years, so we use the first two years of data to generate the training data set. The training data set is generated by solving the deterministic optimisation problem using DP over two-days because we wanted to obtain exact solutions. Note that the

training data set should have the optimal electrical grid power decisions for the corresponding battery states under different PV output, electrical demand and price signals in order to obtain quality ELM models. We can use these ELM models for a long period of time (i.e months) without updating them and still obtain similar quality solutions, so we can afford to use a computationally expensive DP to generate the training data set, however, ADP and MILP can also be used here. The ADP and DP solutions are made in real-time using the value functions and VFAs that are obtained during the offline planning phase. The PV output and electrical demand for the off-line planning are according to Chapter 2. The device characteristics are in Fig 2.3 and Table 2.1. The ToUP signal is in Fig. 2.2.

6.4.1 Quality of the ELM solutions over a day

We first compare the proposed PFAs using ELM (with parametric policy model) with stochastic DP to illustrate the performance over one day. The battery SOC, electrical grid power and actual and estimated PV output and electrical demand for Scenarios 1, 2, 3 and 4 are in Fig. 6.3, Fig. 6.4, Fig. 6.5, and Fig. 6.6, respectively. Our aim in this section is only to compare the performance of the proposed PFA approach over a day with the best possible solution. The rest of the methods are compared in the year-long simulations section (Section 6.4.3).

Our results show that PFAs using ELM (with parametric policy model) result in better quality solutions compared to the stochastic DP solutions when the forecast error is high, as shown in Table 6.1. This is because the value functions from DP are obtained from the kernel estimated PV and demand models so the quality of the solutions depends on the accuracy of the estimates. Note that DP results in close to optimal solutions when the estimates are 100% accurate. However, when the forecast error is low stochastic DP results in better quality solutions. The Scenarios 3 and 4 have a MAE (mean-absolute error) above 0.5 for electrical demand while Scenarios 1 and 2 have a low MAE.

6.4.2 Year-long simulation

In this section, we present simulation results from the proposed PFA approach using ELM, ELM (with parametric model), ANN, FDNNE and SVM; ADP; two-stage lookahead; stochastic MILP; and DP for two households over a year in Table 6.2. Our simulation results indicate that ADP using a two-day decision horizon results in the best solutions followed by the DP solution, which is expected from the simulation results in Chapter 5. However, we have to estimate the PV and demand models before the decision horizon so the quality of the solutions from ADP and DP depend on the accuracy of the estimates. Our proposed hierarchical

Table 6.1 Daily simulation results for PFAs using ELM and DP for four scenarios

Total daily:	Scenario 1	Scenario 2	Scenario 3	Scenario 4
PV output (kWh)	5.82	13.24	9.9	32.14
MAE PV output	0.039	0.008	0.041	0.026
Electrical demand (kWh)	9.08	9.77	41.91	44.7
MAE electrical demand	0.106	0.093	0.503	0.595
Benchmark ($)	1.54	1.40	5.95	6.91
With PV ($)	1.26	0.42	5.21	3.07
Stochastic DP	0.172	0.02	4.05	1.865
PFAs using ELM with parametric policy ($)	0.196	0.01	3.865	1.704

Table 6.2 Year-long simulation results for two households

	Household 1	Household 2
Electrical demand (MWh)	4.29	9.82
PV output (MWh)	2.91	5.99
Benchmark cost ($)	568.09	1208.3
With PV cost ($)	440.52	821.7
Stochastic DP ($)	253.62	546.86
Deterministic DP (lower quality prediction)	276.31	598.54
PFA (ELM) ($)	275.41	620.57
PFA ($) (ELM + parametric model)	267.50	574.36
PFA (no clustering) ($) (ELM)	337.62	721.35
PFA (no clustering) ($) (ELM + parametric model)	286.92	648.79
PFA (ANN) ($)	274.73	592.75
PFA (SVM) ($)	292.43	621.17
PFA (FDNNE) ($)	267.41	622.21
Two-stage lookahead ($)	248.34	567.36
Stochastic MILP ($)	371.2	704.39
ADP (two-days) ($)	247.03	542.41

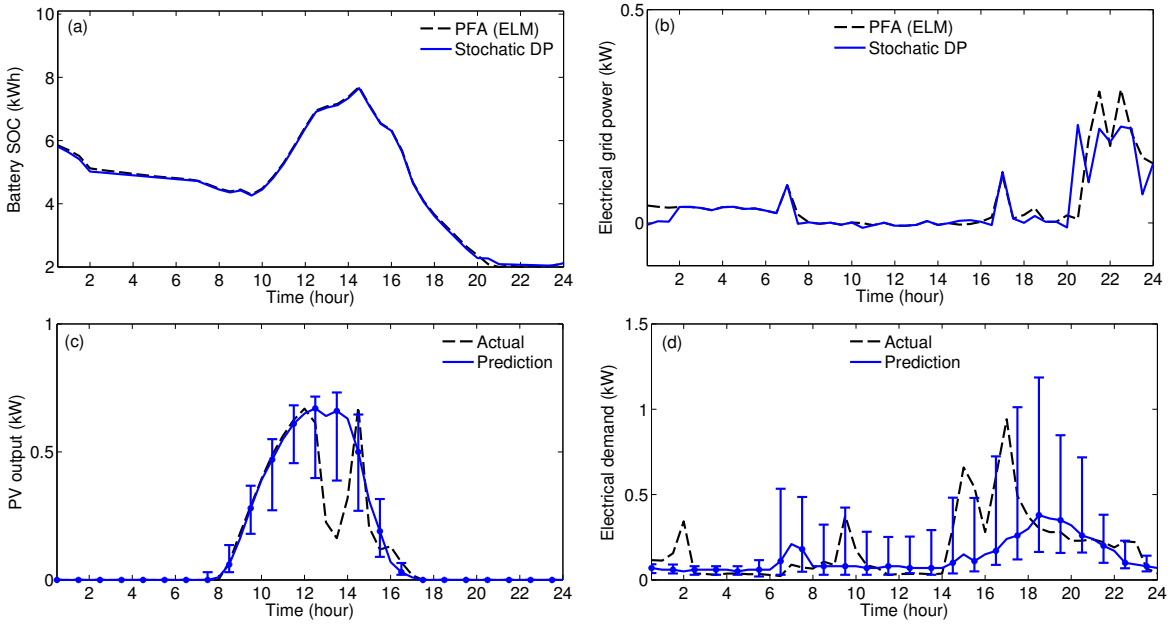

Fig. 6.3 Scenario 1, residential building A on 29th July, 2012, (a) battery SOC and (b) electrical grid power from PFA and stochastic DP; and actual and predicted (c) PV output and (d) electrical demand.

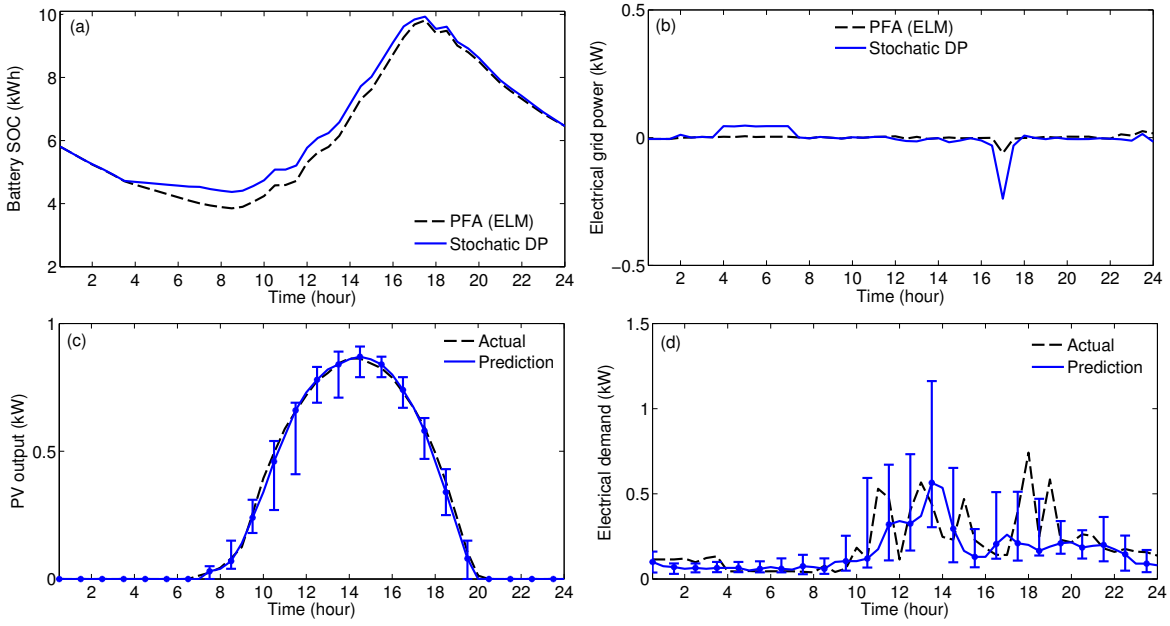

Fig. 6.4 Scenario 2, residential building A on 1st January, 2013, (a) battery SOC and (b) electrical grid power from PFA and stochastic DP; and actual and predicted (c) PV output and (d) electrical demand.

approach in Chapter 2, results in good quality estimates but still in practical applications users will have to identify the corresponding clusters before the start of the decision horizon. Failure to identify the correct clusters for PV and demand may result in increased costs from ADP and DP.

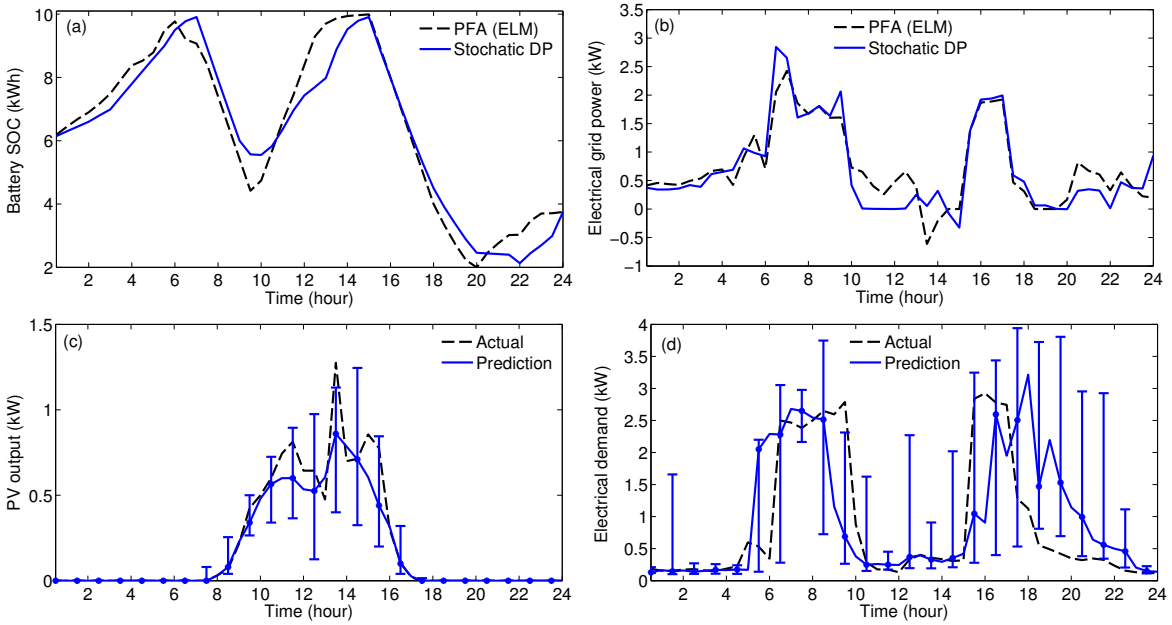

Fig. 6.5 Scenario 3, residential building B on 29th July, 2012, (a) battery SOC and (b) electrical grid power from PFA and stochastic DP; and actual and predicted (c) PV output and (d) electrical demand.

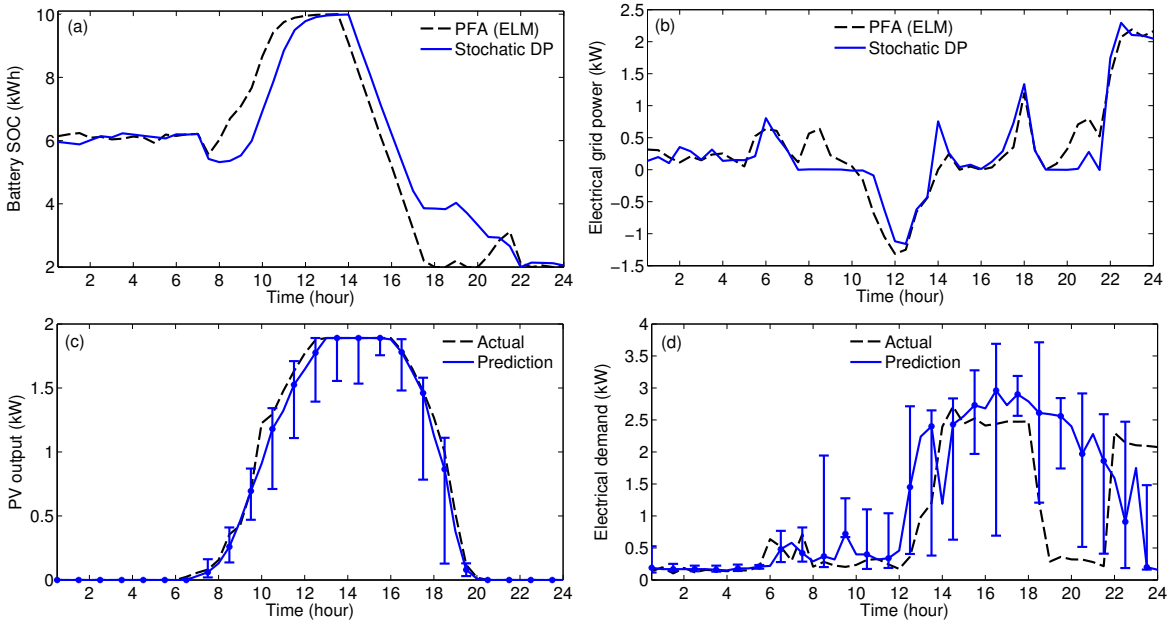

Fig. 6.6 Scenario 4, residential building B on 1st January, 2013, (a) battery SOC and (b) electrical grid power from PFA and stochastic DP; and actual and predicted (c) PV output and (d) electrical demand.

The solutions from the PFAs are slightly lower quality because we do not solve an optimisation problem. However, the training process of the ELM, ANN, FDNNE models are in the range of seconds. PFAs using ELM is computationally fast compared to PFAs using ANN but results in lower quality solutions. The error between the solutions are 0.25% and

5.8% for Households 1 and 2, respectively. The quality of the solutions from ANN depends on the parameter settings used, such as learning rate and the hidden layer size. However, we stick with the same default setting for all the scenarios because it is not possible to change these parameters in practical applications. PFAs using ELM and FDNNE result in similar quality solutions and speed.

The SHEMS using stochastic DP can reduce the total yearly electricity cost by 55.36% and 54.74% for Households 1 and 2, respectively while PFAs using ELM (with parametric model) reduces the total cost by 52.91% and 52.47%. Even though the solutions are slightly lower quality, the proposed approach is extremely fast and can easily be embedded in existing smart meters. Moreover, PFAs perform better than stochastic MILP in terms of both the solution quality and the computational time. The only drawback is that we have to define the parametric model in order to get the solutions close to the DP solutions, which requires a prior understanding of the problem structure. For example, in this situation we know the electricity price is a ToU so we can easily identify the peak electricity price signal.

6.5 Summary

This chapter proposed a PFA algorithm, which can use non-parametric learning methods such as ELM, SVM, FDNNE and ANN to solve the SHEMS problem. These non-parametric methods can learn models that map states and decisions at each time-step of different day types. This process only takes seconds compared to the considerable amount of time that takes to generate value functions and VFAs using DP and ADP, respectively. Moreover, we don't have to estimate day ahead PV and demand models in order to obtain decisions from PFAs using Algorithm 4. However, the solutions are lower quality compared to the DP and ADP solutions from good estimates because we don't solve an optimisation problem.

The real-time decision making process of PFAs using ELM, DP and ADP takes approximately the same time compared to the slightly increased computational time from PFAs using ANN and SVM. However, ADP and DP require us to store value functions for every time-step in the smart meter, which requires a higher memory compared to storing ELM or ANN models. We believe that the proposed PFA algorithm will be beneficial in situations where the computational power of the smart meters is limited or when it is difficult to estimate the day ahead PV and demand models. Moreover, we can use the same PFA models for months without updating and still get similar quality solutions.

Conclusions and Future Work

This thesis has proposed three fast solution techniques for implementing an efficient SHEMS. That is:

- Two-stage lookahead stochastic optimisation framework;
- ADP approach with temporal difference learning;
- PFA algorithm using ELM, ANN, FDNNE, and SVM.

Throughout the thesis, these methods have been compared with each other and against DP and stochastic MILP using a range of PV-storage systems. PV-storage (thermal and battery) systems have been chosen in this thesis because of the Australia's increasing penetration of rooftop PV and battery storage systems in response to rising electricity costs, decreasing technology costs and existing fleet of hot water storage devices.

The main objective of a SHEMS is to minimise energy costs while providing suitable levels of comfort to the inhabitants. The underlying sequential stochastic decision making problem has been presented in Chapter 2. The PV output and electrical and thermal demand data that have been used in this thesis were collected during Smart Grid Smart City project. The contributions of this thesis are summarised below.

An hierarchical approach has been proposed in Chapter 2 to estimate PV and demand models, which first cluster empirical data and then learns probability density functions using kernel regression. This kernel estimator conforms with the MDP construction (i.e. Markov property of the transition functions). Moreover, in practical applications, the user only has to choose the type of day, which is reasonable compared to having to estimate entire day's PV and demand models.

Deterministic and stochastic SHEMSs using DP and stochastic MILP have been compared with each other in Chapter 3. This chapter has concluded that DP results in better quality solutions as it considers non-linear constraints and appropriate probability distributions. Moreover, value functions generated during the off-line planning phase can be used to make fast real-time solutions using the Bellman optimality condition. However, it is

computationally difficult to extend the decision horizon, incorporate the stochastic nature and integrate multiple controllable devices using DP because of dimensionalities of state, decision and outcome spaces.

Given this, a two-stage lookahead method has been proposed in Chapter 4 to identify the benefits of extending the decision horizon. In detail, a longer decision horizon solver that uses deterministic MILP, while its end-of-day battery SOC is used in a daily DP solver. Our results have showed that considering uncertainties using the two-stage lookahead results in significant financial benefits compared to a daily DP approach. However, fixing the end-of-day battery SOC has negative influence when the actual PV output and demand deviates from the forecasts.

Building on this, an ADP approach using temporal difference learning has been proposed to implement a computationally efficient SHEMS in Chapter 5. ADP results in better quality solutions than stochastic MILP as it incorporate stochastic input variables using appropriate probabilistic models and non-linear constraints. However, the solutions are lower quality compared to the optimal DP solutions because the value functions used are approximations. On the other hand, ADP enables us to extend the decision horizon to up to two days with high resolution while considering multiple devices. Our results have indicated that these improvements provide financial benefits to households employing them in a SHEMS. Moreover, stochastic ADP always performs better over deterministic ADP under uncertainty without a noticeable increase in the computational effort. Even thought ADP is computationally efficient compared to both DP and stochastic MILP, it still requires a considerable amount of time to generate VFAs during the off-line planning phase.

A PFA algorithm using ELM has been proposed in Chapter 6 to overcome these challenges. Here ELM was used to generate models that map input states and output decisions. Similar to ADP and DP, on-line decisions can be made within seconds, however, storing ELM models in an existing smart meter is feasible compared to storing VFAs for every time-step. PFAs generated during the off-line planning phase can be used over a long period of time without updating and still obtain quality solutions. However, off-line planning phase require training data, which has to be generated by solving the deterministic SHEMS problem over couple of years. We can use a more powerful cloud or home computer to do this as it is only needed once. The decisions from PFAs are lower quality compared to decisions from ADP and DP because we don't solve an optimisation problem. However, under high uncertainty PFAs performs better than both ADP and DP.

The possible future research directions are described below:

- In this research we only focused on fast solution techniques for implementing efficient SHEMSs. Hence we decided to stick with well established models for battery and

TES units. Given this, the first possible future work is to include more comprehensive battery and TES models. The TES model can be modified to include the indoor household temperature, hot water tank's temperature and the properties (i.e thermal) of the material (i.e polypropylene) used to make the hot water tank. The battery model can include constraints for the battery depreciation and the number of useful life cycles.

- The second possible avenue for future work is to incorporate additional devices to the household model, such as an EV and a HVAC system. The HVAC system model can include the thermal inertia of the building with phase changing materials.
- The third possible research direction is to develop an off-grid system for a large consumer. Here the electrical demand will have to be satisfied by the DG units (i.e PV system) and the battery. In such situations ADP will be beneficial as we have to plan over a longer decision horizon (i.e. a week).
- The fourth possible future work is to implement the proposed SHEMSs on a Raspberry Pi board and then develop a prototype.

In conclusion, the results of this research have shown that PFAs using ELM and ADP with temporal difference learning can incorporate the stochastic variables, extend the decision horizon and integrate multiple controllable devices with low computational burden. As such, SHEMSs implemented using these methods result in significant financial benefits for the residential users. Given this, we recommend the use of ADP for SHEMSs, when the available device has enough computational power and PFAs for SHEMSs, when the available device has low computational power.

List of Publications

[1] C. Keerthisinghe, G. Verbič, and A. C. Chapman, *"A Fast Technique for Smart Home Management: ADP with Temporal Difference Learning",* IEEE Transactions on Smart Grid.

[2] C. Keerthisinghe, G. Verbič, and A. C. Chapman, *"Energy management of PV-storage systems: ADP approach with temporal difference learning,"* in Power Systems Computing Conference (PSCC), 2016, Jun 2016, pp. 1-7.

[3] C. Keerthisinghe, G. Verbič, and A. C. Chapman, *"Addressing the stochastic nature of energy management of smart homes,"* Power Systems Computing Conference (PSCC), 2014, Aug 2014, pp. 1-7.

[4] C. Keerthisinghe, G. Verbič, and A. C. Chapman, *"Evaluation of a multi-stage stochastic optimisation framework for energy management of residential PV-storage systems,"* in Power Engineering Conference (AUPEC), 2014 Australasian Universities, Sept 2014, pp. 1-6.

[5] G. Verbič, C. Keerthisinghe, and A. C. Chapman, *"A Project-Based Cooperative Approach to Teaching Sustainable Energy Systems",* IEEE Transactions on Education.

[6] C. Keerthisinghe, G. Verbič, and A. C. Chapman, *"Estimating residential PV and demand models for a Markov decision process formulation of a home energy management problem",* To be published.

[7] C. Keerthisinghe, G. Verbič, and A. C. Chapman, *"Energy Management of PV-Storage Systems: Policy Approximations using Extreme Learning Machines",* To be published.

References

[1] The conversation. 50% renewable energy would put Australia in line with leading nations. [Online]. Available: http://theconversation.com/50-renewable-energy-would-put-australia-in-line-with-leading-nations-45152

[2] CSIRO. Future Grid Forum. [Online]. Available: http://www.csiro.au/en/Research/EF/Areas/Electricity-grids-and-systems/Economic-modelling/Future-Grid-Forum

[3] A. C. Chapman and G. Verbič and D. J. Hill, "Algorithmic and strategic aspects to integrating demand-side aggregation and energy management methods," *IEEE Transactions on Smart Grid*, vol. PP, no. 99, pp. 1–13, 2016.

[4] Rocky Mountain Institute, Homer Energy, Cohnreznick Think Energy, "The economics of grid defection when and where distributed solar generation plus storage competes with traditional utility service," Tech. Rep., 2014.

[5] S. Li, D. Zhang, A. B. Roget, and Z. O'Neill, "Integrating home energy simulation and dynamic electricity price for demand response study," *IEEE Transactions on Smart Grid*, vol. 5, no. 2, pp. 779–788, March 2014.

[6] M. Muratori and G. Rizzoni, "Residential demand response: Dynamic energy management and time-varying electricity pricing," *IEEE Transactions on Power Systems*, vol. 31, no. 2, pp. 1108–1117, March 2016.

[7] S. Lu, N. Samaan, R. Diao, M. Elizondo, C. Jin, E. Mayhorn, Y. Zhang, and H. Kirkham, "Centralized and decentralized control for demand response," in *Innovative Smart Grid Technologies (ISGT), 2011 IEEE PES*, 2011, pp. 1–8.

[8] M. Pipattanasomporn, M. Kuzlu, and S. Rahman, "An algorithm for intelligent home energy management and demand response analysis," *IEEE Transactions on Smart Grid*, vol. 3, no. 4, pp. 2166–2173, 2012.

[9] C. Chen, J. Wang, and S. Kishore, "A distributed direct load control approach for large-scale residential demand response," *IEEE Transactions on Power Systems*, vol. 29, no. 5, pp. 2219–2228, Sept 2014.

[10] US Energy Information Administration. Demand response can lower electric power load when needed . [Online]. Available: http://www.eia.gov/todayinenergy/detail.php?id=130#

[11] Australian Government Bureau of Resources and Energy Economics. Energy in Australia 2014. [Online]. Available: http://www.industry.gov.au/Office-of-the-Chief-Economist/Publications/Documents/energy-in-aust/bree-energyinaustralia-2014.pdf

[12] Reposit, Canberra, Australia. Reposit at your home. [Online]. Available: http://www.repositpower.com/at-your-home/

[13] Pi Australia. Buy a Raspberry Pi Australia. [Online]. Available: http://raspberry.piaustralia.com.au/

[14] Ausgrid, NSW, Australia. Time-of-use pricing. Ausgrid, NSW, Australia. [Online]. Available: http://www.ausgrid.com.au/Common/Customer-Services/Homes/Meters/Time-of-use-pricing.aspx#.V38KM6JGRJA

[15] Flexible pricing FAQs. Energy Australia. [Online]. Available: https://www.energyaustralia.com.au/faqs/residential/flexible-pricing-plan-information

[16] S. Baltaoglu, L. Tong, and Q. Zhao, "Online learning and pricing for demand response in smart distribution networks," in *2016 IEEE Statistical Signal Processing Workshop (SSP)*, June 2016, pp. 1–5.

[17] K. McKenna and A. Keane, "Residential load modeling of price-based demand response for network impact studies," *IEEE Transactions on Smart Grid*, vol. 7, no. 5, pp. 2285–2294, Sept 2016.

[18] J. Kwac and R. Rajagopal, "Data-driven targeting of customers for demand response," *IEEE Transactions on Smart Grid*, vol. 7, no. 5, pp. 2199–2207, Sept 2016.

[19] D. T. Nguyen, H. T. Nguyen, and L. B. Le, "Dynamic pricing design for demand response integration in power distribution networks," *IEEE Transactions on Power Systems*, vol. 31, no. 5, pp. 3457–3472, Sept 2016.

[20] M. Ali, M. Z. Degefa, M. Humayun, A. Safdarian, and M. Lehtonen, "Increased utilization of wind generation by coordinating the demand response and real-time thermal rating," *IEEE Transactions on Power Systems*, vol. 31, no. 5, pp. 3737–3746, Sept 2016.

[21] D. E. M. Bondy, O. Gehrke, A. Thavlov, K. Heussen, A. M. Kosek, and H. W. Bindner, "Procedure for validation of aggregators providing demand response," in *2016 Power Systems Computation Conference (PSCC)*, June 2016, pp. 1–7.

[22] S. Sebastian and V. Margaret, "Application of demand response programs for residential loads to minimize energy cost," in *2016 International Conference on Circuit, Power and Computing Technologies (ICCPCT)*, March 2016, pp. 1–4.

[23] G. Parkinson. (2013, December) People power: Rooftop solar PV reaches 3GW in Australia. [Online]. Available: http://reneweconomy.com.au/2013/people-power-rooftop-solar-pv-reaches-3gw-in-australia-99543

[24] Electric Power Research Institute (EPRI), "The integrated grid realizing the full value of central and distributed energy resources," Tech. Rep., 2014.

[25] Sophie Vorrath. (2016, November) Tesla Powerwall 2 battery storage opens for orders in Australia. REnewEconomy. [Online]. Available: http://reneweconomy.com.au/tesla-powerwall-2-battery-storage-opens-orders-australia-32360/

[26] Solar Quotes. (2016, June) Solar battery storage comparison table. [Online]. Available: https://www.solarquotes.com.au/battery-storage/comparison-table/AccessedonJanuary2016

[27] G. Parkinson. (2016, April) ACT opens big solar and wind auction to boost battery storage. [Online]. Available: http://reneweconomy.com.au/2016/act-opens-big-solar-wind-auction-to-boost-battery-storage-74992

[28] Australian Energy Market Operator (AEMO), "Emerging technologies information," Tech. Rep., 2015.

[29] Vector, New Zealand. Bringing the Tesla Energy Powerwall to New Zealand. [Online]. Available: https://vector.co.nz/tesla-energy

[30] PV magazine. Germany's solar and storage subsidy extended to 2018. [Online]. Available: http://www.pv-magazine.com/news/details/beitrag/germanys-solarstorage-subsidy-extended-to-2018_100023314/#axzz4CIVyvd7x

[31] Smart-Grid Smart-City Customer Trial Data. [Online]. Available: https://data.gov.au/dataset/smart-grid-smart-city-customer-trial-data

[32] E. L. Ratnam, S. R. Weller, C. M. Kellett, and A. T. Murray, "Residential load and rooftop PV generation: an Australian distribution network dataset," *International Journal of Sustainable Energy*, vol. 0, no. 0, pp. 1–20, 0.

[33] Government UK. Feed-in tariffs: get money for generating your own electricity . [Online]. Available: https://www.gov.uk/feed-in-tariffs/overview

[34] Z. Chen, L. Wu, and Y. Fu, "Real-time price-based demand response management for residential appliances via stochastic optimization and robust optimization," *IEEE Transactions on Smart Grid*, vol. 3, no. 4, pp. 1822–1831, 2012.

[35] M. Pedrasa, T. Spooner, and I. MacGill, "Coordinated scheduling of residential distributed energy resources to optimize smart home energy services," *IEEE Transactions on Smart Grid*, vol. 1, no. 2, pp. 134–143, 2010.

[36] E. L. Ratnam, S. R. Weller, and C. M. Kellett, "Scheduling residential battery storage with solar pv: Assessing the benefits of net metering," *Applied Energy*, vol. 155, pp. 881 – 891, 2015. [Online]. Available: http://www.sciencedirect.com/science/article/pii/S0306261915008193

[37] C. Keerthisinghe and G. Verbič and A. C. Chapman, "Evaluation of a multi-stage stochastic optimisation framework for energy management of residential PV-storage systems," in *2014 Australasian Universities Power Engineering Conference (AUPEC)*, Sept 2014, pp. 1–6.

[38] D. Jiang, T. Pham, W. Powell, D. Salas, and W. Scott, "A comparison of approximate dynamic programming techniques on benchmark energy storage problems: Does anything work?" in *Adaptive Dynamic Programming and Reinforcement Learning (ADPRL), 2014 IEEE Symposium on*, Dec 2014, pp. 1–8.

[39] M. Bozchalui, S. Hashmi, H. Hassen, C. Canizares, and K. Bhattacharya, "Optimal operation of residential energy hubs in smart grids," *IEEE Transactions on Smart Grid*, vol. 3, no. 4, pp. 1755–1766, 2012.

[40] T. Hubert and S. Grijalva, "Realizing smart grid benefits requires energy optimization algorithms at residential level," in *Innovative Smart Grid Technologies (ISGT), 2011 IEEE PES*, 2011, pp. 1–8.

[41] Z. Zhu, J. Tang, S. Lambotharan, W. Chin, and Z. Fan, "An integer linear programming and game theory based optimization for demand-side management in smart grid," in *GLOBECOM Workshops (GC Wkshps), 2011 IEEE*, 2011, pp. 1205–1210.

[42] F. De Angelis, M. Boaro, D. Fuselli, S. Squartini, F. Piazza, and Q. Wei, "Optimal home energy management under dynamic electrical and thermal constraints," *IEEE Transactions on Industrial Informatics*, vol. 9, no. 3, pp. 1518–1527, 2013.

[43] J. Wang, Z. Sun, Y. Zhou, and J. Dai, "Optimal dispatching model of smart home energy management system," in *Innovative Smart Grid Technologies - Asia (ISGT Asia), 2012 IEEE*, 2012, pp. 1–5.

[44] H. Joumaa, G. De-Oliviera, S. Ploix, and M. Jacomino, "Energy management problem in dwellings: Combining centralized and distributed solving approaches," in *Innovative Smart Grid Technologies (ISGT Europe), 2012 3rd IEEE PES International Conference and Exhibition on*, 2012, pp. 1–8.

[45] K. C. Sou, J. Weimer, H. Sandberg, and K. Johansson, "Scheduling smart home appliances using mixed integer linear programming," in *Decision and Control and European Control Conference (CDC-ECC), 2011 50th IEEE Conference on*, 2011, pp. 5144–5149.

[46] A. C. Luna, N. L. D. Aldana, M. Graells, J. C. Vasquez, and J. M. Guerrero, "Mixed-integer-linear-programming based energy management system for hybrid pv-wind-battery microgrids: Modeling, design and experimental verification," *IEEE Transactions on Power Electronics*, vol. PP, no. 99, pp. 1–1, 2016.

[47] M. Pedrasa, E. Spooner, and I. MacGill, "Improved energy services provision through the intelligent control of distributed energy resources," in *PowerTech, 2009 IEEE Bucharest*, 2009, pp. 1–8.

[48] ——, "Robust scheduling of residential distributed energy resources using a novel energy service decision-support tool," in *Innovative Smart Grid Technologies (ISGT), 2011 IEEE PES*, 2011, pp. 1–8.

[49] M. Pedrasa, T. Spooner, and I. MacGill, "Scheduling of demand side resources using binary particle swarm optimization," *IEEE Transactions on Smart Grid*, vol. 24, no. 3, pp. 1173–1181, 2009.

[50] L. Wang, Z. Wang, and R. Yang, "Intelligent multiagent control system for energy and comfort management in smart and sustainable buildings," *IEEE Transactions on Smart Grid*, vol. 3, no. 2, pp. 605–617, 2012.

[51] Z. U. Abedin, U. Shahid, A. Mahmood, U. Qasim, Z. A. Khan, and N. Javaid, "Application of pso for hems and ed in smart grid," in *Complex, Intelligent, and Software Intensive Systems (CISIS), 2015 Ninth International Conference on*, July 2015, pp. 260–266.

[52] S. K. Nayak, N. C. Sahoo, and G. Panda, "Demand side management of residential loads in a smart grid using 2d particle swarm optimization technique," in *2015 IEEE Power, Communication and Information Technology Conference (PCITC)*, Oct 2015, pp. 201–206.

[53] H. Tischer and G. Verbič, "Towards a smart home energy management system - a dynamic programming approach," in *Innovative Smart Grid Technologies Asia (ISGT), 2011 IEEE PES*, 2011, pp. 1–7.

[54] L. Jiang, H. Tang, Q. Jiang, and L. Zhou, "Optimal control of smart home energy management based on stochastic dynamic programming," in *Intelligent Control and Automation (WCICA), 2014 11th World Congress on*, June 2014, pp. 570–575.

[55] H. T. Nguyen, D. Nguyen, and L. B. Le, "Home energy management with generic thermal dynamics and user temperature preference," in *Smart Grid Communications (SmartGridComm), 2013 IEEE International Conference on*, Oct 2013, pp. 552–557.

[56] C. Keerthisinghe and G. Verbič and A. C. Chapman, "Addressing the stochastic nature of energy management in smart homes," in *2014 Power Systems Computation Conference*, Aug 2014, pp. 1–7.

[57] Xiaohui Hu. PSO tutorial. [Online]. Available: http://www.swarmintelligence.org/tutorials.php

[58] Guang-Bin Huang and Qin-Yu Zhu and Chee-Kheong Siew, "Extreme learning machine: Theory and applications," *Neurocomputing*, vol. 70, pp. 489 – 501, 2006, neural NetworksSelected Papers from the 7th Brazilian Symposium on Neural Networks (SBRN '04)7th Brazilian Symposium on Neural Networks. [Online]. Available: http://www.sciencedirect.com/science/article/pii/S0925231206000385

[59] MathWorks. Neural network toolbox MATLAB documentation. [Online]. Available: http://au.mathworks.com/help/nnet/index.html

[60] ——. MATLAB support vector machine regression documentation. [Online]. Available: http://au.mathworks.com/help/stats/support-vector-machine-regression.html

[61] M. Alhamdoosh and D. Wang, "Fast decorrelated neural network ensembles with random weights," *Information Sciences*, vol. 264, pp. 104 – 117, 2014, serious Games. [Online]. Available: http://www.sciencedirect.com/science/article/pii/S0020025513008669

[62] D. F. Salas and W. B. Powell, "Benchmarking a scalable approximate dynamic programming algorithm for stochastic control of multidimensional energy storage problems," Technical report, Working Paper, Department of Operations Research and Financial Engineering, Princeton, NJ, Tech. Rep., 2013.

[63] R. Anderson, A. Boulanger, W. Powell, and W. Scott, "Adaptive stochastic control for the smart grid," *Proceedings of the IEEE*, vol. 99, no. 6, pp. 1098–1115, 2011.

[64] Powell, Warren B. and George, Abraham and Simao, Hugo and Scott, Warren and Lamont, Alan and Stewart, Jeffrey, "SMART: A Stochastic Multiscale Model for the Analysis of Energy Resources, Technology, and Policy," *INFORMS Journal on Computing*, vol. 24, no. 4, pp. 665–682, 2012.

[65] W. B. Powell, *Approximate Dynamic Programming - Solving the Curses of Dimensionality*. John Wiley and Sons, Inc., 2007.

[66] ——, "Approximate dynamic programming for large-scale resource allocation problems," Princeton University, Princeton, New Jersey 08544, USA,, 2005.

[67] F. Borghesan, R. Vignali, L. Piroddi, M. Prandini, and M. Strelec, "Approximate dynamic programming-based control of a building cooling system with thermal storage," in *Innovative Smart Grid Technologies Europe (ISGT EUROPE), 2013 4th IEEE/PES*, Oct 2013, pp. 1–5.

[68] M. Strelec and J. Berka, "Microgrid energy management based on approximate dynamic programming," in *Innovative Smart Grid Technologies Europe (ISGT EUROPE), 2013 4th IEEE/PES*, Oct 2013, pp. 1–5.

[69] P. Samadi, H. Mohsenian-Rad, V. Wong, and R. Schober, "Real-time pricing for demand response based on stochastic approximation," *IEEE Transactions on Smart Grid*, vol. 5, no. 2, pp. 789–798, March 2014.

[70] J. L. Williams, J. W. Fisher, and A. S. Willsky, "Approximate dynamic programming for communication-constrained sensor network management," *IEEE Transactions on Signal Processing*, vol. 55, no. 8, pp. 4300–4311, Aug 2007.

[71] K. Al-jabery, Z. Xu, W. Yu, D. Wunsch, J. Xiong, and Y. Shi, "Demand-side management of domestic electric water heaters using approximate dynamic programming," *IEEE Transactions on Computer-Aided Design of Integrated Circuits and Systems*, vol. PP, no. 99, pp. 1–1, 2016.

[72] W. Li, G. Xu, Z. Wang, and Y. Xu, "Dynamic energy management for hybrid electric vehicle based on approximate dynamic programming," in *Intelligent Control and Automation, 2008. WCICA 2008. 7th World Congress on*, June 2008, pp. 7864–7869.

[73] W. Guo, F. Liu, J. Si, D. He, R. Harley, and S. Mei, "Online supplementary adp learning controller design and application to power system frequency control with large-scale wind energy integration," *IEEE Transactions on Neural Networks and Learning Systems*, vol. PP, no. 99, pp. 1–1, 2016.

[74] N. Sharma, P. Sharma, D. Irwin, and P. Shenoy, "Predicting solar generation from weather forecasts using machine learning," in *Smart Grid Communications (SmartGridComm), 2011 IEEE International Conference on*, Oct 2011, pp. 528–533.

[75] K. Bao, F. Allerding, and H. Schmeck, "User behavior prediction for energy management in smart homes," in *Fuzzy Systems and Knowledge Discovery (FSKD), 2011 Eighth International Conference on*, vol. 2, July 2011, pp. 1335–1339.

[76] D. Lachut, N. Banerjee, and S. Rollins, "Predictability of energy use in homes," in *Green Computing Conference (IGCC), 2014 International*, Nov 2014, pp. 1–10.

[77] C. Keerthisinghe and G. Verbič and A. C. Chapman, "Energy management of PV-storage systems: ADP approach with temporal difference learning," in *2016 Power Systems Computation Conference (PSCC)*, June 2016, pp. 1–7.

[78] ——, "A Fast Technique for Smart Home Management: ADP with Temporal Difference Learning," *IEEE Transactions on Smart Grid*, vol. PP, no. 99, pp. 1–1, 2016.

[79] E3 - Equipment Energy Efficieny, "Water heating data collection and analysis," Tech. Rep., 2012.

[80] MathWorks. Kernel Distribution. [Online]. Available: https://au.mathworks.com/help/stats/kernel-distribution.html

[81] T. Jaakkola, M. I. Jordan, and S. P. Singh, "Convergence of stochastic iterative dynamic programming algorithms," *Neural Computation*, vol. 6, pp. 1185–1201, 1994.

[82] G. A. Godfrey and W. B. Powell, "An adaptive, distribution-free algorithm for the newsvendor problem with censored demands, with applications to inventory and distribution," *Management Science*, vol. 47, no. 8, pp. 1101–1112, 2001.

[83] G.-B. Huang, "Learning capability and storage capacity of two-hidden-layer feedforward networks," *IEEE Transactions on Neural Networks*, vol. 14, no. 2, pp. 274–281, Mar 2003.

[84] G.-B. Huang and H. A. Babri, "Upper bounds on the number of hidden neurons in feedforward networks with arbitrary bounded nonlinear activation functions," *IEEE Transactions on Neural Networks*, vol. 9, no. 1, pp. 224–229, Jan 1998.